

Hanna Birgitte Sletta
Kristin Serck-Hanssen

Integration of Renewable Energy Sources into Electricity Markets via Optimized Wind Farm and Hydropower Scheduling

Master's thesis in Energy and Environmental Engineering (Energi og Miljø)

Supervisor: Umit Cali

Co-supervisor: Michael Belsnes & Marthe Fogstad Dyrge

June 2023



Norwegian University of
Science and Technology

Hanna Birgitte Sletta
Kristin Serck-Hanssen

Integration of Renewable Energy Sources into Electricity Markets via Optimized Wind Farm and Hydropower Scheduling

Master's thesis in Energy and Environmental Engineering (Energi og Miljø)

Supervisor: Umit Cali

Co-supervisor: Michael Belsnes & Marthe Fogstad Dynge

June 2023

Norwegian University of Science and Technology

Faculty of Information Technology and Electrical Engineering

Department of Electric Power Engineering



Norwegian University of
Science and Technology



Kunnskap for en bedre verden

DEPARTMENT OF ELECTRIC ENERGY

TET4900 - ELECTRICAL ENERGY AND ENERGY SYSTEMS

Integration of Renewable Energy Sources into Electricity Markets via Optimized Wind Farm and Hydropower Scheduling

Authors:

Hanna Birgitte Sletta

Kristin Serck-Hanssen

Supervisor:

Umit Cali

Co-supervisors:

Michael Belsnes

Marthe Fogstad Dyngre

June 8, 2023

Abstract

Power companies in Norway are increasing their investments in variable renewable energy sources, like windpower, to meet increased power demand while simultaneously decarbonizing the power system. By optimizing the schedule of operation, one can enhance the price balance in the power markets that have seen significant volatility in recent years. This is particularly relevant for the intraday and balancing markets. The price volatility also makes it increasingly important for producers of unpredictable energy sources to have reliable methods for optimal bid scheduling to avoid penalty costs. This thesis seeks to utilize SINTEF's Short-term Hydropower Optimization Program (SHOP) to develop a wind optimization model for production scheduling and market bidding. The goal on a long-term basis is that this model can be expanded to become a Wind-Hydro Optimization Program (WHOP) for joint scheduling. A *Wind Optimization Model* is developed and its functionality tested on a case study at Geitfjellet Vindpark, located within the focus area price zone NO3. The analysis investigates the impact of a volatile up-regulation price on the day-ahead market power bid and total profit of a windpower producer. Historical data from the case study was inserted as scenarios into a scenario reduction algorithm. Stochasticity was utilized to assess the variations that arise from incorporating a varying number of scenarios.

The results showed that, from the required data, the afternoon has more volatile prices and production than the morning and noon. Additionally, utilizing yearly data points does not properly account for the seasonal dependency observed in windpower production, nor the market prices based on the seasonal variations seen in hydropower-dominated power markets. Another assessment deducted from the results is that the windpower producer mostly bid under their expected production to avoid the high penalty costs. This demonstrates that there could be ways to utilize the market to improve bidding practices, for instance by joint scheduling of wind and hydro. The case study concludes that the functionality of the developed *Wind Optimization Model* has been proven efficient.

Sammendrag

Kraftselskaper i Norge øker investeringene i variable fornybare energikilder som vindkraft for å imøtekomme økt etterspørsel og dekarbonisere kraftsystemet. Ved å optimalisere driftsplanen kan man forbedre balansen i kraftmarkedene, som de siste årene har sett betydelig ustabilitet og usikkerhet. Dette er spesielt relevant for intradag- og balansemarkedene. Denne prisvolatiliteten gjør det også stadig viktigere for produsenter av variable energikilder som vindkraft å ha pålitelige metoder for optimal planlegging av bud for å unngå straffekostnader. Denne master-avhandlingen tar sikte på å utnytte SINTEFs programverktøy for korttids produksjonsplanlegging av vannkraft (SHOP) for å utvikle et liknende optimeringsprogram for vind for produksjonsplanlegging og markedsbud. Målet på lang sikt er at denne modellen kan utvikles til å bli et vind-vann kraftoptimeringsprogram (WHOP) for felles planlegging. En *vindoptimeringsmodell* er derfor utviklet og testet gjennom en casestudie ved Geitfjellet Vindpark i prisområde NO3, det området denne avhandlingen er rettet mot. Analysen undersøker effekten av den volatile oppreguleringsprisen på markedsbudet og profitten til vindkraftprodusenten. Historiske data fra casestudien ble inkludert i en scenario-reduksjonsalgoritme. Stokastisitet ble brukt for å analysere forskjellene ved å inkludere ulike antall scenarioer.

Resultatene viste at ettermiddagen har mer volatilitet i priser og produksjon enn morgenen og formiddagen. Videre viser analysen at bruk av årlige datapunkter ikke tilstrekkelig hensyntar den sesongmessige avhengigheten som observeres i vindkraftproduksjonen, og heller ikke markedsprisene basert på sesongvariasjonen observert i vannkraftdominerte kraftmarkeder. En annen vurdering basert på resultatene er at vindkraftprodusenten stort sett byr under forventet produksjon for å unngå høye straffekostnader, noe som viser at det kan være måter å utnytte markedet for å forbedre budpraksisen, for eksempel ved felles planlegging av vind- og vannkraft. Casestudien konkluderer med at funksjonaliteten til den utviklede *vindoptimeringsmodellen* har vist seg å være effektiv.

Preface

This master's thesis is written at the Norwegian University of Science and Technology (NTNU) in the Department of Electrical Energy. The authors are a part of the MSc Energy and Environmental Engineering program. The project was developed through the research teams Power System Operation and Analysis (PSOA) and Electricity Markets and Energy System Planning (EMESP) at the Department, in collaboration with researchers in the field of hydro- and windpower in SINTEF Energy. The thesis explores the potential for wind to interact in various power markets and adapts a short-term hydropower scheduling tool for wind farm operation scheduling. A project thesis covering a literature review and preliminary market analysis was conducted for the course *TET4510 "Electric Energy and Energy Systems"*, and functions as preparatory work for the background sections in this master thesis.

We chose this topic for our master thesis as the Norwegian power system has been historically dominated by hydropower, affecting the focus in many of our courses during our studies. We wanted to learn more about windpower and how it affects the power system and power markets, and a thesis coupling these two would be a great learning experience. The increased focus on windpower globally has also been a great motivation throughout this year. Both SINTEF and the Department have been great supporters of our work, and through them, we have been able to travel to Oslo to attend the Offshore Wind Conference 2022, participate with a poster in the DeepWind 2023 Conference in Trondheim, and write a conference paper in collaboration with Argonne National Laboratory for the SEST 2023 Conference. The latter work also gave us the opportunity to visit Argonne at their laboratory to learn more about the work they are doing and to write the paper together. This year has given us insight into the research field and provided us with great tools to continue our careers as Energy and Environmental engineers.

We want to thank our supportive supervisor Umit Cali for guiding us during this year. We would also like to thank our two co-supervisors Michael Belsnes from SINTEF Energy Research and Marthe Fogstad Dynge, a PhD candidate at NTNU, for valuable assistance and always being available to answer all our questions - big or small. This group has offered insightful advice and encouraging guidance in our weekly meetings. Per Aaslid and Bjørnar Fjellidal from SINTEF have also contributed to our collaboration by answering all practical questions regarding the use of SHOP, and we want to thank them for spending their time on this. We also want to mention Jonghwan Kwon and the team from Argonne National Laboratory for welcoming us to their laboratories and projects. Jonghwan Kwon has later been helpful in answering any questions regarding the scenario reduction algorithm used in this thesis. Additionally, we would like to thank our families for their support and a shoulder to cry on. Lastly, we could not have finished this thesis without the presence of our fellow students and friends, making the countless hours at school enjoyable and memorable throughout all five years of our master's program. We would not be here without you.

We would like to thank each other for a wonderful collaboration during this last year of our study. Having somebody to lean on during hard times in our research has made writing this master thesis a wonderful experience.

Contents

Preface	iii
Contents	v
Acronyms	vii
Figures	ix
Tables	xi
1 Introduction	1
1.1 Motivation and background	1
1.2 Project description	2
1.2.1 Project objectives	2
1.3 Chapter overview	2
2 Wind and Hydropower	5
2.1 Wind energy technology	5
2.1.1 Wind patterns	6
2.1.2 The basic principles of windpower	6
2.1.3 Modern wind turbines	7
2.1.4 Wind turbine technology and control	9
2.1.5 Wind turbine siting, system design and integration	10
2.1.6 Windpowers effect on the power grid	10
2.1.7 Offshore wind	11
2.2 Hydropower	12
2.2.1 The basic principles of hydropower	13
2.2.2 Hydropower in river systems	13
2.2.3 Hydropower with reservoir storage	13
2.2.4 Turbines used in hydropower	14
2.2.5 The limitations of operating turbines	14
2.2.6 Pumped hydro storage	15
3 Power Markets	17
3.1 The Nordic power market	17
3.2 Deregulated power markets	18
3.3 Day-ahead market and intraday market	19
3.4 Calculation of electricity price in a power pool	19
3.5 The merit order effect	19
3.6 Balancing market	20
3.7 Norwegian power generation	21
3.8 The evolution of cross border transmission cables	22
4 Scheduling Methods for Combined Hydro and Windpower Production	25
4.1 Optimization methods	25
4.1.1 Summary optimizing methods	26
4.1.2 Stochastic programming	26
4.1.3 Big M method	27
4.2 The basics of hydropower scheduling	28
4.2.1 Short term hydro scheduling	29
4.2.2 MILP and MINLP used in hydropower scheduling	30
4.3 SHOP	31

4.4	SHARM: Handling uncertainty in SHOP	33
4.5	Differences in stochastic and deterministic programming	34
4.6	Uncertainty in windpower production	34
4.7	Optimization tools	35
5	Methodology	39
5.1	Data collection	39
5.1.1	Geitfjellet Vindpark	40
5.1.2	Data from Nord Pool	40
5.2	Input scenario generation	41
5.3	Developing a <i>Wind Optimization Model</i> using SHOP	42
5.3.1	Procedure	42
5.3.2	The impact of up and down regulation prices	42
5.4	Flowchart	46
6	Results	51
6.1	Input scenario generation algorithm	51
6.1.1	365 scenario case at 4-5 PM	51
6.1.2	Yearly data points 25 and 50 scenario cases at 4-5 PM	52
6.1.3	Seasonal 25 and 50 scenario cases at 4-5 PM	54
6.1.4	Summary of all input scenario cases	57
6.2	Results from the <i>Wind Optimization Model</i>	59
6.2.1	Expected power production, power price and profit	59
6.2.2	The impact of up and down regulation prices, yearly data	61
6.2.3	The impact of up and down regulation prices at 4-5 PM, seasonal data	63
7	Discussion	67
7.1	Seasonal dependency	67
7.2	Benefits of including uncertainty	68
7.3	Number of scenarios included	70
7.4	Input values	72
7.5	Challenges with using SHOP	73
8	Conclusion	75
9	Future Work	77
9.1	Expanding to WHOP	77
9.2	Modifying SHOPs hydropower attributes	77
9.3	Extending the input data to the case study	79
9.4	Connecting wind and hydro production	79
9.5	Large scale energy storage	79
	Bibliography	81
A	Appendix	89
A.1	Optimization of Wind Scheduling for Improved Power Market Integration	89
A.2	V136-4.2MW Turbine	96
A.3	Input scenario generation for 8-9 AM and 12-1 PM across all yearly cases	98
A.3.1	365 scenario cases	98
A.3.2	Yearly 25 and 50 scenario cases for 8-9 AM and 12-1 PM	99
A.3.3	Seasonal 25 scenario cases for 4-5 PM for winter, spring and summer	101
A.4	Yearly model results from 8-9 PM and 12-1 PM for 25, 50 and 365 scenarios	103

Acronyms

- AC** Alternating Current. 11, 22
- ANL** Argonne National Laboratory. 35, 77
- ANN** Artificial Neural Network. 35, 36
- ARIMA** Auto-regressive integrated moving average. 35, 36
- BM** Balancing Market. 17, 20, 21, 40–42, 48, 49, 68, 70, 72
- CFD** Computational Fluid Dynamics. 35, 36
- DAM** Day-ahead Market. 1, 2, 19–21, 30, 33, 34, 39, 40, 42, 44, 45, 48, 49, 61, 63, 67, 68, 70, 71, 75, 77, 79
- DL** Deep Learning. 35, 36
- EU** European Union. 19, 22
- HVDC** High Voltage Direct Current. 11, 22
- IDM** Intraday market. 17, 19–21, 40, 41, 48, 49, 72, 75
- LP** Linear Programming. 27, 30, 37
- LTS** Long Term Scheduling. 28, 30
- MILP** Mixed Integer Linear Programming. 30–32, 34, 37
- MINLP** Mixed Integer Nonlinear programming. 30, 31
- MIP** Mixed Integer Programming. 30, 37
- MTS** Medium Term Scheduling. 28, 30
- NEMO** Nominated Electricity Market Operator. 17, 19
- NLP** Nonlinear Programming. 30, 37
- NREL** National Renewable Energy Laboratory. 35, 37
- NVE** The Norwegian Water Resources and Energy Directorate. 12, 21
- pdf** Probability Density Function. 8, 9
- PSH** Pumped-Storage Hydroelectric Power. 15, 28, 30, 79
- SD** Standard Deviation. 51, 60, 67

- SHARM** Short-term Hydro Application with Risk Modeling. 1, 2, 33–35, 40, 43, 74, 75, 79
- SHOP** Short-term Hydro Optimization Program. 1–3, 28, 31–35, 37, 39, 40, 42–45, 48, 68, 73–75, 77, 79
- STHS** Short Term Hydro Scheduling. 29–33, 48
- STS** Short Term Scheduling. 28, 30
- SVR** Support Vector Regression. 35, 36
- TSO** Transmission System Operator. 17–21, 40, 48
- UC** Unit Commitment. 29, 32, 48, 49, 77
- ULD** Unit Load Dispatch. 29, 32, 48, 49, 77
- VRE** Variable Renewable Energy. 1, 12, 15, 17, 19, 21, 22, 25, 29, 68, 77
- WHOP** Wind Hydro Optimization Program. 2, 39, 46, 48, 75, 77, 79

Figures

2.1	Production sources of electric power in Norway in 2022 [5], where "other energy sources" cover other renewables, fossil fuels, coal, gas and nuclear power. These renders almost equal share.	5
2.2	Global wind systems and their characteristics [7].	6
2.3	Surface roughness length for various terrains [11].	7
2.4	Most common wind turbine designs [8, p. 413].	8
2.5	Idealized power curve for a wind turbine [8, p. 437].	8
2.6	Power curves when a) increasing rotor diameter, and b) increasing generator size [8, p. 438].	9
2.7	A detailed overview of the principal components in most wind conversion systems [8, p. 415].	10
2.8	DFIG generator system with grid connection [10, p. 288].	10
2.9	An overview of the status of Nordic offshore wind farms [21].	12
2.10	The main components in a hydroelectric plant with reservoir storage [27].	14
2.11	Maximum efficiency as a function of non-dimensional turbine specific speed [N_{St}] for a Pelton, Francis and Kaplan turbine [24, p. 186].	15
3.1	A timeline of the electricity market [31].	17
3.2	Map over Nord Pools price zones [32].	18
3.3	A graph showing electricity demand, supply and the SMP	20
3.4	Illustration of the timeline for the different responses, based on the figure found in [46]. . .	21
3.5	The electrical connections between Norway and other countries. AC (red), existing HVDC (orange), HVDC under construction (green), HVDC currently under consideration (green stapled). [59]	23
4.1	A scenario tree with three stages and eight scenarios [64].	27
4.2	Scheduling toolchain for a decentralized model and a centralized model [59].	29
4.3	SHOP modules currently available [65].	32
4.4	The solution strategy in SHOP [65].	33
5.1	The process of generating scenarios for the <i>Wind Optimization Model</i>	39
5.2	Location of Geitfjellet Vindpark [107].	40
5.3	System created in SHOP	43
5.4	The physical system that the model is to represent.	46
5.5	Flowchart showing the solution strategy for the WHOP model. The black-marked SHOP part of the flowchart is based on the flowchart in [65].	47
6.1	Scatter plot showing input data for 365 scenarios at 4-5 PM. Each point is a scenario, each with the same probability. The colors represent the four seasons and the scenarios within the respective season. Extreme points are numbered.	52
6.2	Scatter plot showing input data for 25 scenarios at 4-5 PM. Each point is a scenario, and the size of the plot indicates its probability. The color represent the different scenarios.	53
6.3	Scatter plot showing input data for 50 scenarios at 4-5 PM. Each point is a scenario, and the size of the plot indicates its probability. The color represents the different scenarios.	53

- 6.4 Scatter plot showing input data for 25 scenarios at 4-5 PM for the fall months. Each point is a scenario, and the size of the plot indicates its probability. The color is the same as the fall color from the 365 plot. 54
- 6.5 Scatter plot showing input data for 50 scenarios at 4-5 PM for the winter months. Each point is a scenario, and the size of the plot indicates its probability. The color is the same as the winter color from the 365 plot. 55
- 6.6 Scatter plot showing input data for 50 scenarios at 4-5 PM for the spring months. Each point is a scenario, and the size of the plot indicates its probability. The color is the same as the spring color from the 365 plot. 55
- 6.7 Scatter plot showing input data for 50 scenarios at 4-5 PM for the summer months. Each point is a scenario, and the size of the plot indicates its probability. The color is the same as the summer color from the 365 plot. 56
- 6.8 Scatter plot showing input data for 50 scenarios at 4-5 PM for the fall months. Each point is a scenario, and the size of the plot indicates its probability. The color is the same as the fall color from the 365 plot. 57
- 6.9 Profit when running the *Wind Optimization Model* with 25, 50 and 365 scenarios from yearly data points at 4-5 PM. 62
- 6.10 A comparison of the profits from running the 25 and 50 scenario case in the *Wind Optimization Model* for data based on the winter season at 4-5 PM. 63
- 6.11 A comparison of the profits from running the 25 and 50 scenario case in the *Wind Optimization Model* for data based on the spring season at 4-5 PM. 64
- 6.12 A comparison of the profits from running the 25 and 50 scenario case in the *Wind Optimization Model* for data based on the summer season at 4-5 PM. 65
- 6.13 A comparison of the profits from running the 25 and 50 scenario case in the *Wind Optimization Model* for data based on the fall season at 4-5 PM. 66

- 7.1 Degree of filling for 2019. Values provided by reservoir statistics by NVE [47]. 69
- 7.2 Graph showing the yearly consumption [MWh] in price zone NO3. 69

- 9.1 Proposal for future additions to the WHOP tool. 78

- A.1 Scatter plot showing input data for 365 scenarios at 8-9 AM. Each point is a scenario, each with the same probability. The colors represent the four seasons and the scenarios within as shown in the bar to the right. Extreme points are numbered. 98
- A.2 Scatter plot showing input data for 365 scenarios at 12-1 PM. Each point is a scenario, each with the same probability. The colors represent the four seasons and the scenarios within as shown in the bar to the right. Extreme points are numbered. 99
- A.3 Scatter plot showing input data for 25 scenarios at 8-9 AM. Each point is a scenario, and the size of the plot indicates its probability. The color represent the different scenarios. 99
- A.4 Scatter plot showing input data for 50 scenarios at 8-9 AM. Each point is a scenario, and the size of the plot indicates its probability. The color represent the different scenarios. 100
- A.5 Scatter plot showing input data for 25 scenarios at 12-1 PM. Each point is a scenario, and the size of the plot indicates its probability. The color represent the different scenarios. 100
- A.6 Scatter plot showing input data for 50 scenarios at 12-1 PM. Each point is a scenario, and the size of the plot indicates its probability. The color represent the different scenarios. 101
- A.7 Scatter plot showing input data for 25 scenarios at 4-5 PM for the winter months. Each point is a scenario, and the size of the plot indicates its probability. The color is the same as the winter color from the 365 plot. 101
- A.8 Scatter plot showing input data for 25 scenarios at 4-5 PM for the spring months. Each point is a scenario, and the size of the plot indicates its probability. The color is the same as the spring color from the 365 plot. 102
- A.9 Scatter plot showing input data for 25 scenarios at 4-5 PM for the summer months. Each point is a scenario, and the size of the plot indicates its probability. The color is the same as the summer color from the 365 plot. 102

Tables

2.1	The sizes of hydropower plants according to NVE from [23].	12
4.1	Summary of optimization methods described in [61] and [60]	26
4.2	A table summarizing the differences between methods used for solving hydro scheduling problems.	31
4.3	Possible forecasting and simulation methods to predict wind speed and windpower generation.	36
4.4	An overview of optimization software tools used to schedule operation of renewable energy sources.	37
6.1	A summary of the input values for 25 and 50 scenario cases for all hours. The respective scatter plots are either presented in the Chapter 6 or in Appendix A.3.	58
6.2	Expected production, power price and profit for the yearly scenario cases at 8-9 AM.	59
6.3	Expected production, power price and profit for the yearly scenario cases at 12-1 PM.	59
6.4	Expected production, power price and profit for the yearly scenario cases at 4-5 PM.	60
6.5	Expected production, power price and profit for the seasonal scenario cases at 4-5 PM.	60
6.6	Standard deviation for the yearly 25 and 50 scenario cases across all hours.	60
6.7	Standard deviation for the seasonal scenario cases at 4-5 PM.	60
6.8	Results from running the <i>Wind Optimization Model</i> with 25 scenarios from data between 4-5 PM. The input data is shown in Figure 6.2.	61
6.9	Results from running the <i>Wind Optimization Model</i> with 50 scenarios from data between 4-5 PM. The input data is shown in Figure 6.3.	61
6.10	Results from running the <i>Wind Optimization Model</i> with 365 scenarios from data between 4-5 PM. The input data is shown in Figure 6.1.	62
6.11	Result from the <i>Wind Optimization Model</i> with both 25 and 50 input scenario cases based on data from the winter season at 4-5 PM.	63
6.12	Result from the <i>Wind Optimization Model</i> with both 25 and 50 input scenario cases based on data from the spring season at 4-5 PM.	64
6.13	Result from the <i>Wind Optimization Model</i> with both 25 and 50 input scenario cases based on data from the summer season at 4-5 PM.	65
6.14	Result from the <i>Wind Optimization Model</i> with both 25 and 50 input scenario cases based on data from the fall season at 4-5 PM.	66
7.1	Average degree of filling in reservoirs located in NO3.	70
A.1	Results from running the <i>Wind Optimization Model</i> with 25 scenarios from data between 8-9 AM. The input data is shown in Figure A.3.	103
A.2	Results from running the <i>Wind Optimization Model</i> with 50 scenarios from data between 8-9 AM. The input data is shown in Figure A.4.	103
A.3	Results from running the <i>Wind Optimization Model</i> with 365 scenarios from data between 8-9 AM. The input data is shown in Figure A.1.	104
A.4	Results from running the <i>Wind Optimization Model</i> with 25 scenarios from data between 12-1 PM. The input data is shown in Figure A.5.	104
A.5	Results from running the wind optimization model with 50 scenarios from data between 12-1 PM. The input data is shown in Figure A.6.	104

A.6 Results from running the *Wind Optimization Model* with 365 scenarios from data between 12-1 PM. The input data is shown in Figure A.2. 105

Chapter 1

Introduction

1.1 Motivation and background

In recent years there has been a substantial surge in the use of Variable Renewable Energy (VRE) sources like wind and solar power. This trend is driven by their ability to produce renewable energy with minimal climate impact, a crucial consideration as global energy demand continues to rise. However, the integration of large amounts of intermittent energy sources, like wind and solar power, into the power grid poses significant challenges, including the maintenance of a stable and reliable power supply, as well as the preservation of power frequency. [1]

The integration of wind and solar power has increased the importance of balancing supply and demand in real time, as the output of these sources can be unpredictable and fluctuate rapidly. This differs from more traditional power sources like thermal and hydropower which can schedule their production in advance. This has created a shift in the traditional power market, where scheduling has been dominantly decided in the Day-ahead Market (DAM) sometime before production [2]. As a consequence, divergent pricing has emerged across different power markets, compelling power producers to adjust their participation. Effective scheduling becomes a critical factor, as producers must adapt their operations to the requirements and conditions of each power market.

Short-term Hydro Optimization Program (SHOP) is a cutting-edge optimization tool developed by SINTEF, a leading research organization in Scandinavia. It is specifically designed to optimize hydropower production, one of the world's most important renewable energy sources. By using advanced algorithms and mathematical modeling techniques, SHOP can determine the optimal operating conditions for hydropower plants, considering factors such as water inflow, energy demand, and environmental regulations. It can help operators to find the most efficient way to balance energy production with other requirements in the hydropower system, such as flood control and ecosystem management. Overall, SHOP is an invaluable tool for hydropower producers, providing them with the ability to make informed decisions that can significantly improve the efficiency and sustainability of their operations. The incorporation of power markets into its optimization is also one of the key features that make SHOP a powerful tool for hydropower producers looking to optimize their operations and increase their profitability. SHOP can provide decision support before and during the establishment of the DAM prices. Decision support can also be provided for the regulation market and decision support for when unexpected events occur. [3]

Short-term Hydro Application with Risk Modeling (SHARM) is an extension to SHOP that allows the hydropower producer to account for the uncertainty in inflow and DAM prices. The goal of this extension is to more accurately schedule hydropower production in a future power market that has an increased penetration of renewable energy sources like solar and wind [4]. Both the integrated optimization with power markets and the possibility to optimize production with regard to uncertainty in price and inflow data are functionalities that can be incorporated into combined windpower scheduling.

Because of the price volatility experienced in today's power market, it is a clear benefit for windpower

producers to explore the possibilities of participating in multiple markets. Utilizing SHOP with the SHARM extension, which has power market interaction incorporated, could benefit the windpower producers when evaluating their profits while considering uncertainty in both power market prices and windpower production. A *Wind Optimization model* in SHOP is therefore created in this thesis to find the optimal bid for the windpower producer into the DAM.

1.2 Project description

State of problem:

Integration of Renewable Energy Sources into Electricity Markets via Optimized Wind Farm and Hydropower Scheduling

The master thesis aims to continue the work done in the project thesis in the fall of 2022. The thesis' main objective is to utilize methods in the SHOP tool created by SINTEF to develop a wind optimization model, that could help develop a joint Wind Hydro Optimization Program (WHOP) in the future. This initial *Wind Optimization Model* is to be tested in a case study. In addition to providing a *Wind Optimization Model* and a first structure proposal for the WHOP tool, this thesis will provide a literature analysis of the basic principles of windpower, hydropower, power markets and optimization methods for production scheduling. These chapters are drawn extensively from the project thesis.

This master thesis has gathered information on historical market prices, production, and consumption in the Nord Pool price zone NO3, in order to use the SHOP tool to create the *Wind Optimization Model*. This region was picked for the thesis since hydropower traditionally has dominated the area. Additionally, a new wind project of multiple wind farms, Fosen Vind DA, started production in 2020, significantly increasing the penetration of windpower in the NO3 price zone. To test the functionality of the developed *Wind Optimization Model*, a case study based on the Geitfjellet Vindpark is conducted in this thesis, also gathering relevant data concerning wind speed and technical specifications of the wind turbines. The methodology will therefore highlight the process by giving insight through input data processing through a scenario reduction algorithm, code development and flowcharts. The case study investigates the impact of the up-regulation prices on the optimal market bid for the windpower producer.

1.2.1 Project objectives

This master thesis contributes with the following:

- Literature review of the basic principles of windpower, hydropower, the Nordic power market and optimal scheduling methods.
- Documenting and demonstrating the use areas of SHARM, SINTEF's extension for stochastic modelling in SHOP.
- Development of a *Wind Optimization Model* that integrates market bidding and optimal scheduling practices using the SHOP environment.
- Creating an initial proposal for the structure of a hybrid wind-hydro scheduling tool (WHOP) by expanding the current hydropower scheduling model (SHOP) through the incorporation of the developed *Wind Optimization Model*.
- Techno-economic case study of the *Wind Optimization Model* for multiple scenarios aided by a scenario reduction algorithm.
- Recommendations for future work regarding extensions to the techno-economic study and further development of the SHOP tool.

1.3 Chapter overview

This master's thesis is divided into multiple chapters for easier comprehension. The background chapters address the necessary theory to cover this thesis's objectives. All chapters are organized as follows.

Chapter 1 - Introduction

The introduction emphasizes the context and driving motives behind the masters thesis. Along with the objectives of the master project, the chapter also includes a description of the problem being addressed.

Chapter 2 - Wind and Hydropower

This chapter begins with an introduction to wind energy technology and its fundamental theoretical concepts, including wind patterns and offshore wind. A similar review of the basic principles of hydropower technology is provided, covering hydropower with and without storage.

Chapter 3 - Power Markets

Theory regarding the general function of power markets, as well as the Nordic power market and its development is reviewed. This chapter ends by looking at trends seen in the Norwegian power market and the evolution of cross-border transmission cables connected to Norwegian price zones.

Chapter 4 - Optimization and Scheduling Methods

This chapter will briefly give an introduction to general optimization methods before going into the state-of-the-art methods for hydropower planning for short-term scheduling with an emphasis on the SHOP tool developed by SINTEF. Lastly, optimization programs for power system planning and operation will be investigated and presented, comparing them to the SHOP program.

Chapter 5 - Methodology

The master thesis looks into ways to expand the SHOP tool so that windpower output may be scheduled as efficiently and economically as possible. This chapter will give the methodology for achieving the goals through data collection, the development of the *Wind Optimization Model* and a flowchart outlining the suggested strategy for enhancing joint wind and hydropower operations.

Chapter 6 - Results

The results from the scenario reduction algorithm and the results from the *Wind Optimization Model* are presented based on both yearly and seasonal scenario data. Calculations of expected values and standard deviation are also performed. Initial comments are made.

Chapter 7 - Discussion

The identified topics in the thesis and result section are discussed, and the limitations and areas of improvement are identified. The focus of the discussion is on seasonal dependency, benefits of the model of including uncertainty, inaccuracies in the model's input values and limitations in SHOP. Additionally, the included number of scenarios and their impact on the model will be discussed.

Chapter 8 - Conclusion

The conclusion summarizes the findings in the results and discussion and emphasizes the contributions of this master thesis.

Chapter 9 - Future Work

Future work for possible research papers and further project and master thesis' work are identified and specified.

Chapter 2

Wind and Hydropower

Norwegian power production has the highest proportion of renewable energy in Europe, resulting in low greenhouse gas emissions. This renewable energy production has historically consisted of hydropower but has recently met a growing amount of windpower [5]. It can be seen in Figure 2.1 that the penetration of windpower production in the Norwegian power system in 2022 was at 12%. Learning how these energy sources function together is therefore crucial for Norway's future of energy production. The following theory sections on the technology of wind and hydropower are taken from the specialization project report [6] written by the authors, with the exception of Section 2.2.5.

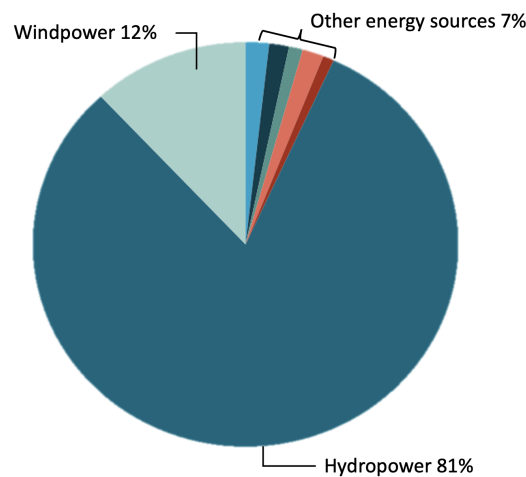


Figure 2.1: Production sources of electric power in Norway in 2022 [5], where "other energy sources" cover other renewables, fossil fuels, coal, gas and nuclear power. These renders almost equal share.

2.1 Wind energy technology

Understanding the basic principles of windpower generation is essential to this master thesis. This section emphasizes on the topics most relevant for the continuation of this thesis, some of them being the basic principles of windpower production, wind turbines and their characteristics, control and siting. Lastly the section will touch briefly on offshore wind globally and in Norway.

2.1.1 Wind patterns

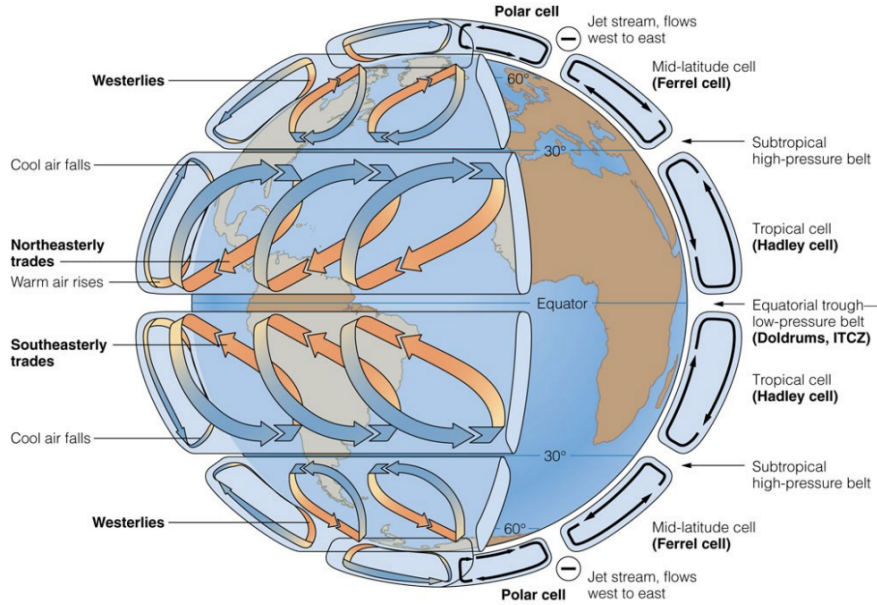


Figure 2.2: Global wind systems and their characteristics [7].

Wind as a phenomenon is a result of uneven distribution of heat over geographical locations caused by the sun [8]. The earth is divided into three circulation cells on both sides of the equator, covering approximately 30° each to the Poles [9]. These are the Hadley, Ferrel, and Polar cells, as can be observed in Figure 2.2 [7]. In addition, the cells have prevailing wind belts associated with them; the trade winds, westerlies and polar easterlies, respectively. The transport of air masses from the equator to the poles, and the opposite, cause the pressure differences that drive the continuous wind circulation. The latitudes where two cells and prevailing wind systems meet, at 0° , 30° and 60° North and South, are called convergence zones. These zones are characterized by their lack of prevailing winds. The doldrums at 0° and horse latitudes at 30° have calm and variable winds, while the zone around 60° is unstable and highly wind-prone. The Nord Pool price zone NO3 lies in this area, at $62 - 65^\circ$ N. [9]

2.1.2 The basic principles of windpower

Power from wind [W] can be thought of as the rate at which air particles with a certain amount of energy pass through an area A [m^2]. This is shown in Eq. (2.1) where ρ is air density [kg/m^3], v is wind speed [m/s] and C_p is a coefficient of performance of the wind turbine. Because it is theoretically and practically impossible for the wind turbine to capture all the kinetic energy in the wind, the C_p is determined by the Betz limit. The maximum possible energy extraction is defined to be 0.593 [10, p. 284].

$$P_w = \frac{1}{2} \rho A v^3 C_p \quad (2.1)$$

It is important to observe that the produced power is cubic with wind speed, meaning that the power produced is sensitive to changes in wind speed. Wind speed is highly dependent on the friction to the surface of the earth, also known as surface roughness length, as given in Figure 2.3.

This surface roughness, z_0 [m], is often used for calculating the wind speed v_2 [m/s] at desired hub height z_2 [m]. Eq. (2.2) [11] shows how this is calculated.

$$\frac{v_2}{v} = \frac{\ln\left(\frac{z_2}{z_0}\right)}{\ln\left(\frac{z_1}{z_0}\right)} \quad (2.2)$$

Terrain Description	Surface lengths (m)
Very smooth, ice or mud	0.0001
Calm open sea	0.0002
Blown surface	0.0005
Snow surface	0.003
Lawn grass	0.008
Rough pasture	0.01
Fallow field	0.03
Crops	0.05
Few Trees	0.10
Many trees, few buildings	0.25
Forest and woodlands	0.5
Suburbs	1.5
City center, tall Buildings	3.0

Figure 2.3: Surface roughness length for various terrains [11].

Here z_1 [m] represents the surface anemometer height, often standardized to 10 meters [8, p. 452], and v [m/s] the wind speed. It can be observed that for a higher z_0 , the wind speed at hub height z_2 will decrease.

In addition to the friction of the surface, [8, p. 426-429] mentions that the air density ρ gets corrected by the temperature and altitude. By rewriting the ideal gas law for an air mass with a molecular weight (M.W.) they get

$$\rho = \frac{p \cdot M.W.}{RT} \quad (2.3)$$

From Eq. (2.3) it can be observed that air density is inversely proportional to temperature and altitude. Eq. (2.1) showed that air density and power in the wind have a linear relationship. By looking at the two equations, it can be concluded that power extracted from the wind will also depend on the air density and altitude. This is a crucial characteristic to consider when planning a wind farm.

2.1.3 Modern wind turbines

The authors of [8, p. 413] and [12, p. 2-4] classify the turbines that capture the energy in the wind by their axis around the turbine rotor blades, as presented in Figure 2.4. Most wind farms use the upwind Horizontal Axis Wind Turbine (HAWT) technology as it delivers more power and operates more smoothly compared to other turbine technologies. However, these turbines require complex yaw control to keep the blades facing the changing wind direction while decreasing the wake effect for downstream turbines [8, p. 413-415]. The advantage of the Vertical Axis Wind Turbine (VAWT) is that yaw control is unnecessary because it is designed to accept and utilize wind from all directions. Despite this, the VAWT has not been accepted in the market due to fatigue and stress issues on the blades [12].

The importance of a wind turbine's performance characteristics, more specifically the power curve, is highlighted in both [8, p. 433-440] and [13]. Figure 2.5 displays a general idealized power curve. This technical information provides insight into the amount of electricity the turbine can produce at various wind speeds [13]. Production will be zero for winds below the cut-in wind speed V_C and will follow Eq. (2.1) for winds between V_C and the rated wind speed V_R . P_W will be equal to the generator's rated power at wind speeds between V_R and the fixed wind speed V_F , and this is the ideal area. The turbine must furl or halt operation if the wind speed exceeds V_F . This prevents overcompensation causing fatigue and stress to the mechanical equipment like the turbine and the power converters. Where the values of the different wind speeds lays will vary from turbines and are specified in the technical information.

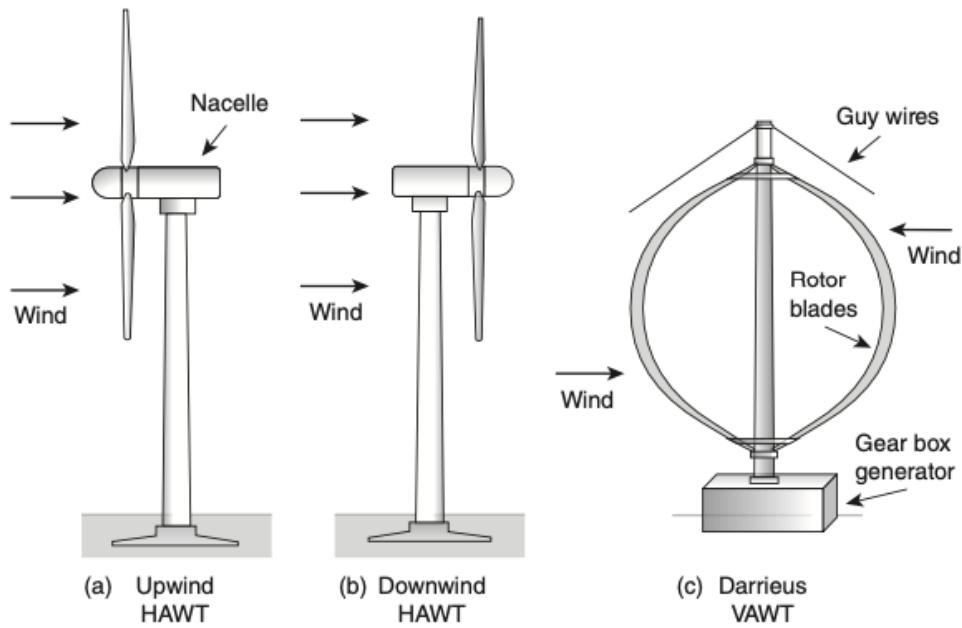


Figure 2.4: Most common wind turbine designs [8, p. 413].

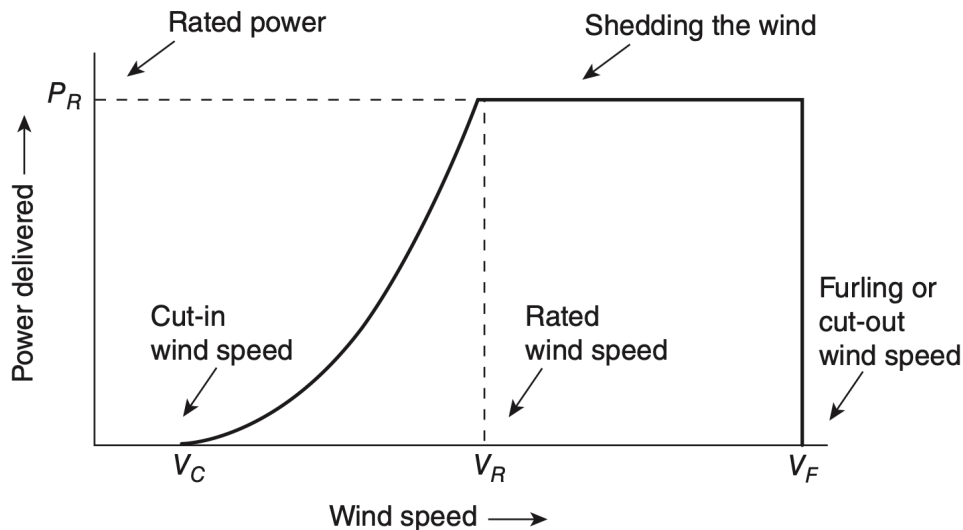


Figure 2.5: Idealized power curve for a wind turbine [8, p. 437].

Figure 2.6 in [8, p. 438] demonstrates the impact of changing the rotor diameter and generator size on the power curve. By increasing the rotor diameter, V_R is shifted to the left, making it possible to harness energy at rated power for lower wind speeds. A larger generator increases the rated power P_R and shifts the V_R to slightly higher wind speeds. These are important aspects to evaluate when planning a wind farm depending on weather characteristics and desired power output. The surrounding area can also limit the size of turbines and generators due to transporting and maneuvering, which needs to be considered. Additionally, the generator's size and the blades' length also affect the cost, and there will be a need to perform a cost-benefit analysis.

Another important factor is the cumulative statistical distribution of the wind speed, often characterized by Weibull statistics and the Weibull Probability Density Function (pdf), Eq. (2.4). Histograms are a common way of visual representation. [8, p. 443-454]

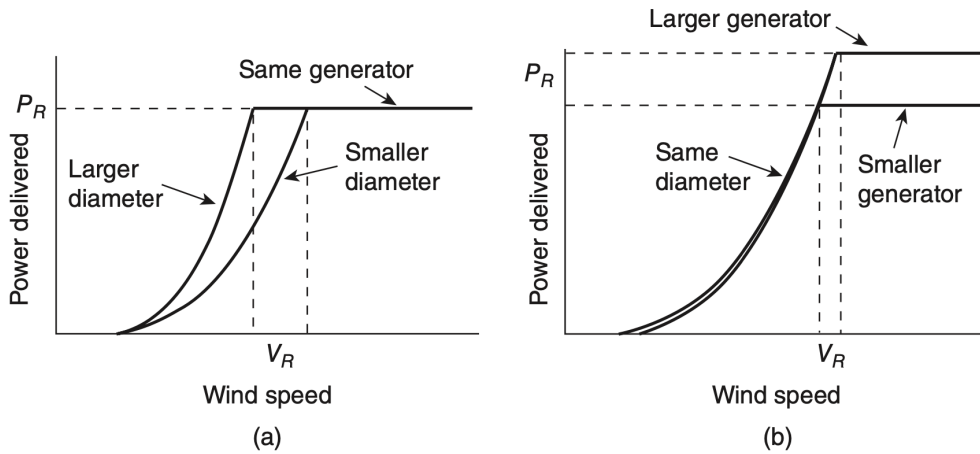


Figure 2.6: Power curves when a) increasing rotor diameter, and b) increasing generator size [8, p. 438].

$$f(v) = \frac{k}{c} \left(\frac{v}{c}\right)^{(k-1)} \exp\left[-\left(\frac{v}{c}\right)^k\right] \quad (2.4)$$

Here k and c are the shape and scale parameters, respectively. As presented above, an ideal wind farm site should have fairly consistent periods of wind above cut-in wind speeds to extract the energy in the wind. Such a shape is characterized by setting $k = 2$ and has its own name, Rayleigh pdf. This is also the assumed approach when the wind distribution of a potential wind site is unknown. The Rayleigh pdf is shown in Eq. (2.5). [13]

$$f(v) = \frac{2v}{c^2} \exp\left[-\left(\frac{v}{c}\right)^2\right] \quad (2.5)$$

Average windpower is another factor that could be interesting to evaluate for a potential wind site. Continuing on the assumption of Rayleigh pdf, the average wind speed becomes [8, p. 448-450]:

$$\bar{v} = \int_0^{\infty} v \cdot f(v) dv = \int_0^{\infty} 2\left(\frac{v}{c}\right)^2 \exp\left[-\left(\frac{v}{c}\right)^2\right] dv = \frac{\sqrt{\pi}}{2} c \quad (2.6)$$

2.1.4 Wind turbine technology and control

A detailed overview of the principal components in most wind energy conversion systems can be observed in Figure 2.7. The most important components will be discussed in this section. Conventional power systems like gas, coal and hydropower use synchronous (fixed speed) generators, which provide system stability through natural inertia. However, most grid-connected wind turbines do not usually use these types of generators as they are unable to handle the turbulent frequency of wind energy production. Ref. [10] explains that this is because constant speed causes stiff coupling between the generator and grid which makes the produced transient torque in the turbine drive shaft cause mechanical stress on the gears. Eventually, this leads to reduced system stability and reliability. To avoid this, a Doubly-fed Induction Generator (DFIG) is commonly used. The structure of such a system is shown in Figure 2.8, where 1:n specifies the ratio of the gear. [10, p. 287-289]

According to [14, p. 145-159] and [12, p. 328-334], the rotor speed and power capture can be controlled. The goal is to maximize energy production, minimize operation and maintenance costs, reduce wake effects and ensure safe turbine operation. There are several ways to do this. Pitch regulation controls the

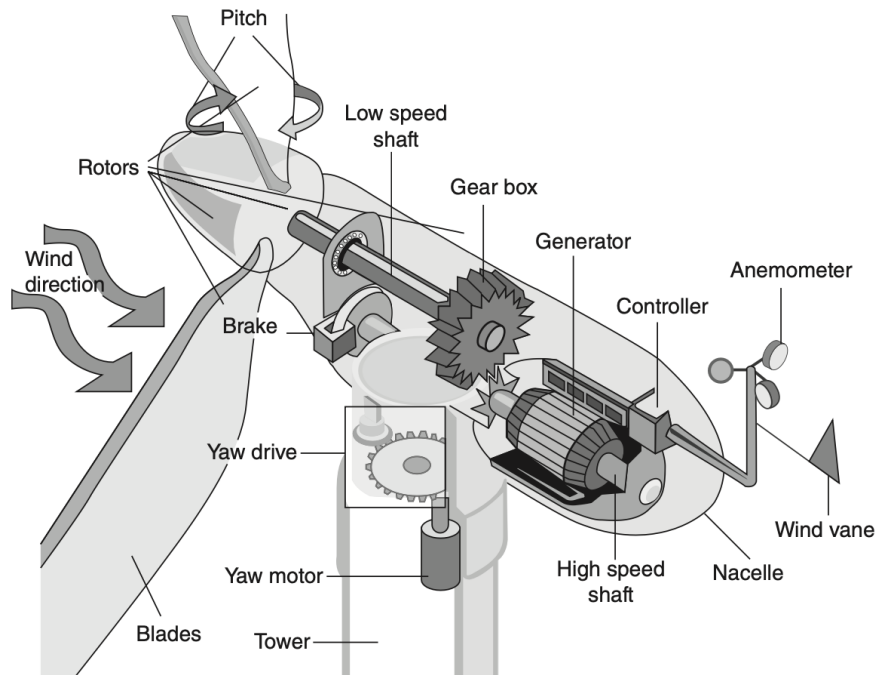


Figure 2.7: A detailed overview of the principal components in most wind conversion systems [8, p. 415].

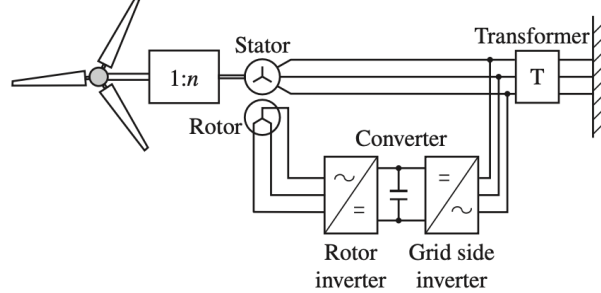


Figure 2.8: DFIG generator system with grid connection [10, p. 288].

blade angle, hence the wind capture, and can be done individually for each blade or collectively. Yaw angle control involves the alignment of the turbine head into the wind direction. This control measure is also a common way to deflect wakes for downstream turbines in a wind farm by slightly misaligning the angle between wind direction and yaw angle from the orthogonal standard.

2.1.5 Wind turbine siting, system design and integration

There are many different aspects to evaluate when deciding the location, system design, grid integration and topology for a wind farm. As shown in Figure 2.3, a smooth surface is desired to achieve high and stable winds to produce as much energy as possible. Wind speed and direction may also vary due to local terrain. Additionally, the power producer wants to minimize wake losses created by the up-stream turbines upwind by spacing them at an appropriate distance from each other. This also avoids wake-affected efficiency losses and mechanical fatigue on turbines downwind. Considering these two mentioned necessities, most wind farms, at least onshore, do not have a geometric park design. [12]

2.1.6 Windpower's effect on the power grid

Windpower is known to have an intermittent generation that is hard to predict because of weather conditions. This results in windpower plants posing a threat to system security if one compares it with more

conventional plants. Scheduling methodologies are currently based on minimizing operation costs subject to system security. To implement the optimal generation mix in a system with windpower, one must consider essential factors such as production costs, environmental costs and emissions. These factors usually work against each other, so this means that one would need to find the optimal combination of the amount of these factors. [1]

It has been shown that a low penetration level of wind generation can improve the economic, environmental and security performance of a system without system reinforcement if generation is carefully scheduled. The study referenced in [1] shows the impact on cost, emissions and security violations when increasing wind penetration in a power system. The analysis shows that the security performance of the system improved after introducing a small amount of windpower into the grid. However, the simulations had a maximum wind penetration rate of 5.37% and it is unknown if a more significant penetration rate would have a negative effect. Especially on system security since a higher penetration would mean higher intermittency in the system.

2.1.7 Offshore wind

There are many advantageous aspects with offshore windpower making it increasingly more common. Most importantly, compared to onshore winds, offshore winds are typically stronger and more reliable. There are many reasons for this, including the lack of geographical and topological variances causing the wind to divert. Additionally, the smooth surface offshore means there is very low friction, as can be observed in Figure 2.3. This lets the winds stay at a consistently higher speed than would be possible onshore. Changing terrain and local wind influences also increase turbulence intensity and risk of fatigue damage, which can be avoided offshore. There are also significantly fewer planning issues related to the environmental impacts, although there are still some issues related to life below the water surface and the fishing industry. These strong winds and reduced impacts have allowed the turbines to increase in size, efficiency and capacity factor far past what is functional onshore, enabling even more energy to be captured. [12, p. 403-409]

However, many considerations in offshore windpower differ from onshore. The long transmission lines are one of them. Long Alternating Current (AC) cables have an increased risk for electrical losses caused by reactive effect, while the long High Voltage Direct Current (HVDC) cables have a much higher cost. There are also foundational issues offshore, regarding bottom-fixed or floating turbines, depending on the water depth. Operation and maintenance costs are also higher and need better planning as wind farm location is far from land and in areas of more extreme weather. This also means that compared to onshore wind farms, there might be longer periods where the turbines need to furl the wind to avoid mechanical stress and damage. [12, p. 403-409]

Offshore wind in Norway

Any type of electricity generation on the Norwegian territorial sea and the continental shelf is only subject to regulation by the Norwegian Government, according to the Norwegian Offshore Energy Act of 2010 [15]. This indicated that any areas set aside for production must first undergo impact and license reviews by the government. Since then, Tampen, Utsira Nord, and Sørilige Nordsjø II have all been opened. The partners of the two oil and gas platforms, Snorre and Gullfaks received the first, Tampen, with Equinor receiving the largest partner share of 47%. The wind farm, which goes by the name Hywind Tampen, began production from its first turbine in November 2022 and will be the largest floating wind farm in the world when fully completed [16].

The Norwegian government declared in early December 2022 that they planned to tender phase one at Utsira Nord and Sørilige Nordsjø II by the end of 2023's first quarter [17]. The government announced the opening of the application period for offshore wind projects in these areas in a new press release at the end of March 2023, with a deadline for applications set for the coming fall [18]. A press conference was conducted a month later, on April 25, announcing the identification of 20 new North Sea regions for

more research and impact evaluations for potential offshore wind projects [19]. This is a component of the government's long-term aim to open up regions to generate 30 GW of offshore wind energy by 2040 [20]. Norway has a long history in the North Sea and on its continental shelf, from fishing to the recovery of oil and gas. The oil and gas partners excellent technological proficiency in floating offshore constructions has given the Norwegian government tremendous ambitions to become the industry pioneer in floating wind turbine technology. [20]

Figure 2.9 depicts the existing and planned offshore wind activity in the Nordic countries. Utsira Nord and Sørilige Nordsjø II are located south-west of Norway.

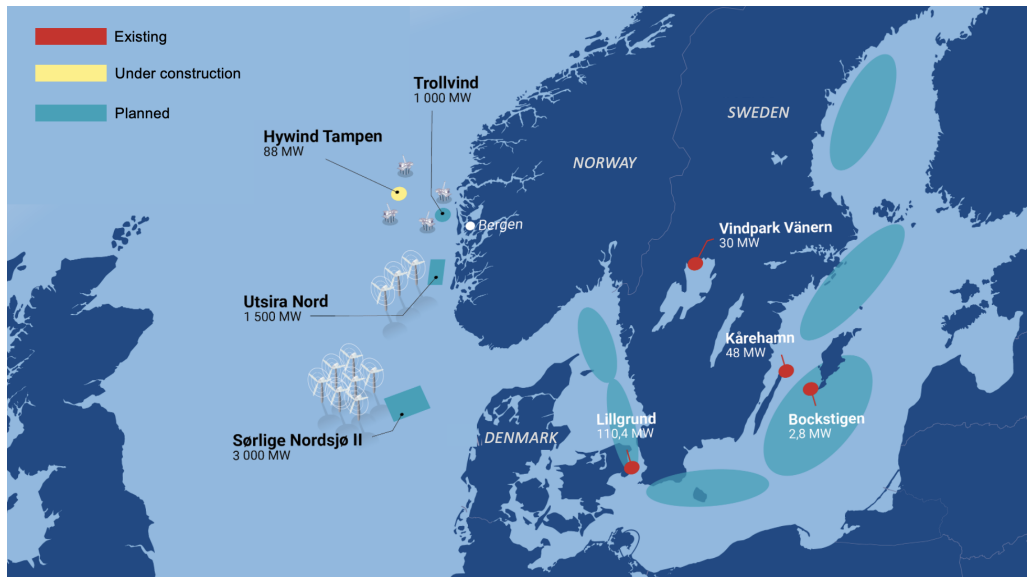


Figure 2.9: An overview of the status of Nordic offshore wind farms [21].

2.2 Hydropower

Hydropower makes up for about 16.5% of the world's energy production and is the biggest producer of renewable energy [8, p. 491]. In Norway, almost 90% of power generation comes from hydropower [22]. Compared to other renewable energy sources, hydropower is a much more flexible resource. This is in contrast to other unpredictable VRE resources like windpower because it has the ability to store energy, making it possible to schedule energy production to a greater degree. It can also deliver a baseload, provide spinning reserve and provide peaking power. This helps to maintain the system's stability and frequency response. Types of hydro plants can broadly be divided into run-of-the-river plants with no storage capacity and plants with conventional reservoir storage. [8, p. 491-492]

Conventional hydropower plants are also usually separated by their size. The Norwegian Water Resources and Energy Directorate (NVE) separates the hydro plants after the sizes described in Table 2.1.

Table 2.1: The sizes of hydropower plants according to NVE from [23].

Name	Production size
Small power plants	< 1 MW
Medium power plants	1-10 MW
Large power plants	10-100 MW
Very large power plants	> 100 MW

2.2.1 The basic principles of hydropower

For hydroelectric power, one uses the potential energy from water being stored at a certain height above the reference point. The reference point depends on what turbine type is used, but it is usually located at the water surface after the discharge from the turbine. This is called the tailrace area. The height between the original water level and the reference level is called the gross head. Flowing fluid also has flow energy created by the fluid's pressure. Lastly, fluids can obtain kinetic energy by flowing at a certain speed. These three energy types accumulate to mechanical power per unit mass shown by Eq. (2.7). [24, p. 165-171]

$$e_{mech} = \frac{P}{\rho} + \frac{V^2}{2} + gh \quad (2.7)$$

Where:

- e_{mech} : Mechanical energy [J/kg]
- P : Pressure in the penstock [N/s^2]
- V : Velocity of the water [m/s]
- ρ : Mass density of water [kg/m^3]
- g : Gravitational acceleration [m/s^2]
- h : Gross head [m]

During incompressible flows, the change in mechanical energy equals the change in potential energy. This is because the water pressure, density and velocity are identical at the reservoir's water surface and tailrace area. The first law of thermodynamics states that energy in a system can neither be created nor destroyed, just change to other forms [25]. Therefore, all the change in potential energy has converted into mechanical energy by going through a turbine that forms electrical power with the help of a generator. This is except for the energy losses in the turbine, generator and piping. To find the level of hydropower produced, one has to multiply the potential energy per unit mass by the mass flow rate of the water and the efficiency of the turbine and generator. The losses that come from piping depend on the smoothness of the pipe, the length, diameter and how straight the pipeline is. To account for these losses a dynamic head is used in the calculations called net head, instead of the original gross head. One can then rewrite Eq. (2.7) to Eq. (2.8). [24, p. 165-171]

$$P_h = Q \cdot \eta \cdot \rho \cdot g \cdot H_n \quad (2.8)$$

Where:

- P_h : Power produced by hydropower [W]
- Q : Flow rate [m^3/s]
- η : Efficiency of the turbine and generator [-]
- ρ : Mass density of water [kg/m^3]
- g : Gravitational acceleration [m/s^2]
- H_n : Net head [m]

2.2.2 Hydropower in river systems

Run-of-the-river plants are installed directly into the river and usually have a short or non-existent intake tunnel. The net head of the plant is therefore quite low and the power plant depends on a high volumetric flow rate. Some sources say that small hydro plants that lack storage possibilities, even if they have penstocks and high net head, belong in this category [8, p. 500-501], [24, p. 186-189], [26]. Run-of-the-river plants have a negligible impact on the ecosystem compared to manufactured dams and reservoirs. The investment cost of these plants is also smaller due to fewer construction costs regarding the building of a dam. These advantages come at the cost of having no storage capacity, and therefore no flexibility. [26]

2.2.3 Hydropower with reservoir storage

When constructing hydropower with reservoir storage, the biggest construction that has to be built is the dam. There are different types of dams, and the type is decided based on the topography of the area. When the dam gets built, precise calculations must be done on the forces that the dam is affected by,

simply because the consequences of a dam failure are massive. The water located in the reservoir enters an intake before it travels down the penstock to the turbine. The most common reaction turbine used is the Francis turbine, which works well on both low and high net heads and flows. The reservoir's water level will depend on the inflow, spillage and the water released to produce power. Spillage happens when the reservoir overflows, and to prevent this from damaging the dam, spillways are installed. For the hydropower producer, spillage is the same as lost revenue. This means that when scheduling the hydro production, the producer would try to minimize this spillage. Figure 2.10 shows the main components in the hydroelectric plant with reservoir storage. There are also systems with multiple reservoirs whose inflow depends on one another. [8, p. 491-501]

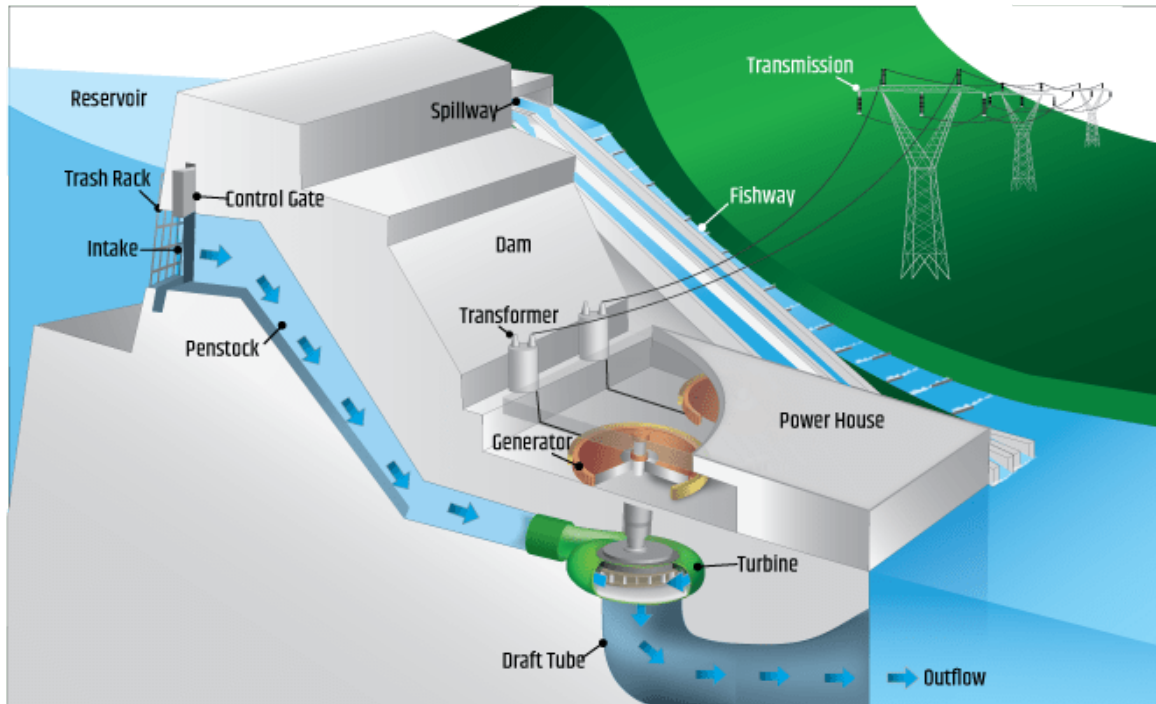


Figure 2.10: The main components in a hydroelectric plant with reservoir storage [27].

2.2.4 Turbines used in hydropower

The turbines used when producing hydropower can be divided into impulse and reaction turbines. The impulse turbine is known as the simplest type of turbine. A nozzle sends water jets at high speed on a wheel where the water is caught in bucket-shaped vanes making the wheel spin. This transfers energy to the turbine shaft. The most used impulse turbine is the Pelton wheel. A reaction turbine differs from an impulse turbine by filling the casing completely up with water and utilizing the kinetic energy and the water's pressure. A reaction turbine has to be submerged under the tailrace area to be able to utilize this pressure. The two most known reaction turbine types are Francis and Kaplan turbines. [24, p. 173-186]

Every turbine has a specific speed that characterizes the operation of the turbine and its optimal conditions. It also has a best efficiency point for a specific speed where the turbine works optimally. This information is used when deciding what turbine to use for a specific system. Figure 2.11 shows the efficiency curve of the three mentioned turbine types along the non-dimensional turbine specific speed N_{St} . [24, p. 185-186]

2.2.5 The limitations of operating turbines

Over longer periods, turbines used in hydropower production have a slow decline in performance as they get damaged. During low loads, turbines can be damaged by a process named cavitation. Cavitation happens when pressure variations in water can cause small cavities to form and implode. These cavities get

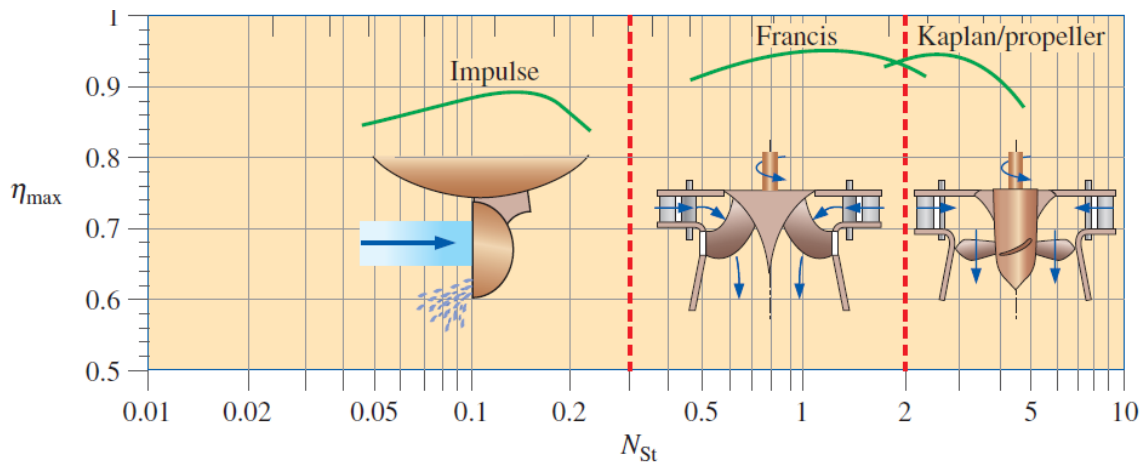


Figure 2.11: Maximum efficiency as a function of non-dimensional turbine specific speed [N_{St}] for a Pelton, Francis and Kaplan turbine [24, p. 186].

filled with liquid vapor that begins to boil locally because of pressure reduction. It is when the pressure rises above vapor pressure that the bubbles implode. This results in high-pressure shock waves that can cause significant damage to the turbine metal. [28]

Reaction turbines, like the Francis turbines, are more disposed to cavitation. During hydropower production, this process repeats itself many thousand times per second until the material eventually fails by fatigue. This process may also completely tear away certain parts of the turbine, such as the runner blades. While it is challenging to prevent cavitation in hydro turbines completely, it is possible to mitigate its effects to a level that is economically acceptable. [29]

2.2.6 Pumped hydro storage

Pumped-Storage Hydroelectric Power (PSH) can be produced by a hydropower plant that can pump water back into the reservoir by utilizing a pump. Using a reversible Francis as a pump and turbine is the most common. The penstocks running from the upper to the lower reservoirs can have a 2-way flow. Pumped hydro storage is especially profitable when the difference between peak and off-peak power prices are high. The pumped storage hydro plant then utilizes the low power prices to pump water back into the upper reservoir. They then have more power to sell when prices are high. Enough installed PSH would result in a flattened-out power peak during the day. Additional benefits of PSH are avoiding curtailment on VRE production like wind or solar. This can be done by utilizing the excess power produced by VRE, to pump hydro. When there is excess power from these energy sources, hydropower is usually not producing energy. [8, p. 501-503]

As mentioned in Section 2.2.1 there are some losses in energy during production. There are also losses in the pump when pumping the water up. These combined losses are represented by the round-trip efficiency. According to SINTEF, modern PSH plants can have a round trip efficiency of around 85% [30]. This efficiency represents how big the difference in power prices must be for PSH to be profitable while not including maintenance or investment costs. PSH can also make an additional profit from selling into the reserve market, mentioned in Section 3.6 [30]. Since the profitability of PSH depends on the normally volatile power prices, investment comes at a high risk.

Chapter 3

Power Markets

With the recent rise of VREs the traditional Nordic power markets must be reconsidered. Hydropower producers have a high degree of flexibility in their production and have participated in these markets for a long time, while windpower production is more challenging to predict because of the lack of storage capacity. The Nordic power market is therefore described in Section 3. This Power markets chapter is taken from previous work [6], except for Section 3.5.

3.1 The Nordic power market

Trading electricity between producer and consumer can be done in many ways. In the Nordic market, Nord Pool is the Nominated Electricity Market Operator (NEMO) and are responsible for merging the bids in the day-ahead spot market (Elsport) and the intraday market (Elbas). Selling or buying electricity could also be done by power purchase agreements. These agreements are usually long-term contracts between parties where the future price is set. Since the predictions made in the Intraday market (IDM) on power consumption and production can never be certain, there is also a need for a Balancing Market (BM) that functions short-term and corrects possible imbalances. This market is operated by the regions Transmission System Operators (TSOs), which is Statnett in Norway. For power trading, there is also a financial market operated by Nasdaq consisting of futures and other derivatives. The financial market aims to hedge against the risks that affect market participants from the volatility in the spot prices. [31]

A timeline showing when the use of different markets occurs is shown in Figure 3.1. The financial market will not be discussed further in this thesis.

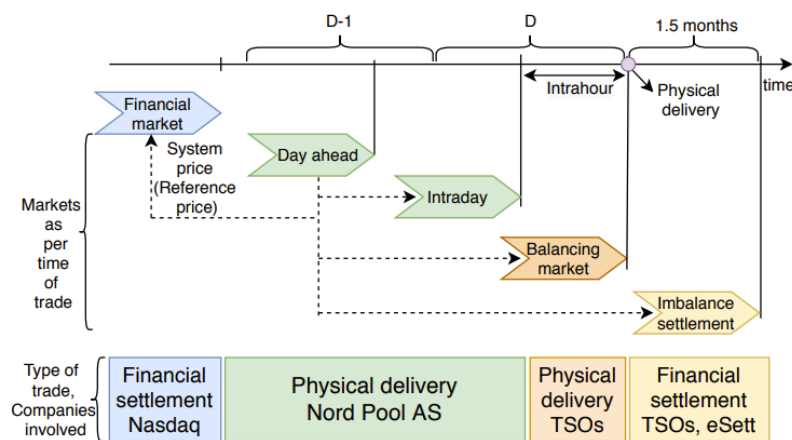


Figure 3.1: A timeline of the electricity market [31].

Nord Pool operates with 15 different market price areas shown in Figure 3.2. These zones are set by the local

TSO based on the transmission capacity. Between the zones, there is often power congestion and a maximum import and export have to be calculated. This results in different power prices in the different zones. How this price is set is further explained in Section 3.4. As seen in Figure 3.2, Norway, Sweden and Denmark have multiple price zones, while Finland and the Baltic countries have one price zone spanning the whole country. International cables have now opened the possibilities for increased trading with countries outside the Nordic market. This is covered in Section 3.8.

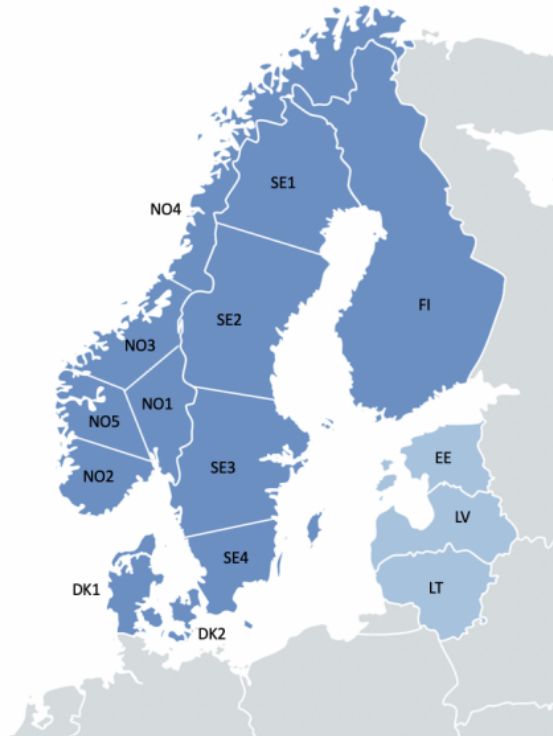


Figure 3.2: Map over Nord Pools price zones [32].

3.2 Deregulated power markets

A deregulated power market is a type of electricity market in which the generation, transmission, and distribution of electricity are managed by a network of independent entities rather than a single, centralized authority. The Nordic market is a deregulated power market [33]. Because deregulated power markets are based on the same assumption for a perfectly competitive market and market forces, they are able to provide consumers with potentially lower prices than a regulated market. This is because a perfectly competitive market is designed to find the most socio-economically optimal solution, meaning the solution that works best for society as a whole. Multiple conditions must be upheld for a market to be considered a perfectly competitive market. One of them is that there have to be multiple participants, and none of the participant can be of the size that they can exercise market power. A regulated power market works as a monopoly with an efficiency loss that hinders achieving the socio-economical optimum. In a regulated power market, the authority is typically a government agency or a utility company responsible for overseeing electricity production, transmission, and distribution to consumers. [34, p. 172-178]

3.3 Day-ahead market and intraday market

The DAM is a wholesale electricity market where the power prices for all 24 hours the following day are determined by competitive closed auctions. The bids for all 24 hours from buyers and sellers must be submitted before noon, 12:00 CET, the previous day. All participants must also define in what price area they are located. The local TSOs have to release the trading capacities for every trading area before 10:00 CET. For all 24 hours and each price zone, the prices are then calculated and released at 12:42 CET by Nord Pool [31]. The largest power volumes in the Nordic market are traded in the DAM. [2]

The Nordic power market gets more connected to the rest of Europe as more international cables get built, as will be described in Section 3.8. To couple the DAM bids that come from different regions in Europe, many regions TSOs and NEMOs have collaborated on a single day-ahead coupling (SDAC). SDAC aims to create more efficient utilization of power generation across Europe while also making trading more efficient. This is done by using a common algorithm called price coupling of regions (PCR) EUPHEMIA. The different NEMOs use this algorithm to calculate prices while taking cross-border capacity into consideration. As much as 98.6% of the European Union (EU)'s consumption is coupled. [35], [36]

The DAM works optimally for flexible generation sources like hydropower, where one can plan a set generation ahead of time. However, now that the penetration rate of VREs are increasing, it is more difficult to predict generation 12-36 hours from the bidding deadline. This prediction is made more accurate by using forecasting tools, but this does not guarantee precise power production information. This is why the importance of the IDM is now increasing. The IDM opens at 14:00 CET, two hours after the DAM closes, and closes 1 hour before the delivery time. Meaning that the producers now have a clearer picture of what the generation will be. It is also possible to correct the market if new information regarding outages or consumption is received. In Nord Pool's IDM it is possible to trade in 15 min, 30 min, hourly increments or other types of blocks. This is to provide flexibility to the market participants. It is possible to trade across 14 countries with Nord Pool's IDM. [37]

3.4 Calculation of electricity price in a power pool

An electricity pool works in a flowing manner: all the producers submit bids on how much energy they can produce in a time period. From all these different bids, one can create the market supply curve where the bids are ranked with increasing prices that are equal to their marginal costs. The demand for electricity is mainly inelastic because consumers often need power, and they are not willing to change their need for electricity based on the price. Instead of consumers submitting bids on how willing they are to pay, a forecast of the load is often used. This forecast creates the market demand curve, illustrated as a slightly tilted vertical line, as shown in Figure 3.3. An electricity pool is used in deregulated markets. [38, p. 49-86]

The point where these two functions meet is the market equilibrium. The demand and supply curve and the market equilibrium are illustrated in Figure 3.3. Only the bids from producers that bid in at a lower or equal price than the equilibrium price is accepted. The market clearing price is called the system marginal price (SMP), which is the price that the producers are paid per MWh produced, and this is the spot price that all the consumers pay per MWh consumed. The power plant that bids in at the SMP is the price setter. Renewable generation sources usually have low marginal costs since they are not dependent on fuel prices, but utilize natural resources. The plants that have a high marginal cost are known as peaking plants. These are expensive plants that only get utilized during times of high demand. The plants with low marginal costs get paid the same price as plants with higher costs. This is to encourage producers to bid in at their marginal cost so that there is an optimal use of the available resources. [38, p. 49-86]

3.5 The merit order effect

The growth of VRE sources, like wind and solar power, has changed how electricity prices are calculated in a power pool, described in Section 3.4. These energy sources depend on the availability of stochastic wind

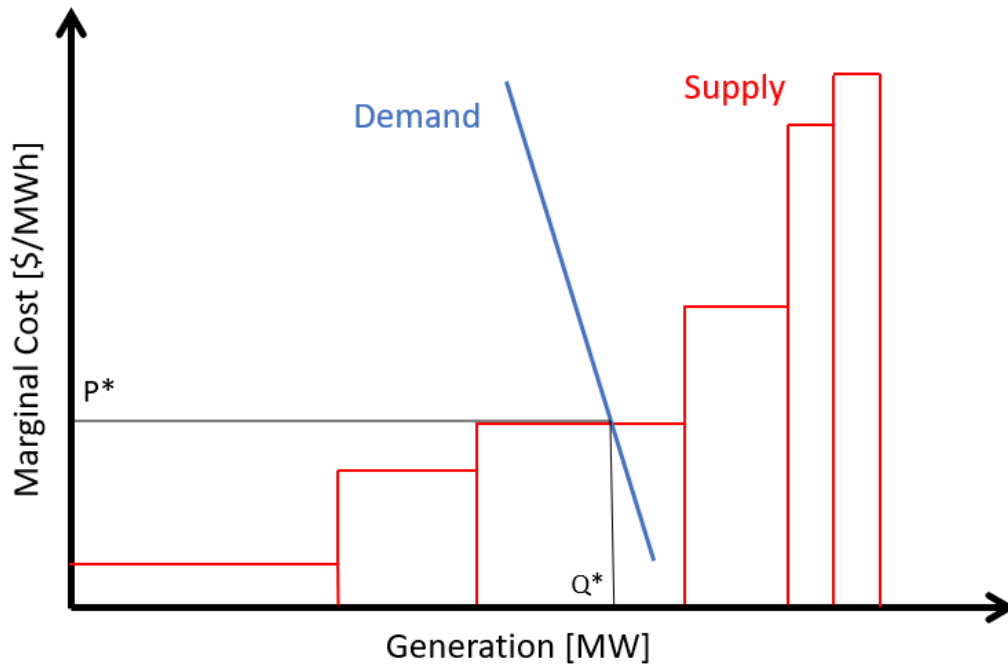


Figure 3.3: A graph showing electricity demand, supply and the SMP

speeds and solar radiation. They also have a very low variable cost since they are not dependent on fuel or human resources, making it favorable to produce even when the electricity price is low [39].

These low variable costs shift the supply curve, shown in Figure 3.3, to the right, something that results in lower electricity prices. This is known as the merit order effect. While hydro and nuclear power also possess low variable costs that contribute to the merit order effect, they lack the unpredictable production fluctuations seen in wind and solar power. Such unpredictability can lead to greater volatility in electricity prices, a phenomenon compounded by the intermittent nature of wind and solar production. The merit order effect results in an increase in consumer welfare and a reduction in investment returns for the power producer. The increased volatility also increases the risk for the investor and the long-term effects are still very uncertain. [40]

In numerous markets, negative electricity prices have been observed during high solar radiation and wind speeds. This is because government-support schemes make it profitable to produce even with electricity prices around zero. It is documented that this can not only happen during the night when demand is low but also during the day when demand is high. [41]

3.6 Balancing market

TSOs are responsible for ensuring an equal amount of consumption and production in the power grid at all times. The DAM and the IDM plan a certain amount of production and consumption in advance, but the TSOs use the BM to make sure it equals in real-time. The European market is considered balanced when there is a frequency band of 49.9 – 50.1 Hz [42]. The system's frequency decreases when the power grid is experiencing a lack of supply. This can not be tolerated for an extended amount of time and if the problem is left unattended, some customers will eventually be disconnected. If the grid experiences excess supply, one would observe a high frequency in the power grid and some producing units would have to be ramped down. Irregular frequency can be tolerated for short amounts of time so that the TSOs have enough time to ramp up or down supply. However, if the irregularity lasts for a long time, there is a risk of damaging different system components in the power grid. [43]

To handle these frequency irregularities, the TSOs manages a portfolio of frequency reserves. The frequency changes can come from malfunctioning equipment, sudden change in consumption or intermittent production. The latter is becoming more relevant with increasing VREs in the grid. TSOs can trade reserves with other Nordic countries TSOs. The BM in the Nordics is divided into three different reserves. These are primary reserves (FCR), secondary reserves (aFRR) and tertiary reserves (mFRR). The primary and secondary reserves are automatically operated in response to the changing frequency. Primary reserves are used if the imbalance lasts for some seconds, but if the changes last for several minutes, the secondary reserves are activated. This makes it so the primary reserves can be ready to handle new possible imbalances in frequency [2]. In Norway, the primary reserve is traded in two markets, D-1 and D-2. The D-2 market happens before the DAM and the D-1 market happens after to cover cross-border trading and other needs that may have appeared in the market. The Nordic countries TSOs have collaborated on a program called the Nordic balancing model (NBM). The main function of this program is to make trading within the BM more efficient and therefore enhance the common Nordic socioeconomic benefit [44]. The BM in the Nordic countries still have differences, making it more difficult to harmonize than the DAM and IDM. These differences are documented in [31]. One of the Nordic balancing models main objectives is to create a common Nordic market for aFRR trading.

If a fault in the system lasts longer than 15 minutes, the tertiary reserves are activated manually. The timeline for different frequency responses is shown in Figure 3.4. All Nordic countries are required to have tertiary reserves equal to the dimensioning error for their subsystem. In Norway, the dimensioning error is at 1200 MW and Statnett deems it necessary to ensure 500 MW additional tertiary reserves in the Norwegian power grid. This is to accommodate regional imbalances and bottlenecks [45]. Participants in the tertiary reserves market submit their bids into the TSO and if their bids get accepted, they get paid even if their resources are unused. They get paid to have their resources ready to produce on short notice if needed. Therefore these resources have to be power sources that can quickly ramp up and down [2]. The TSOs accept the tertiary reserves bids based on price, where in the power grid production is needed and if there is congestion.

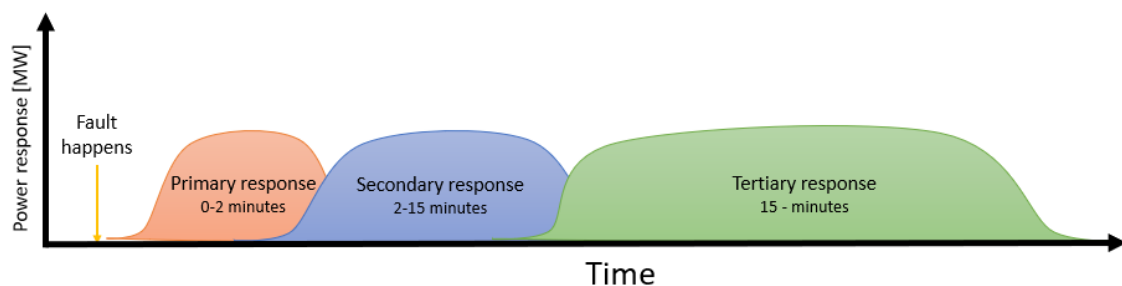


Figure 3.4: Illustration of the timeline for the different responses, based on the figure found in [46].

3.7 Norwegian power generation

Norwegian power production mainly consists of hydropower. This makes the electricity prices in Norway seasonally dependent on when there is much rainfall during the year and therefore, high water levels in the reservoirs. The water level is usually low in winter before it rises in spring when the mountain snow melts. This is shown by the reservoir statistics released by NVE in real-time [47]. During winter there also is a huge need for heating in Norway something that increases the load during this time and therefore subsequently the power prices. Norway has also been working on adding new power production capacity to the grid, most of which has been in the form of wind turbines. In 2020 86% of new capacity connected to the grid consisted of windpower [48]. A lot of this windpower was the Fosen Vind DA project.

Fosen Vind DA is a wind project located in Mid-Norway and consists of six wind farms that combined have the capacity of 1057 MW. This is the biggest land-based windpower project in Europe. The different

parks are located on the coast where there are good wind conditions and the wind parks are estimated to produce 2.7 TWh yearly [49]. As mentioned, historically the power production in Mid-Norway (NO3 zone in Figure 3.2) has been dominated by hydro production and wind has not had a significant penetration rate. However, mainly due to Fosen Vind, wind production in Mid-Norway has increased from 1.1 TWh in 2018 to 5.4 TWh in 2021 [50].

3.8 The evolution of cross border transmission cables

To enhance electricity trading between zones and countries, the power system needs sufficient transmission capacity. This is to prevent bottlenecks and congestion that result in high price peaks in the local market. As the penetration rate of VRE increases, so does the fluctuation characteristics that come with wind and solar power. If interregional transmission lines increase, the possibilities for efficiently operating these VRE sources also increase. Building transmission projects is complex and takes a long time to complete. Studies have shown that missing regulatory design and increasing coordination while creating institutional change might be required [51]. The European association for the cooperation of transmission system operators for electricity (ENTSO-E) releases a 10-year network development plan (TYNDP) every two years that describe what projects should be developed to reinforce the grid. They estimate that an additional 64 GW of cross-border capacity is needed by 2030 in the EU. [52]

From Norway, the first international cable was an AC connecting Nea in Mid-Norway to Järpströmmen in Mid-Sweden, and started its operation in 1960. This linked Nord Pools' present price zones, NO3 and SE2. The cable was originally built to supply the Stockholm area with excess power from the Norwegian hydropower system. However, the same year as the operation of the cable started, Norway experienced drought and a low degree of filling of reservoirs, and the benefit of cross-border transmission lines was brought to attention. This was the beginning of the cross-border transmission cables connecting Norway to the rest of Northern Europe. This specific cable has been one of the most recent points of debate in the current power price discussions as it enables the power to travel from north to south through Sweden, causing significant price differences between zones. [53], [54]

The most recent new international cables were put into operation in 2021. The first one is a HVDC cable called the North Sea Link. It is between Norway and England and has a capacity of 1400 MW [55]. The other one is called NordLink and is connected between Norway and Germany. This is also a HVDC cable and has a capacity of 1400 MW [56]. Both cables are connected to the NO2 price zone, a zone in Norway that often experiences a lack of supply [42]. The two cables are shown in Figure 3.5, a figure that also shows that Norway is connected to both the Netherlands and Denmark through HVDC cables. These are named NorNed and Skagerrak 1, 2, 3 and 4 respectively. See [57], [58] for further reading.



Figure 3.5: The electrical connections between Norway and other countries. AC (red), existing HVDC (orange), HVDC under construction (green), HVDC currently under consideration (green stippled). [59]

Chapter 4

Scheduling Methods for Combined Hydro and Windpower Production

The production and scheduling of renewable resources, in particular VREs, pose significant challenges. To address these challenges, a multitude of optimization methods have been developed and implemented in the industry. This chapter provides an overview of the most commonly employed optimization techniques, particularly those utilized in short-term hydropower planning. Additionally, existing software for power system planning is discussed, with a focus on their application to the optimization of renewable resource production and scheduling. The general optimization and application for hydropower planning were also covered in previous work [6] and remain mostly the same, with the addition of Section 4.1.3. Sections 4.5 and 4.7 have been added at the end and look more closely at stochastic programming compared to deterministic programming for renewable energy technologies, as well as existing optimization programs as an investigation of relevant software for this master thesis.

4.1 Optimization methods

One can use different types of optimization models to find the optimal solution to a problem. To utilize an optimization method, one first has to define the problem. What is it that the methods should optimize and what are the restrictions from achieving the optimal solution? An optimization model is a mathematical model representing the problem's essence. The problem describes a function that is to be maximized or minimized, this is called the objective function. To achieve this optimal value there are certain decisions that have to be made, these can be expressed as decision variables. The variables are often affected by a multiplicative factor represented by a coefficient. When working with energy production, typical objective functions are maximizing energy production, maximizing profit, or minimizing CO₂ emissions. There also have to be some constraints that restrict the values of the decision variables. These have to be formulated mathematically by the means of inequalities or equations. Constant values in the objective function and constraints are called parameters and these are decided outside the optimization problem. The parameters chosen in the model are not always certain, therefore one might be interested in what change would happen in the objective function if one parameter is changed. Doing an analysis of these consequences is called a sensitivity analysis. [60, p. 10-21]

In an optimization problem, there is a feasible region which is a collection of all feasible solutions. This is where the decision variables have values that do not cross any constraints. The feasible region is filled with possible solutions for the optimization problem, but this does not mean that the solution is optimal with the most favorable value of the objective function. It is possible for a problem not to have an optimal solution. This happens if the constraint leaves no feasible solutions or the objective function is unbound. This means that the objective value can be improved indefinitely, either negatively or positively. [60, p. 10-21]

4.1.1 Summary optimizing methods

Table 4.1 shows a summary of some basic optimization programming methods. It is also possible to combine these methods, e.g., mixed linear programming and stochastic dynamic programming. Power system optimization can utilize these methods to get the most optimal operation. It is essential to consider the specific functions and qualities of each tool to determine its suitability for a given scheduling problem. A comprehensive evaluation of the strengths and limitations of these methods is necessary for informed decision-making and optimal outcomes.

Table 4.1: Summary of optimization methods described in [61] and [60]

Optimization method	Short description
Linear Programming (LP)	Assumes linear relationship between all variables
Linear Integer Programming (LIP)	Assumes integer variables
Mixed Integer Programming (MIP)	Assumes a mixture of integer and noninteger variables
Non Linear Programming (NLP)	Assumes some nonlinear constraints or objective function
Stochastic programming (SP)	Handles problems with uncertainty
Dynamic programming (DP)	Divides complex problems into easier subproblems

4.1.2 Stochastic programming

When attempting to optimize a real-life problem, there will always be some uncertainty, making it challenging to perform evaluations as desired. To be able to deal with this in linear programming, stochastic programming can be added to result in stochastic linear programming. Solution techniques that can be used for stochastic linear programming use numerical approximation and statistical estimation [62, p. 1-14]. A general description of a stochastic optimization problem is described in the following model.

$$\min_x f(x) + E_{\xi} * Q(x, \xi) \quad (4.1a)$$

$$\text{s.t. } g_j(x) \leq b_j \quad j \in J \quad (4.1b)$$

$$x \geq 0 \quad (4.1c)$$

When dealing with uncertainty, there is often some first decision variable that has to be decided before one has the complete information, in this general model called x . When the complete information is received, some second-stage decision variables y_s have to be decided for each scenario s , based on the realization of some random vector ξ . $Q(x, \xi)$ is a function that represents the gain from making a decision y under scenario s , based on the first decision x that has been made. E_{ξ} represents the probability of each scenario in vector ξ . As a result, the model gives the best first decisions when there is uncertainty regarding which scenario will happen. [62, p. 1-14]

Recourse problems are problems where decisions must be made based on previous decisions. In this case, that means that the decision variable y has to be made with regard to the decision already made in x . A way to represent this problem is through a scenario tree. A scenario tree describes in an ordered fashion

how the stochastic elements evolve over time. Each scenario is represented by a branch of nodes and they are associated with a subset of decisions. [63, p. 1-22]

The scenario tree in Figure 4.1 shows a stochastic problem with three stages and two outcomes for each decision. The number of scenarios is given as the number of outcomes raised in the number of stages. Stages are defined as every time a problem-altering decision has to be made. It is therefore easy to see how fast the problems can increase in size when adding scenarios or stages. Node number one is known as the parent node and it is known as the first decision variable. All the other nodes depend on their parent node. [63, p. 1-22]

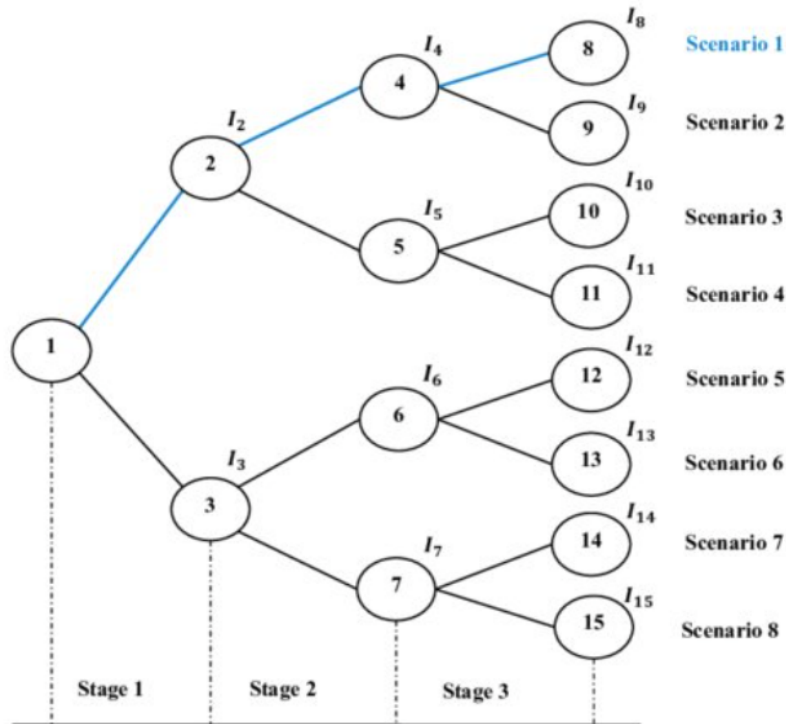


Figure 4.1: A scenario tree with three stages and eight scenarios [64].

4.1.3 Big M method

The big M method is a solution method for Linear Programming (LP) problems where an artificial non-negative variable \bar{x}_i is introduced to the problem like a slack variable would be. This is usually introduced when the constraints of the optimization problem require equality rather than \leq or \geq , or when a logical restriction must hold. Additionally, a sufficiently high value M is assigned to the artificial variable in the objective function. The M represents a symbolically high positive value and forces the variable \bar{x}_i to become zero in the optimal solution, and hence will not affect the solution other than enabling feasibility. [60, p. 115-125]

The general problem formulation

$$\max_x f(x) \tag{4.2a}$$

$$\text{s.t.} \quad \sum_i a_i x_i = b \quad i \in I \tag{4.2b}$$

$$x_i \geq 0 \tag{4.2c}$$

Thus becomes

$$\max_x f(x_i) - M\bar{x}_i \quad (4.3a)$$

$$\text{s.t.} \quad \sum_i a_i x_i + \bar{x}_i = b \quad i \in I \quad (4.3b)$$

$$x_i \geq 0 \quad (4.3c)$$

when adding the big M method.

4.2 The basics of hydropower scheduling

The primary purpose of hydropower scheduling is to optimally produce power with regard to the power market prices and the availability of water. The objective function of hydropower scheduling depends on what is to be optimized. As described in Section 3.2, some countries have regulated markets where power scheduling is decided by either the government or a single utility company. The main objective for countries with regulated markets is to maximize power production while minimizing operational costs and meeting the electricity demand. The Nordic power market is deregulated and the hydro producer schedules hydropower production to maximize their profit and, consequently, the socio-economic surplus.

There can be simple hydro systems with one reservoir and more complex hydro systems with multiple power stations. There are also PSH facilities and simple run-of-the-river plants. The hydropower scheduling problem's complexity depends on the hydropower productions system type. Including all details in a full-scale optimization model when dealing with bigger systems is not possible because of the size of the problem. Scheduling therefore has to be divided into different models based on the time horizon and the scheduling considerations. The most common categories are long-term, mid-term, short-term and actual real-time scheduling. [65]

The Long Term Scheduling (LTS), Medium Term Scheduling (MTS) and Short Term Scheduling (STS) models are coupled in different ways depending on if there is a regulated or deregulated market. In a deregulated market, the scheduling problem is solved by each individual producer, therefore decentralized scheduling is used. While in regulated markets, the authority aims to optimize the system as a whole. This results in a different approach called centralized scheduling. The different approaches are shown in Figure 4.2. The graph to the right shows how the three models represent the whole system in centralized scheduling. This means that the problem has the same space dimensions while the time horizon decreases. In decentralized scheduling shown to the left, LTS utilizes a fundamental approach, a long-time modeling of the hydro system. While MTS and STS modeling are both unit based and are decoupled in time. They take on the profit maximization objective [59]. This master thesis will focus on short-term scheduling in a decentralized market because the short-term scheduling tool, SHOP, will be utilized to simulate wind-power production.

As discussed in Section 2.2, the net head of the system depends on water flow, water volume in the reservoir and tail-race level. Since these values in a typical hydro optimization problem are variable, the net head function becomes nonlinear. In [66] it is discussed that the variations in net head can only be ignored for relatively large reservoirs. In these large reservoirs, the net head can be accurately approximated only to be dependent on the flow rate. The main problem in hydropower scheduling is finding the relationship between the power produced and water discharge. It is shown in Eq. (2.8) that the electric power produced depends on the net head and the efficiency of the turbine and generator. The generator efficiency depends on the power produced and the turbine efficiency depends on the water discharge and net head. To show these dependencies, one can rewrite Eq. (2.8) to Eq. (4.4). The flow rate also has a nonlinear effect on the amount of head loss, which changes the net head. The problem also does not comply with the requirements for nonlinear convex optimization problems, making it a nonconvex problem. The function for hydropower produced per water discharge is therefore a complex state-dependent, nonlinear and nonconvex problem.

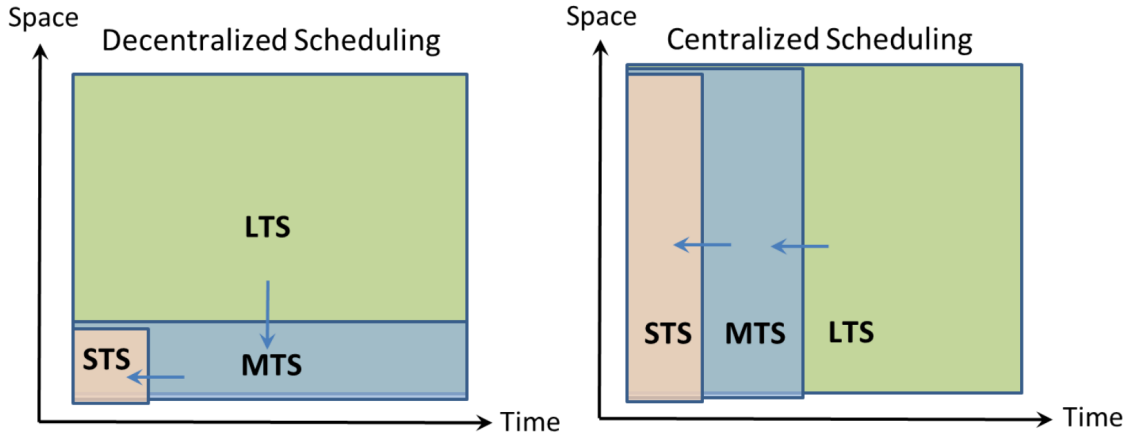


Figure 4.2: Scheduling toolchain for a decentralized model and a centralized model [59].

It is often referred to as hydro unit generating input/output (I/O) characteristics. [65]

$$P_h(Q) = Q \cdot \eta_{gen}(P_h) \cdot \eta_{tur}(H_n, Q) \cdot \rho \cdot g \cdot H_n \quad (4.4)$$

4.2.1 Short term hydro scheduling

Short Term Hydro Scheduling (STHS) is used to find the optimal operating policy for a hydropower system. In the Nordic region, power is sold to the power markets described in Chapter 3 with the goal of maximizing the producers' profit. The optimization model can either be plant-based or unit-based. Plant-based models often look at a system where all hydro-turbine generator units are aggregated into one unit. Doing this reduces the size of the optimization problem significantly. Because of the recent rise of VRE sources, the benefits from participating in the capacity markets have also increased. This means that the information on the available capacity during production is more important, making unit-based models more beneficial. Increased VRE penetration in the power grid has also led to increased variation in power prices, something that leads to detailed planning becoming even more important. Advances in software and hardware packages have made it possible to solve bigger models. The time horizon for STHS is from a single day to one week. [67]

Two main points have to be decided when scheduling hydropower on a short-term basis. Firstly the on/off status of the power producing units has to be decided. This is known as the Unit Commitment (UC) problem. Secondly, the dispatch from each specific committed unit has to be decided. This is known as the Unit Load Dispatch (ULD) problem. These two problems can be solved in separate optimization problems or as one combined. [65]

When creating a model to optimize STHS some constraints must be included. The objective function also has to be formulated in a manner that correctly describes the problem. When both the constraints and objective function are correctly formulated, the model should describe the systems' characteristics and operational requirements. [65]

The objective function could include three objectives, where the first two are for a deregulated market. Firstly, it should maximize the total revenue by multiplying the production with the prices from the different markets described in Chapter 3. Secondly, it should minimize the total operational cost. The units' startup and shutdown costs are the highest costs for operating hydropower production. The model would therefore like to minimize each unit's startup and shutdown. Frequent startups can drastically reduce the lifetime of a unit because of mechanical stress. To estimate the cost for each startup and shutdown, it is possible to use historical data to see the expenses related to maintenance and repairs per number of startups. Thirdly, if there is a regulated market, the producer would aim to minimize the value of energy used or spilled. In this case, power would not be sold to the spot market and the load obligated is predefined.

Here, in a regulated market, the main objective is to minimize the water used by turbines while fulfilling the demand for electricity. [65]

The main constraints that should be included in the STHS problem are listed here. They are further described in [65] and are general for STHS.

1. A constraint that balances the water in the reservoir. It changes the reservoir level between each time step by adding inflow and removing water discharged for production and spillage. The water flow between reservoirs has to be included when having multiple connected reservoirs.
2. A constraint that sets the reservoir's storage limits and sets limits for controllable spillage. The reservoirs will have a minimum operating level, and the power plants can not produce power when the reservoir level is lower than this because of environmental and operational reasons. The maximum flood level is to prevent possible damage to the dam.
3. A constraint that accounts for head variation and flow-related head losses. As mentioned in Section 4.2, head loss can be ignored for large reservoirs, so if this constraint should be included depends on the reservoir size.
4. A constraint that sets the connection between water discharge and power produced. As also mentioned in Section 4.2, this is a nonlinear function. One can simplify this formulation in different systems to obtain better computational traceability. This can be done by assuming the turbine efficiency as fixed or only flow dependent.
5. A constraints that set the limits for power production and water discharge depending on the unit and system data. The generator sets the upper and lower power output, while the turbine sets the upper and lower water discharge. The power limits can be fixed while the discharge limits can be fixed or head-dependent.
6. A constraint that describes the operating status of each unit. The constraint should reflect the startup decision of the units. If needed a constraint with a minimum or maximum number of producing units can be added
7. A constraint that balances power produced to power sold in the market.
8. A constraint that couples the STS to LTS and MTS. This can be done in different ways described [68] and [69].

Other constraints that can be necessary based on the topology of the area are environmental constraints. This could be constraints regarding minimum environmental flows or minimum and maximum flow rates. Ramping rates regard how fast the reservoir level can vary. When a hydropower plant participates in the DAM and capacity markets, the optimization problem must also know the available capacity reserves. Other constraints must also be included if the hydro system is a PSH facility.

4.2.2 MILP and MINLP used in hydropower scheduling

When formulating an optimization model for hydropower scheduling, one has to consider the nonlinearity of the problem as well as the variables' mixture of integer and noninteger variables. Nonlinear programming problems have high complexity, this also applies when introducing integer variables in what then becomes Mixed Integer Nonlinear programming (MINLP). Therefore MINLP solvers are often combined LP, Mixed Integer Programming (MIP) and Nonlinear Programming (NLP) solvers [70]. A STHS problem can be solved as a MINLP problem [71], or it can use piecewise linear approximation and be solved as a Mixed Integer Linear Programming (MILP). [66]

The available software for solving MINLP is less mature than the MILP software, but some algorithms are available. When solving an optimization problem with nonlinearities, it is important to remember that one can have multiple local optima. If an MINLP solver relies on convexity assumptions, it can find a local optimum and represent it as a global optimum [71]. Much research is being done to determine the deterministic global optimum when using NLP and MINLP.

In theory, STHS is also stochastic due to the uncertainty in the unknown inflow, electricity demand, and electricity prices. This can be included in the model using scenario trees, even if this has a negative effect

on the computational time. Many STHS programming programs therefore start with a computationally efficient deterministic model while uncertainty can be added afterward [71]. It therefore has to be evaluated which uncertainties affect the calculated profit by looking at the change in the objective value when the number of scenarios is changed. An analysis done in [72] shows that a reduction in inflow scenarios had a small impact on the profit. While an analysis in [73] shows that in a combined hydro and wind project, a reduction in wind scenarios had a smaller impact on the profit than a change in price scenarios.

Table 4.2 shows the different ways of solving hydro scheduling problems. There are different ways of handling the nonlinearity, nonconvexity and state dependency that occurs in hydro production. The function for hydropower production can be modeled as a high-order polynomial, a quadratic formula or a piecewise linear approximation.

Table 4.2: A table summarizing the differences between methods used for solving hydro scheduling problems.

	Solving method	Usage	References
Mixed Integer Linear Programming (MILP)	Piecewise linear approximation	Backed by a rich body of literature. Will deviate from actual values	[66], [74], [75]
	Piecewise linear approximation with dynamically decided breakpoints	More accurate approximation.	[65]
	Adding iterative method	Used in SHOP Handles state dependency in the hydropower production function	[65]
Mixed Integer Nonlinear Programming (MINLP)	High order polynomial	Can not guarantee global optima. Needed when more nonlinear details are included	[70], [71]
Mixed Integer Nonlinear Quadratic Programming (MINQP)	Quadratic function	More accurate than linear approach. Longer computational time	[76], [77]
Mixed Integer Linear Stochastic Programming (MILSP)	Stochastic Linear Programming	Deals with uncertainty. A more accurate representation of reality. Makes the problem much bigger, resulting in longer computational times	[72], [73]

4.3 SHOP

Optimal short-term scheduling of hydropower is necessary and challenging because of the many stochastic variables and nonlinear functions related to reservoir levels, water value, flow limits and unit efficiency. This is why SINTEF has made an optimal scheduling tool, SHOP, based on the programming language C/C++ to help power producers better perform short-term hydropower scheduling. The SHOP tool is a STHS tool aimed to be functional for hydro producers located across the globe. Multiple strategic, phys-

ical, technical and market constraints are considered during scheduling. Figure 4.3 shows the currently available modules in SHOP. SHOP includes junction, reserve, reservoir, plant and gate information as well as simulation, bidding and uncertainty modules. The nonlinear, nonconvex and state-dependent properties of hydropower are handled in SHOP. There are multiple ways to couple short-term to long and medium-term scheduling, and in SHOP it is possible to choose which alternative the model should use. SHOP uses deterministic electricity prices and inflow. [65]

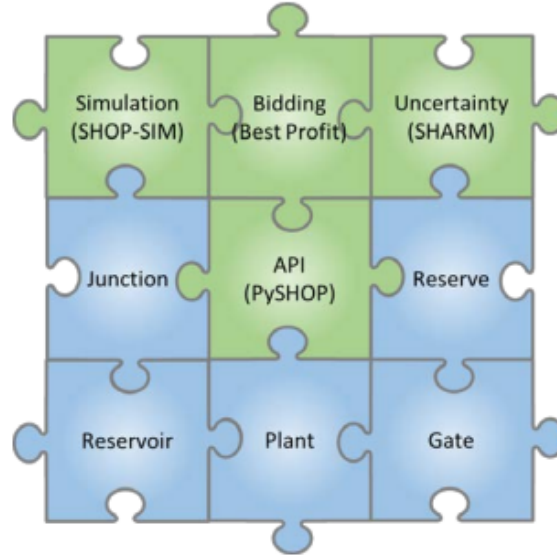


Figure 4.3: SHOP modules currently available [65].

SHOP uses piecewise linearization, but instead of static breakpoints dynamically determines the breakpoints. The breakpoints are also timely updated during the solution process. [65]

Universality, precision and efficiency are the three criteria that researchers use to evaluate which mathematical formulations and solution methodologies can be used in SHOP [65]. Universality has to be considered by creating generic formulations that can be specialized based on the factors that vary between hydropower systems. This is factors like systems equipment, electricity markets in the area and hydraulic systems. SHOP therefore requires input data from the hydro producers to work optimally. Precision has to be included so that SHOP gives reliable results for most system conditions. This is done by accurately including head variation, head losses, turbine and generator efficiency, and penstock structure. First, SHOP should run as an efficient deterministic model before it can incorporate stochastic features. Many factors in hydro production are uncertain and can therefore be included as stochastic scenario trees. However, this should not hinder the code from running efficiently. [65]

In September 2016, SHOP made a change in its default modeling strategy from plant-based to unit-based. This change was initiated by the increased benefits for hydropower producers participating in multi-markets and a need for further development towards autonomous hydropower scheduling. This is now possible because of the advantages that have been made in the workstation hardware and MILP software packages. This makes it so that the larger MILP problems are easier to solve. [65]

To solve the STHS problem, SHOP's algorithm decomposes the problem into a UC and a ULD mode as described in Section 4.2.1. The solution strategy for SHOP is shown in Figure 4.4. Firstly, which units will be running is decided in UC mode before the load of each running unit is decided in ULD mode. The figure shows that the UC mode is an iterative method to stabilize the head variation. Because of the binary variables that describe the units' on/off status and the piecewise linear approximation with dynamically decided breakpoints, this becomes a MILP problem. The iteration method used in UC and ULD updates the gross head after each iteration by updating the volume and reservoir level. This is done because of the hydropower production functions' state dependency. There can be different ways to measure if the problem

convergences. Three main methods are:

1. The change in the highest mismatch of water level.
2. The largest difference between optimized and actual unit power output.
3. The change in objective values between interactions.

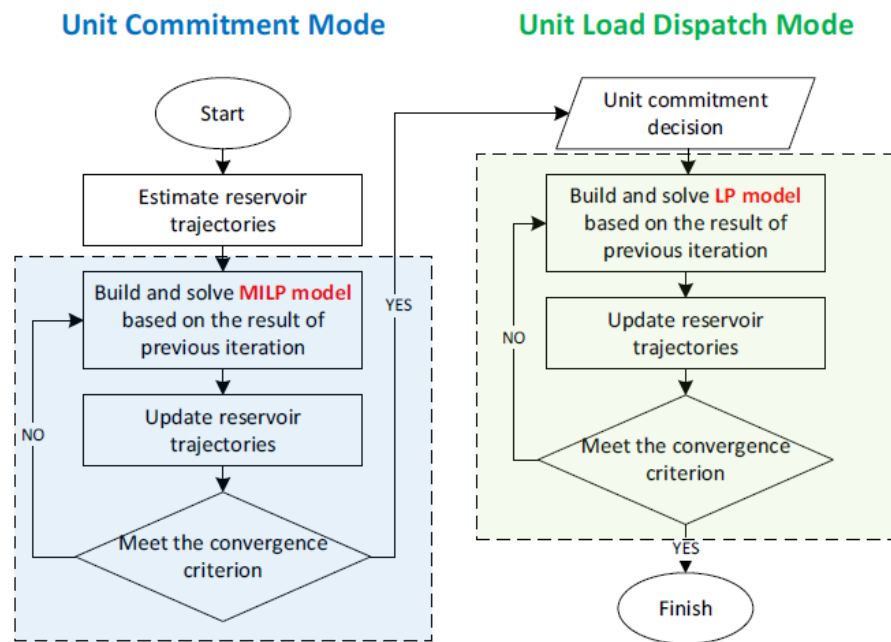


Figure 4.4: The solution strategy in SHOP [65].

4.4 SHARM: Handling uncertainty in SHOP

To incorporate the uncertainty surrounding selling hydropower in the electricity markets, a prototype module named SHARM has been implemented by SINTEF in the framework of SHOP. To achieve this, a stochastic version of the successive linear programming algorithm used in SHOP is built using a discrete representation of scenario trees. Because of the increased profit a hydropower producer can gain from participating in multiple markets, SHARM allows stochastic representation in multiple markets.

In a STHS model, inflow to one or more reservoirs and electricity prices are the most significant options for stochastic variables. In the current implementation of SHARM only the DAM prices are considered to be the stochastic prices in the model. The stochastic variables are represented by a scenario tree as shown in Figure 4.1, where each root-to-leaf path of the tree equals one scenario. The scenario tree branches at each stage of the planning period. Since a hydropower scheduling problem has many decision stages, the problem will quickly become large. It would therefore be favorable if the branching would be limited to only a few number of stages. In a hydropower scheduling problem that looks at the DAM it would be beneficial to set branching every 24 hours as the DAM prices are set. To limit the problem size, a deterministic inflow could be assumed. In literature, several algorithms can be used for scenario tree reduction. Different inflow and price scenarios can be found by studying historical data. It is possible to look at price and inflow uncertainty as a set of multi-dimensional scenarios. One can also assume a coupling between inflow and price scenarios and combine these, or look at both uncertainties separately. [78]

To increase SHARM's speed and accuracy, a method of using a new iteration as an incremental description of the previous iteration is used. In the SHARM prototype, it is possible to have multiple different inflow scenarios in one system and only one price scenario. As mentioned in Section 2.2.5, cavitation may occur during low loads. This can limit minimum generation to 30 – 40% of nominal loading instead of zero, and

this limit varies based on the turbine and the pressure height above it. To handle this, SHOP uses binary variables often combined with modeling of startup costs. Computational time becomes a problem when using a solving algorithm on an optimization problem with many binary variables. [78]

A further detailed description of SHARM's solving method is described in [78].

In the case study conducted in [78], the same system used 165.75 seconds to find the optimal solution for the stochastic inflow and power prices compared to 10.23 seconds to find the solution in the deterministic input version in SHOP. The computational time in SHARM is dependent on the following variables:

- Time-horizon and the topology of the system.
- Some optimal solutions can be more difficult to find if the initial reservoir levels give the system more flexibility.
- The size of the scenario tree is also essential for computational time.

The results from [78] indicate that including uncertainty in the inflow has a larger impact on profit than price. However, this study was conducted before the large variations in power prices that we see today [79], so these results might not be a good representation of today's power market.

4.5 Differences in stochastic and deterministic programming

The authors of [80], [81] and [82] compare deterministic heuristics, usually MILP, to stochastic models for the DAM bidding for hydropower producers. The aim is to evaluate how the different approaches impact the resolution of the solution. In accordance with standard industry practice, inflow scenarios are not included in the uncertainty model. In [80], three approaches for generating bids based on the deterministic model are presented: bidding the expected volume, bids based on the water value given by seasonal scheduling, and bids based on the results from multi-scenario runs of the deterministic model using price forecasts. The paper comes to the conclusion that the stochastic model and the multi-scenario deterministic model outperform any of the two other heuristics by 0.16-3.49% across all days in the case study. Furthermore, depending on the day in the case study, the stochastic model achieves from 0.03-1.51% higher objective function values than the multi-scenario heuristic model. A drawback however, was that the stochastic model had a much longer computational time of around 2.5 times the sequence of all the heuristic methods, meaning the multi-scenario model could be an alternative for producers with limited calculation time.

These findings were also documented in [81], where the stochastic bid optimization method performs better than the heuristic methods in terms of 0.69% higher average prices and 0.61% higher total value. Additionally, the authors of the paper argue that the algorithm is fast enough for daily use and that any daily improvement can be very beneficial for a power producer. This is consistent with other literature, e.g. [82].

4.6 Uncertainty in windpower production

Windpower forecasting is a growing research field seeking to deal with the intermittency and variability of the wind. By minimizing uncertainty, it can enable better production predictions as well as reduce investment risks. In recent years Europe has seen that increased production from inflexible energy sources like windpower has resulted in negative power prices. This has been especially shown in countries like Denmark, Germany and Ireland, where windpower production accounts for 27-49% of the country's total electricity production [83]. Negative prices mean that the producer will pay the consumer to use their power, usually caused by volatile energy sources covering a large share of the supply side. Hence, there is a need for increased knowledge about windpower forecasting.

In [84], the authors distinguish between aleatoric and epistemic uncertainty. Aleatoric uncertainty comprises random variability brought on by a system's stochastic behavior. In contrast, epistemic uncertainty

is associated with a lack of knowledge, often related to measurement errors, model flaws and insufficient sampling. The global wind systems described in Section 2.1.1 are an example of aleatoric uncertainty.

The authors of [84] also present statistical, physical and hybrid uncertainty modeling approaches. Statistical methods are generally based on mathematics, probability theory, stochastic forecasting and historical data. The methods are usually trained and their prediction is based on this approach. Some known statistical techniques are Auto-regressive integrated moving average (ARIMA) (an integrated version of the auto-regressive moving average model), Artificial Neural Network (ANN) and machine learning approaches such as Support Vector Regression (SVR) and Deep Learning (DL), presented in Table 4.3. Because statistical methods are usually trained using historical data samples, their prediction is satisfactory and works as a generalization, but only if the samples are sufficiently consequent and detailed.

The physical forecasting methods deal with the physical aspects impacting the wind speed and windpower production, such as the surface, its roughness and terrain differences. This was pointed out in Section 2.1.2 and 2.1.5. According to [84] numerical weather prediction data are used as boundary conditions, and Computational Fluid Dynamics (CFD) simulations calculate the wind speed and direction at the turbines' hub height. See Table 4.3 for more on CFD. The advantages of physical methods are that they are usually based on the turbines' power curve and hence do not rely on historical data. However, CFD require high computational power to solve the forecasting problem.

The idea behind the hybrid modeling methods is to minimize the chance of forecasting errors by combining statistical and physical methods. A hybridization involves forecasting by several different models, and by averaging one can exclude possible large deviations.

4.7 Optimization tools

Table 4.4 shows the state-of-the-art software used for optimal energy planning and energy system simulations. The different programs have been developed by research institutions worldwide, like the National Renewable Energy Laboratory (NREL), Argonne National Laboratory (ANL), SINTEF and Aalborg University. It can be observed that some of the programs focus more on exploring the interactions within the system, while others are more focused on long-term system expansion planning. SHOP is one of the few programs with a specific focus on short-term operation scheduling of hydropower. This is opposed to most of the others, which are more general for all electricity sources like gas, wind and solar. Therefore, SHOP has some key characteristics regarding hydropower scheduling that other programs do not have: the aforementioned SHARM module for uncertainty calculation, detailed system setup, and possibilities for the respective users to personalize their hydropower plants. SHOP is the program used in this thesis.

Table 4.3: Possible forecasting and simulation methods to predict wind speed and windpower generation.

Modelling method	Short description	Target(s)	Reference(s)
Auto-regressive integrated moving average (ARIMA)	Conventional statistical approach using stationary time series model. Divided into four steps: model identification, parameter estimation, diagnostics checking, and forecasting	Very short-term wind speed forecast	[85], [86], [87]
Support Vector Regression (SVR)	Used to predict chaotic time series through nonlinear mapping of input data from the sample space before performing linear regression to estimate the desired prediction in the feature space	Wind speed prediction	[88], [89]
Artificial Neural Network (ANN)	Time series model that can represent complex linear relationships, imitate natural intelligence and map nonlinear functions through weighting of interconnected neurons	Wind speed and windpower prediction	[90],[91]
Deep Learning techniques (DL)	Considered as a class of machine learning techniques or a subset of computational intelligence	Wind speed and wind energy forecast	[92]
Computational Fluid Dynamics (CFD)	Investigates on a small scale the physical flow of fluids and how they act in relation to objects. This is described through mathematical equations, and are usually solved computationally through numerical simulations	Accurately simulate the resource distribution in wind farms	[93], [94]

Table 4.4: An overview of optimization software tools used to schedule operation of renewable energy sources.

Name	Type of model	Usage	Reference(s)
SHOP	MIP for start/stop in the unit commitment mode. LP for the network model in the unit load dispatch mode.	Optimally schedule short-term hydropower plants. Calculating marginal costs with regulating power notification. The economic trade-off between expected price within the period and future price expectations. SHOP is coupled with seasonal and long-term planning tools, all developed by SINTEF.	[65], [3]
WILMAR	Scenario Tree Tool (STT) and Scheduling Model (SM).	Used to simulate and analyze the optimal operation of international energy systems over a one-year time horizon. The model treats windpower production forecasts and load forecasts as stochastic input parameters. Mostly used for analyzing the integration of new energy sources into the power system.	[95], [96]
A-LEAF	Long term is a least-cost linear program. Short-term is a binary security-constrained unit commitment model.	Divided into long-term expansion planning and short-term operational planning of all assets, such as power plants and transmission lines, across the whole power system. Mostly used for its long-term properties.	[97]
PLEXOS	LP, MILP, NLP with a stochastic approach to uncertainty. Object-oriented. Divides into subproblems solved in a cascade.	Power market modeling, forecasting and simulation software for energy solutions. Used for Integrated Resource Plan (IRP) and to study emerging energy technologies and how policy impacts the market. Includes operational planning across all time horizons and uncertainty for future loads, inflow and price.	[98], [99]
FLORIS	Python-based command line program for simulation and processing.	a wake modeling and wind farm control simulation software developed by NREL. It is based on a Python framework and incorporates steady-state engineering wake models.	[100]

Chapter 5

Methodology

In this master thesis, the *Wind Optimization Model* has been developed in several stages. These are explained in this section. Relevant data to perform the study has been collected from the case location Geitfjellet Vindpark through Renewables.ninja, and market data from Nord Pool. Information regarding this can be read in Section 5.1.1 and 5.1.2. The long-term goal is that this developed *Wind Optimization Model* can be integrated into the SHOP tool to create a joint Wind and Hydropower Optimization Program (WHOP) for short-term scheduling. The authors have also performed a study, see Appendix A.1, based on the topics of this master thesis. The study also investigated the impact of up-regulation prices for windpower producers' bids in the DAM, but for different scenario cases.

5.1 Data collection

As explained in Section 3.7, the power production in Nord Pool price zone NO3 is dominated by hydropower production. In 2020 the wind farms of Fosen Vind DA opened, significantly increasing the windpower penetration in the region by 801 MW. In [6], a market analysis was performed, investigating production and price data before and after the integration of windpower. This analysis gave no conclusive results and will therefore not be continued in this master thesis.

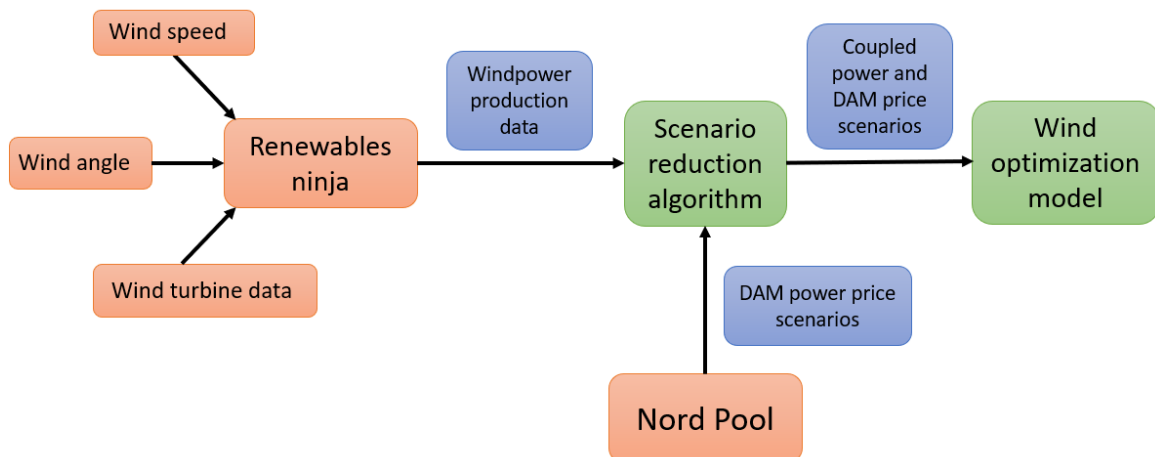


Figure 5.1: The process of generating scenarios for the *Wind Optimization Model*.

Figure 5.1 shows the process of building scenarios based on historical data to be used as input scenarios into the *Wind Optimization Model*. The orange color in the figure represents data collected from Renewables.ninja and Nord Pool and will be described in Sections 5.1.1 and 5.1.2. The blue represents the data transported from one stage in the flowchart to another. The green color represents the algorithms used.

The scenario reduction algorithm takes in the windpower production data and DAM prices for a given year and reduces the data to the desired number of scenarios, described further in Section 5.2. The coupled production and DAM price scenarios are then used as input scenarios in the *Wind Optimization Model* developed in the SHOP virtual lab (vLab) with the SHARM extension. The development and functionality of the *Wind Optimization Model* is presented in Section 5.3.

5.1.1 Geitfjellet Vindpark

In the thesis, the Geitfjellet Vindpark has been employed as a base case for the *Wind Optimization Model*. This is a wind farm located in Norway, see Figure 5.2. The wind farm has an installed capacity of 180.6 MW and consists of 43 wind turbines [101]. The turbines are Vestas V136-4.2 MW, with a hub height of 87 meters. Technical specifications can be found in Appendix A.2 and [102]. This information was fed into Renewables.ninja [103–105] at Geitfjellet Vindpark to extract wind speed and windpower production data from the location of the wind farm. Renewables.ninja is a website based on the MERRA-2 (global) dataset provided by the Global Model and Assimilation Office (GMAO) of NASA [106]. Renewables.ninja gives datasets with information in an hourly time resolution regarding power output [kW], wind speed [m/s], and local date and time for the chosen location. The location used is shown in Figure 5.2 and can be found at latitude 63.365 and longitude 9.497. The data in Renewables.ninja was only provided for 2019, and it has not been possible to extract windpower production and wind speed information for any other year. This limits the amount of data to one year.

It is essential to keep in mind that the wind production data given by Renewables.ninja is for a year when the Geitfjellet Vindpark was yet to be in operation. The sampled weather data provided by MERRA-2 is coupled with the technical turbine specifications given by the user, and Renewables.ninja generates the expected output. This means that the production data is not empirical data but simply an estimation. Additionally, since the Fosen Vind project did not start producing energy until 2020, the power price data is unaffected by the increased windpower penetration rate in the area. It is also not possible to see any effects of today's ongoing energy crisis in Europe.

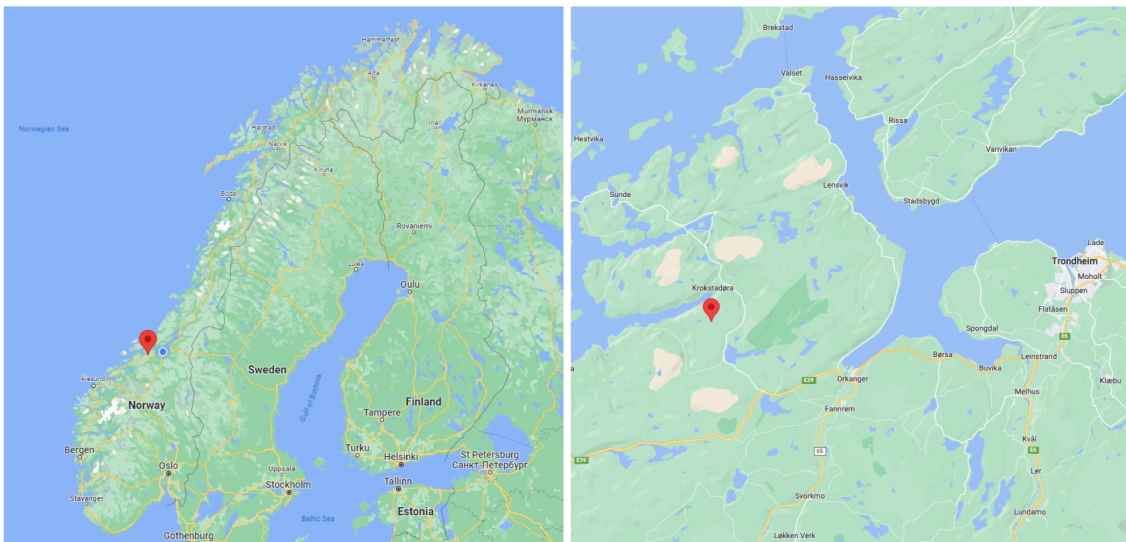


Figure 5.2: Location of Geitfjellet Vindpark [107].

5.1.2 Data from Nord Pool

Data sets for the investigated price zone NO3 for the DAM, IDM and BM have been gathered from Nord Pool, the local TSO. The data sets are in hourly increments and are given in [EUR/MWh]. The DAM prices are

from 2000 to 2022, whereas the IDM and BM price data are available for only one year back. From Nord Pool, the consumption and production data [MWh] has also been sampled in hourly increments for the years 2000-2021. The datasets from 2020-2022 from the NO3 price zone include the supplied production from windpower from Fosen Vind DA. However, the production data given by Nord Pool does not give any details regarding how much of the power is produced from the different electricity sources. Power producers in the region have also been unwilling to share production data due to production security and privacy. This makes it hard to analyze what kind of impact the increased windpower penetration has had on the distribution of power production.

5.2 Input scenario generation

This thesis analyzes the case study at Geitfjellet Vindpark and price zone NO3 for 25, 50 and 365 scenarios throughout the year of 2019. A varying amount of scenarios were chosen to investigate the benefits of including more uncertainty in the model. The 25 and 50 scenario cases have been based on the sampled historical data on a yearly basis as well as on a seasonal basis. This was done to further explore the advantages and disadvantages of considering the seasonal data characteristics when optimizing the plants' production schedule.

In order to select the desired amount of weighted input scenarios, a scenario reduction algorithm has been utilized. For this study, a backward scenario reduction algorithm developed by [108] was applied, the same as was used in the conference paper written by the authors, see Appendix A.1. The general optimal reduction problem described in [108] is shown in the optimization problem (5.1). The algorithm takes wind production and market prices as input data and iteratively remove scenarios based on their similarity to the remaining scenarios. This continues until the desired amount of representative scenarios, each with a set probability, are obtained. The idea is that the new probability of a kept scenario is equal to its former probability as well as the sum of the probabilities of the deleted scenarios closest to it, with respect to c_t . The probability of the deleted scenarios is set to zero. More information on the specific backward reduction strategy used in this thesis can be found in [108] as *Algorithm 1*. The output of the scenario reduction algorithm is a list of the kept scenarios and their corresponding probability.

$$\min \sum_{i \in J} p_i \min_{j \in J} c_t(\xi^i, \xi^j) : J \subset 1, \dots, S, \#J = S - s \quad (5.1a)$$

Nomenclature

- $c_t(\xi^i, \xi^j)$: distance between scenario $\{\xi^i\}_{\tau=1}^T, \{\xi^j\}_{\tau=1}^T$
- p_i : scenario probabilities
- $\{\xi^i, \xi^j\}$: scenarios (sample path)
- $\{\xi^i\}_{\tau=1}^T, \{\xi^j\}_{\tau=1}^T$: n-dimensional stochastic processes with parameter set $\{1, \dots, T\}$
- S : number of scenarios in the initial scenario set
- J : index set of deleted scenarios
- $\#J$: cardinality of the index set J
- $s = S - \#J$: number of preserved scenarios

The algorithm was run for the hours of 8-9 AM, 12-1 PM and 4-5 PM each day. The hours chosen in this model were noon and four hours before and after, approximately peak hours of the day. This was done to investigate the impact of peak hours on the distribution of power produced versus market price and to see how the distribution shifts during the day in set four-hour intervals.

The scenario reduction algorithm's output gives the input to the *Wind Optimization Model*, more specifically, the day number, market price [EUR/MWh], power produced [MWh] and probability for each scenario. The *Wind Optimization Model* is explained in Section 5.3. Given the number of scenarios investigated in this study, a scatter plot best graphically represents the scenario data. These are presented in Chapter 6, Results.

5.3 Developing a Wind Optimization Model using SHOP

The SHOP tool has been utilized to simulate the operation of an operational wind farm through the creation of a *Wind Optimization Model* in the SHOP environment. The objective of this model is to determine the optimal bid for the windpower producer in the DAM when there are stochastic market prices and windpower production. This is done by manipulating the existing hydropower-specific objects and attributes built into SHOP to simulate a wind farm. One must also add the possibility for the windpower producer to buy and sell power to and from the BM. This is for when the windpower production is lower or higher than the DAM.

5.3.1 Procedure

The creation of a wind farm in the SHOP tool involved characterizing the wind farm as a run-of-the-river plant. This was accomplished by configuring the wind farm to function as a hydropower plant with no available storage, such that all inflows into the reservoir could be treated as wind speeds entering the turbines. One can calculate the inflow that should be inserted into the run-of-the-river plants to achieve the desired windpower production. This can be done by inserting the preferred windpower production into the equation for power produced by hydropower, Eq. (2.8). Since the wind turbines are modeled as run-of-the-river plants, the flow rate is equivalent to the inflow, as expressed in Eq. (5.2) and (5.3). Eq. (5.3) demonstrates that, assuming the generator and turbine have a perfect efficiency and the net-head is set to a reference height of $h_{ref} = 1000/9,81m$, the inflow rate [m^3/s] is equivalent to the power output [MW]. This was done to easily check if the *Wind Optimization Models'* results were accurate and identify any differences from what was expected.

$$P_h[MW] \cdot 10^6 = Q[m^3/s] \cdot (\eta \cdot \rho \cdot g \cdot H_n) \quad (5.2)$$

$$P_h[MW] \cdot 10^6 = i[m^3/s] \cdot (100\% \cdot 1000kg/m^3 \cdot 9,81m/s^2 \cdot 1000/9,81m) = i[m^3/s] \cdot 10^6 \quad (5.3)$$

5.3.2 The impact of up and down regulation prices

According to information provided by ANEO [109], the income of a windpower producer is highly dependent on the BM prices. Meaning that during times of lack of supply on the grid, windpower producers have to pay high up-regulation prices when they cannot meet their DAM bids. The down-regulation price is often low, resulting in low profits for windpower producers when they produce more than their DAM bid.

Wind producers are required to bid in at their expected production in the market. With such significant variations in up and down-regulation prices as seen today, this could be very costly for the wind producer. It is therefore beneficial to examine the points at which increases in up-regulation costs result in a deviation from expected levels of production.

If the power producer had perfect information on wind speed and direction, it could bid its precise production into the DAM. One could then find the producers' profit by multiplying the production with the DAM price. This master thesis runs different scenario cases for scenarios with different values and probabilities. One can find the expected production, power price and profit by utilizing Eq. (5.4), (5.5) and (5.6), respectively. Here ρ_s is the probability for scenario s , p_s is the price in scenario s , and x_s is the production in scenario s . This expected profit can be used to compare the benefits of including uncertainty in the model compared to a deterministic solution approach. The expected production, power price and profit for the scenario cases run in this model are presented in Section 6.2.1.

$$Expected\ production = \sum_s^S \rho_s \cdot x_s \quad (5.4)$$

$$Expected\ power\ price = \sum_s^S \rho_s \cdot p_s \quad (5.5)$$

$$\text{Expected profit} = \sum_s^S \rho_s \cdot x_s \cdot p_s \quad (5.6)$$

The wind farm model is made in SHOP with the SHARM extension to simulate the physical system shown in Figure 5.4 with uncertainty regarding windpower production. To add the possibility for up and down-regulation of production to the wind farm created in SHOP, one can not treat the wind farm as just a simple run-of-the-river. The model has to produce one common decision for power bid based on all scenarios. This creates a problem, as run-of-the-river plants can not guarantee production above its lowest inflow scenario. Changes therefore have to be made to the simple wind farm described in Section 5.3.1.

Capacity is added to reservoir 1 so that it is possible to ramp up production if the power bid from the wind producer is too high compared to the actual wind production calculated based on stochastic wind speed. SHOP is then used to price the water stored in reservoir 1 with the up-regulation price, making this an additional cost in the optimization problem. This change is made to illustrate power being bought from the market. Reservoir 2 below the wind turbine is also added. When there is a higher inflow/wind speed than what has been bid from the wind producer, the inflow goes down into this reservoir. The inflow does not accumulate in reservoir 1 because the capacity of the reservoir is set to max at the beginning of the optimization problem. A consequence of this is that the model can only be used for a single time step. The water stored in reservoir 2 is valued as the down-regulation cost and is also added to the optimization problem. The reservoirs and the power station is connected, as shown in Figure 5.3, though river objects in SHOP.

The Wind Optimization Model in SHOP

The objective function for the simulated hydropower problem created in SHOP is shown in the optimization problem (5.7). This is based on the system shown in Figure 5.3. When other hydropower aspects are added to the problem, additional constraints are generated by SHOP. All the different constraints that can be generated are further described in [65].

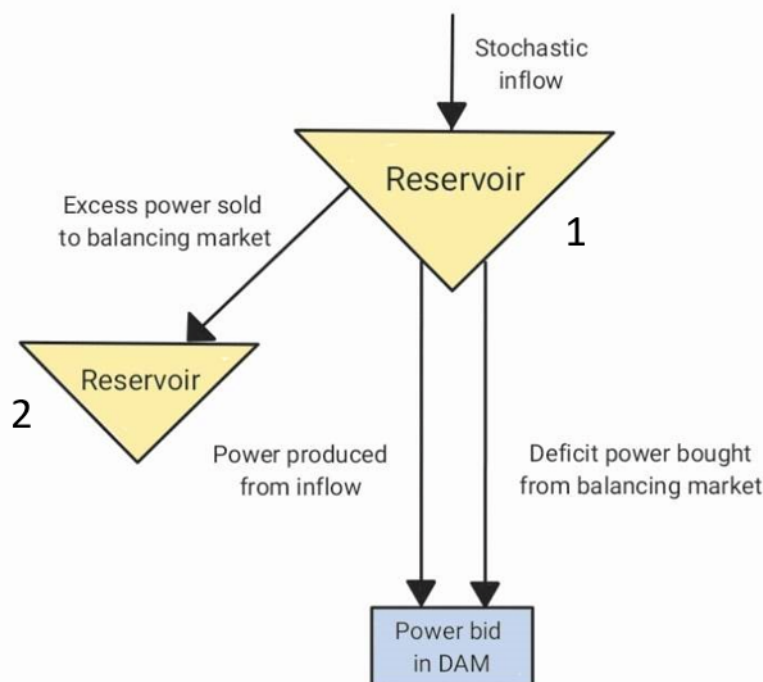


Figure 5.3: System created in SHOP

$$\max z = \sum_s \rho_s \cdot (y_{1,s} - z_{1,s}) \cdot p_s + \sum_s \rho_s \cdot P_d \cdot v_{2,1,s} \cdot \frac{10^6}{3600} + \sum_s \rho_s \cdot P_u \cdot v_{1,1,s} \cdot \frac{10^6}{3600} - P_u \cdot v_{1,0} \cdot \frac{10^6}{3600} \quad (5.7a)$$

s.t.

$$v_{r,0,s} - v_{r,1,s} = 3600 \cdot 10^{-6} \cdot (f d_{1,s} + q_{1,s} - i_{r,0,s}) \quad r \in R \quad s \in S \quad (5.7b)$$

$$y_{1,s} - z_{1,s} = x_s \quad s \in S \quad (5.7c)$$

$$f d_{t,s} = f u_{t,s} \quad t \in T \quad s \in S \quad (5.7d)$$

$$x_{min} \leq x_s \leq x_{max} \quad s \in S \quad (5.7e)$$

$$q_{min} \leq q_s \leq q_{max} \quad s \in S \quad (5.7f)$$

$$x_0 = x_s \quad s \in S \quad (5.7g)$$

$$v_{r,1,s} = v_{r,2,s} \quad r \in R \quad s \in S \quad (5.7h)$$

Sets

S : set of scenarios, $s \in S$

T : set of hours, $t \in T$

R : set of reservoirs, $r \in R$

Parameters

p_s : the power price in the DAM during scenario s

$i_{r,t,s}$: inflow into reservoir r in scenario s

P_u : price for up-regulating production

P_d : price for down-regulating production

ρ_s : probability of scenario s

x_{max} : maximum production

x_{min} : minimum production

q_{max} : maximum discharge

q_{min} : minimum discharge

Variables

x_s : Power produced in the power plant during scenario s . Is set to be equal for every scenario

$q_{t,s}$: Generator discharge in scenario s . Is set to be equal for every scenario

$v_{r,t,s}$: volume in reservoir r at time step t

$f d_{t,s}$: Flow downstream river in scenario s

$f u_{t,s}$: Flow upstream river in scenario s

$y_{t,s}$: Power bid to the DAM in scenario s for the time step t

$z_{t,s}$: Power bought from DAM in scenario s for time step t . Set to zero

The objective for this model is to maximize the production revenue across all scenarios, as seen in Eq. (5.7a). The first summation in this equation represents all the power sold to the DAM. In this case, purchasing electricity from the DAM is not considered, and therefore the corresponding variable (z) is set to zero. The second summation accounts for the value of the stored water in reservoir 2 at the end of the time step and represents the profit from the excess power produced above the DAM bid. The two final components of the objective function represent the loss in profit caused by the water used in reservoir 1. This is done by taking the stored profit found in reservoir 1 at the end of the time step and subtracting the stored profit at the start of the problem. It should be noted that the final component is not incorporated in the final profit estimation provided by the optimization tool used (i.e., SHOP), but it must be included when presenting the windpower producers' total profit. Since this value is a constant across all scenarios, it does not affect the optimal DAM bid.

The reservoir balance constraint is shown in Eq. (5.7b) for the single time step in this problem. To set

the power produced equal to the power sold to the DAM, Eq. (5.7c) is introduced. The constraint (5.7d) displays how there is no inertia in the river system by setting the flow at the start of the river equal to the flow at the bottom. The generators' production and flow limits are shown in Eq. (5.7e) and (5.7f), respectively. Constraint (5.7g) forces the model to make a joint decision for the production across all scenarios. SHOP does not allow for optimization for just one time step, and the code therefor has to be made for two time steps. Eq. (5.7h) is added to force the production to zero in the second time step.

As mentioned in Section 4.2.1, startup and shutdown costs can be implemented in SHOP to account for the damage implemented on the turbine during frequent startups and shutdowns. This is not included in the *Wind Optimization Model*. During windpower production, the turbine blades do not take the same damage as a turbine used for hydropower. Wind turbines also have a cut of speed, as mentioned in Section 2.1.3, to limit mechanical stress. Frequent startups and shutdowns are therefore not a significant problem when scheduling windpower and can be ignored. This means that the binary variables introduced in SHOP during the implementation of startup and shutdown costs is not included in the *Wind Optimization Model*. The exclusion of binary variables reduces the computational time of the problem, making it possible to run the model with more scenarios.

This model is functional when the up-regulation price is below the DAM prices. However, the solution would then prefer to buy water from the regulation market and sell it to the DAM, something that in reality is not possible. Nevertheless, the up-regulation prices in the regulation market are historically higher than the DAM prices.

Some variables and constraints get created in SHOP for the optimization problem (5.7) that is not relevant to the *Wind Optimization Model*. These variables and constraints describe aspects of hydropower optimization that do not exist in the windpower system and are listed below.

- Penalty variables are included in the objective function. These are included when the system is infeasible, like a system where spillage occurs and there are no spillways. The punishment variables add value to the objective function so the user understands something is wrong with the system while making the problem feasible.
- A PQ-curve is generated to describe the relationship between the power produced and water tapped. Since SHOP is based on a linear model, the PQ-curve gets divided into linear segments by piecewise linearization with dynamically set breakpoints. In the *Wind Optimization Model*, there is a constant efficiency curve of 100% for both the generator and turbine because there should be a linear relationship between inflow into the model and power produced. The model generates three different segment variables that combined equal the total generation. Some constraints balance the segment variables compared to the total generation in the model.
- Head optimization generation variables are included to account for the heightened efficiency from a higher magazine level. Since the level of the reservoir in the model is constant, this variable is zero in all cases and therefore not included in the optimization problem (5.7).

Alternative wind optimization

One can also create an optimization model that can solve this problem without the use of SHOP. This system is shown in 5.4. A possible model for this optimization is shown in the optimization problem (5.8). This solution uses binary variables and the big-M method described in Section 4.1.3. It is also possible to

use this model in more than one time-step.

$$\max z = \sum_t \sum_s \rho_s \cdot x_{t,s} \cdot p_{t,s} + \sum_t \sum_s \rho_s \cdot P_d \cdot (w_{t,s} - x_{t,s}) \cdot b_{1s} - \sum_t \sum_s \rho_s \cdot P_u \cdot (x_{t,s} - w_{t,s}) \cdot b_{2s} \quad (5.8a)$$

s.t.

$$w_{t,s} - x_{t,s} \leq M \cdot b_{1t,s} \quad s \in S \quad t \in T \quad (5.8b)$$

$$x_{t,s} - w_{t,s} \leq M \cdot b_{2t,s} \quad s \in S \quad t \in T \quad (5.8c)$$

$$w_{t,s} - x_{t,s} + M \cdot (1 - b_{2t,s}) \leq M \quad s \in S \quad t \in T \quad (5.8d)$$

$$x_{t,s} - w_{t,s} + M \cdot (1 - b_{1t,s}) \leq M \quad s \in S \quad t \in T \quad (5.8e)$$

$$b_{1t,s} + b_{2t,s} = 1 \quad s \in S \quad t \in T \quad (5.8f)$$

$$0 \leq x_{t,s} \leq x_{max} \quad s \in S \quad t \in T \quad (5.8g)$$

Sets

S : set of scenarios, $s \in S$

T : set of hours, $t \in T$

Parameters

$p_{t,s}$: the power price in the DAM in time step t during scenario s

$w_{t,s}$: windpower produced in time step t during scenario s

P_u : price for up-regulating production

P_d : price for down-regulating production

ρ_s : probability of scenario s

x_{max} : maximum production

x_{min} : minimum production

Variables

$x_{t,s}$: Power produced in the power plant in time step t during scenario s .

$b_{1t,s}$: Binary variable. Active when windpower produced is larger than power bid in scenario s .

$b_{2t,s}$: Binary variable. Active when windpower produced is smaller than power bid in scenario s .

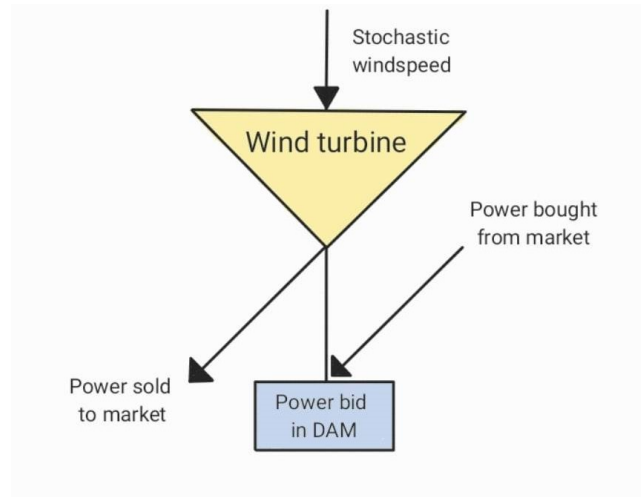


Figure 5.4: The physical system that the model is to represent.

5.4 Flowchart

The flowchart in this masters thesis has been developed through several stages, such as the project thesis [6], a paper for the SEST conference, and finally the version depicted in Figure 5.5. The proposed flowchart gives an overview of the author's version of the joint wind-hydro planning algorithm WHOP for scheduling

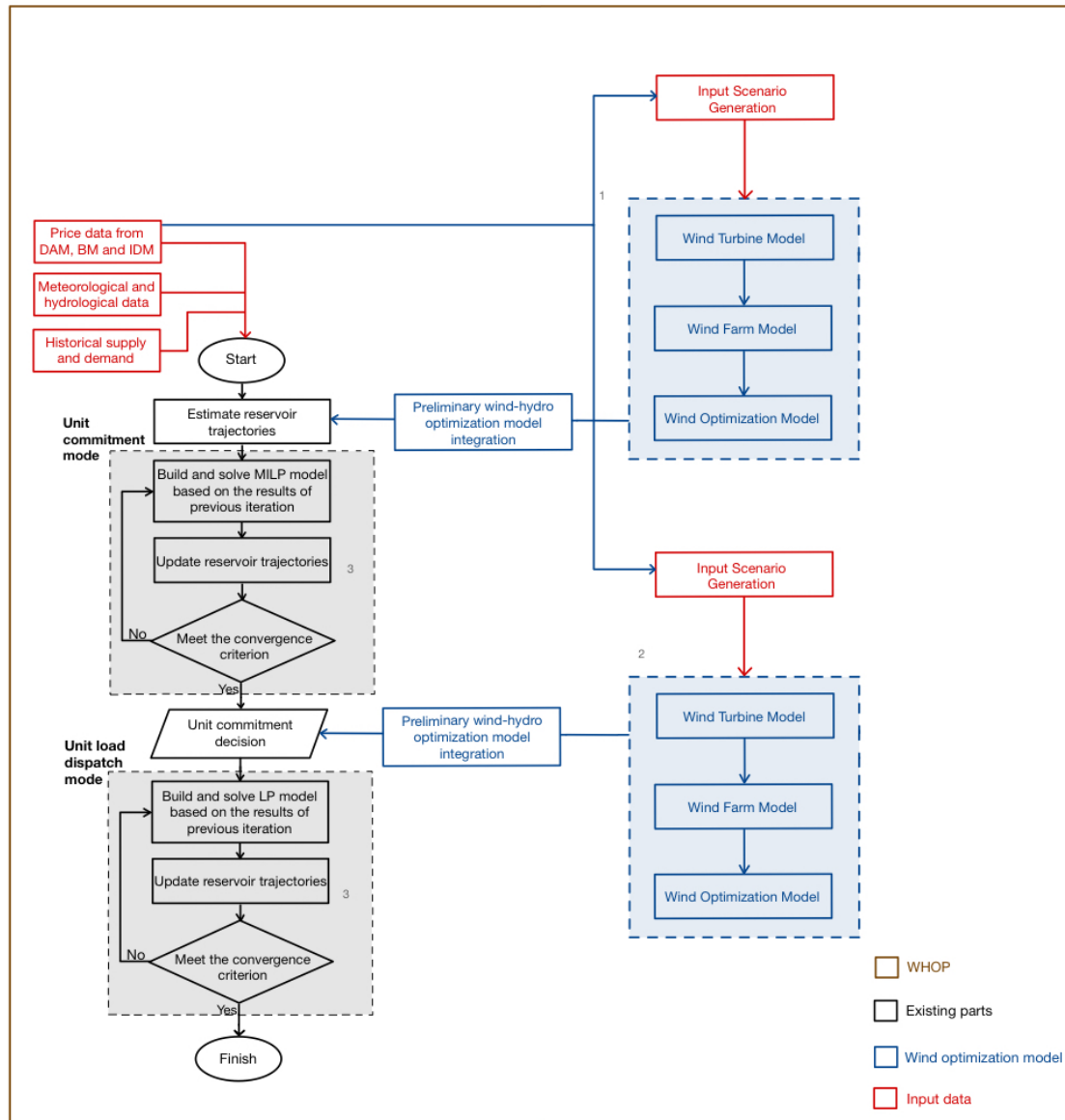


Figure 5.5: Flowchart showing the solution strategy for the WHOP model. The black-marked SHOP part of the flowchart is based on the flowchart in [65].

and cooperation between the power plants. As observed, the model is divided into four color schemes, which will be briefly described, before the boxes labeled 1, 2 and 3 on the flowchart are further elaborated.

The black color represents the existing SHOP tool as how it functions in SINTEF's SHOP VLAB. This is further explained in [65] and Sections 4.2.1 and 4.3. The red boxes are the input data in the model. For the SHOP tool, this means price data from all three markets; DAM, IDM and BM. Local hydrological and meteorological information, as well as historical supply and demand, need to be included. This is to better represent the hydropower reservoirs characteristics. As can be seen, the price data is also critical for the *Input Scenario Generation* entering the blue *Wind Optimization Model*. However, in this stage of the development of the *Wind Optimization Model* only the DAM data is used. The *Input Scenario Generation* model was explained in Section 5.2, and the *Wind Optimization Model* in Section 5.3. The same price data information must be given to both the SHOP tool and the input scenario generation in order to ensure effective and correct co-scheduling.

As SHOP is divided into two stages; the UC mode and the ULD mode, the *Wind Optimization Model* also needs to be divided as such. Hence, there are two blocks of wind optimization and input scenario generation and their integration into the SHOP tool. The *Wind Optimization Model* is divided into three stages. Firstly, a wind turbine model is developed, which builds around the specific characteristics of the wind turbine used. In this thesis, a Vestas V136-4.2 turbine has been used, as was explained in Section 5.1.1. Next, a model for the whole wind farm needs to be developed. The user can scale up the wind turbine into a wind farm by adding the production properties of their number of wind turbines in this stage of the model. Lastly, by incorporating the wind farm model and the input scenarios generated, the *Wind Optimization Model* is created. A more detailed explanation can be found in Section 5.3. A preliminary integration between the *Wind Optimization Model* and the hydro optimization model has also been developed in this master thesis. It is preliminary because it runs the two without a means of affecting the others' price or production, effectively running the models independently. A more advanced integration of power markets needs to be developed in the future and is discussed more in Chapter 9, covering future work. The totality of all parts explained here will be the new WHOP tool. This is shown as the brown square encompassing the three parts in black, red and blue.

The WHOP model has several essential components that make it an important tool for enhancing wind and hydropower operations. These exact qualities were also identified in A.1 and the project thesis [6] and consist of:

1. The *Wind Optimization Model* enters SHOP before the hydropower scheduling's UC mode. This mode of the SHOP model determines the on/off status of each generator and is typically finished in time for the hydropower producers to enter their bids into the DAM. The decisions in this stage is based on the STHS model and constraints the hydropower producer uses in their scheduling and are usually quite certain. However, the initial predictions in the *Wind Optimization Model* may not be accurate for the DAM bids, as wind forecasts are unreliable 12-36 hours in advance. But, they do have a clear indication of whether or not wind can be expected the following day and the general predominant wind speed. With the help of the WHOP tool, the wind producers will receive a preliminary generation optimization model. The hydropower producer can more accurately assess their expected production by considering the estimated windpower production based on these preliminary forecasts. The accuracy of the wind forecasting 12-36 hours prior to the period of production determines how much hydro producers need to consider wind forecasting and wind scheduling. This can be researched by examining wind forecasting data, wind speed data, or studies that have already been done on the subject.
2. The *Wind Optimization Model* enters SHOP prior to the ULD mode and constitutes the second area of interest. Here, the hydropower producer often increases or decreases the regulation of their output in order to submit bids in the IDM or sell any free capacity to the TSO in the BM. The *Wind Optimization Model* entering the ULD stage has a higher degree of precision than the generation estimation created for the DAM in the UC mode, as wind forecasts are more accurate for short-term predictions of just a few hours, as was shown in Section 4.6. The hydropower producer can now adjust their output

accordingly. This model is beneficial, especially for the wind producer as wind speed predictions would still not be entirely accurate. As a result, windpower producers generally have to pay a fee in the BM for inaccurate wind speed forecasting. The windpower generator may suffer a sizable loss if these prices are much higher than the DAM and IDM. If they can rather balance through the hydropower producer, the wind producer can significantly decrease monetary losses.

3. For the third area of interest, the hydro reservoir trajectories are updated concurrently with the new wind energy trajectories in the UC and ULD modes. Here, the generation of wind energy will be updated in comparison to hydropower. It is essential to ensure that market bids for both wind and hydro are met. As long as the UC mode is fixed and the system is in marginal condition, it is possible to make minor adjustments to hydro production in the ULD mode. This depends on whether it is possible or necessary to change the position of the IDM and the BM in accordance with the market load.

Chapter 6

Results

As mentioned in Chapter 5, Methodology, the case study was performed based on data from 8-9 AM, 12-1 PM and 4-5 PM. A selected range of results from the input scenario generation algorithm is presented in this section. This entails the 365 scenario case and the yearly 25 and 50 scenario cases for 4-5 PM. The seasonal cases for 4-5 PM are also presented here. Regarding the input generation for 8-9 AM and 12-1 PM, these can be found in the Appendix A.3. The scenario cases generated for 12-1 PM are excluded from the main text because the market prices were lower than the 4-5 PM cases for all scenarios and were hence deemed less interesting to investigate. The 8-9 AM scenario cases yielded market price values between 12-1 PM and 4-5 PM, in addition to having a more stable market price distribution than the 4-5 PM cases. Hence, the scenario cases for 4-5 PM were the most interesting to analyze and are the ones depicted in this section. For these reasons a seasonal investigation was only performed for the 4-5 PM cases. A table summarizing all scenario input cases is presented in Table 6.1, while the results from running the *Wind Optimization Model* with the different scenario cases are presented in Section 6.2. The expected production, price, and profit, as well as the Standard Deviation (SD) for each scenario case are also presented in the latter.

6.1 Input scenario generation algorithm

The input scenarios generated by the scenario reduction algorithm explained in Section 5.2 are presented in the following sections in the form of scatter plots. A summary of all 25 and 50 scenario cases across all hours is given in Section 6.1.4.

6.1.1 365 scenario case at 4-5 PM

The input values for the 365 scenario case for 4-5 PM can be observed in Figure 6.1. Because all days of the year are used in this case, every input scenario is weighted equally. Hence they have the same probability. Three extreme points for power produced and market price value are numbered in the scatter plot. The point's numbers represent the day of the year, as the scenarios covers every day of 2019. As the right legend shows, the colors of the points represent the different seasons during the year. The winter season includes data points from January, February and December; spring is March, April and May; summer is June, July and August; fall is September, October and November.

It can be observed that the maximum power prices occur on day 19, 21 and 310, with values around 60 EUR/MWh. The lowest power prices were observed on day 157, 159 and 160, at 10-15 EUR/MWh. The power produced is highest on day 45, 82 and 87 at approximately 175 MWh, and lowest on day 128, 286 and 329 at around 5 MWh. From further analysis of the figure, it is clear that the input price scenario centers around 40 EUR/MWh for most of the year. The power produced remains between 10 and 100 [MWh] for most scenario-days.

Additionally, one can observe that the extreme points for the market price values represent different times and seasons of the year. 19, 21 is at the beginning of the year, in the winter month of January, whereas 310 is in the fall month of November. Point 310 looks like an abnormality, but November is temperature wise a

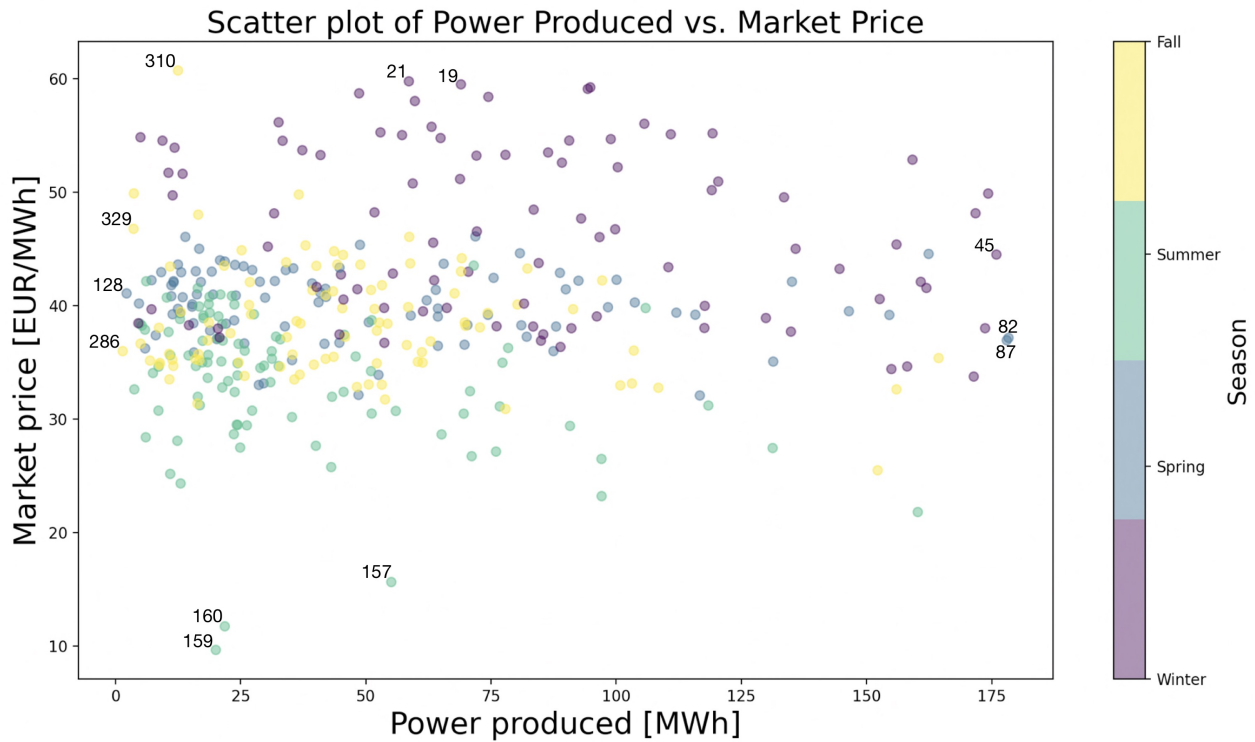


Figure 6.1: Scatter plot showing input data for 365 scenarios at 4-5 PM. Each point is a scenario, each with the same probability. The colors represent the four seasons and the scenarios within the respective season. Extreme points are numbered.

winter month in price zone NO3, and days with high prices is therefore a normal occurrence. Conversely, 157, 159 and 160 are early summer, when power prices are lower. The seasonal effect can be confirmed by observing that the general summer market price distribution is lower than the rest of the year. When it comes to power produced the observed trend is production below 100 MWh for most of the year. The extreme points differs from the market price in that all seasons seem to have an extreme point in the high and low spectrum of power produced. Meaning they do not seem to be as seasonally based as the market price. The 365 scenario scatter plots for 8-9 AM and 12-1 PM can be observed in Figure A.1 and A.2, respectively.

6.1.2 Yearly data points 25 and 50 scenario cases at 4-5 PM

This section presents the generated input values for the 25 and 50 scenario cases at 4-5 PM based on sampled data from the whole year of 2019. The colors in the plots represent the different generated scenarios. The size of the point represents its weighted probability.

Figure 6.2 represents the input data for the 25 scenario case at 4-5 PM. The minimum and maximum market price values are 29.5 EUR/MWh and 56.0 EUR/MWh, respectively. Scenario 11 yielded the highest probability with a production of 18.8 MWh at a market price value of 40.8 EUR/MWh. One can observe that the input price scenarios are located between 30-40 EUR/MWh, except for five more extreme points above 50 EUR/MWh.

The input data for the 50 scenario case with yearly data points from 4-5 PM is shown in Figure 6.3. Simi-

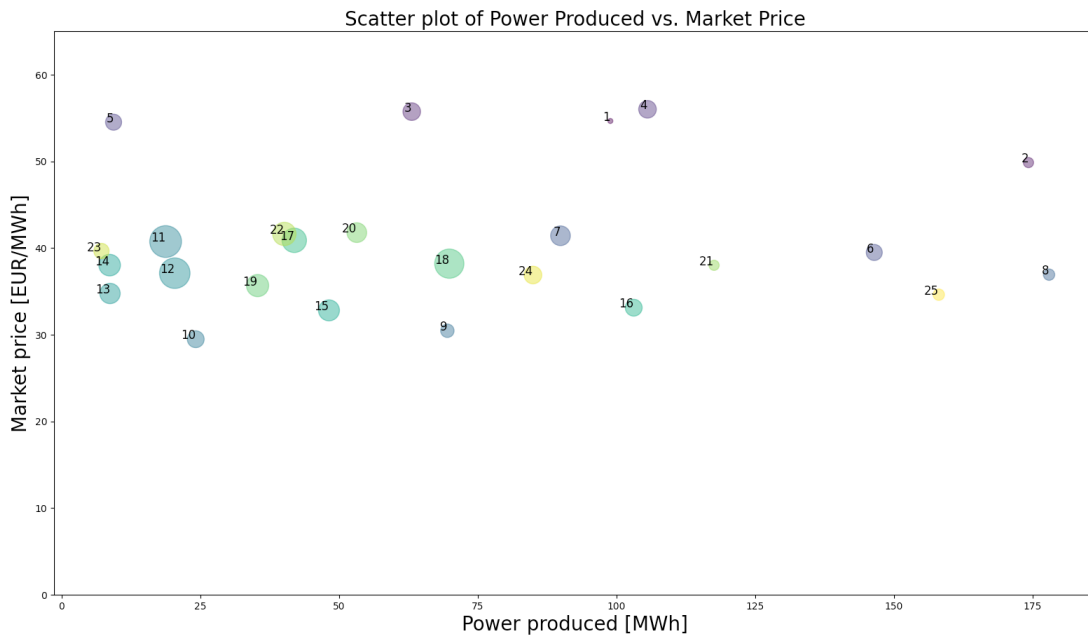


Figure 6.2: Scatter plot showing input data for 25 scenarios at 4-5 PM. Each point is a scenario, and the size of the plot indicates its probability. The color represent the different scenarios.

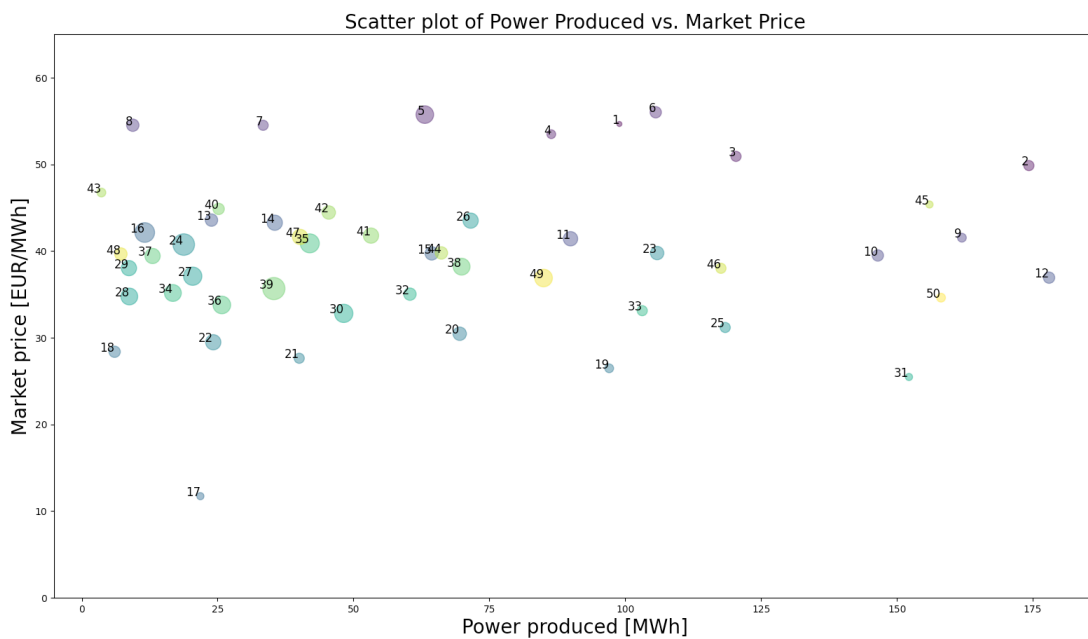


Figure 6.3: Scatter plot showing input data for 50 scenarios at 4-5 PM. Each point is a scenario, and the size of the plot indicates its probability. The color represents the different scenarios.

larly to the 25 scenario case the maximum market price value lies at 56.0 EUR/MWh. The minimum market price value is 11.7 EUR/MWh. The scenario yielding the highest probability is number 39, with a market price value of 35.7 EUR/MWh and power production of 35.3 MWh. For this case the scenarios' input price centers closer to 40 EUR/MWh than it did for the 25 scenario case. The extreme values are also more widely scattered both above and below the general price value. Furthermore, the 50 scenario case include more extreme data points than the 25 scenario case. However, it is worth noting that these extreme points have a relatively smaller probability.

6.1.3 Seasonal 25 and 50 scenario cases at 4-5 PM

This section presents the generated input values for the 25 and 50 scenario cases at 4-5 PM based on sampled data within each season in 2019. This means that the amount of data given to the scenario reduction algorithm has decreased from 365 data points to around 90 data points. In this section, the different scenarios do not have distinct colors. Instead, the color scheme is the same as the 365 scenario scatter plot where winter is purple, spring is blue, summer is green and fall is yellow.

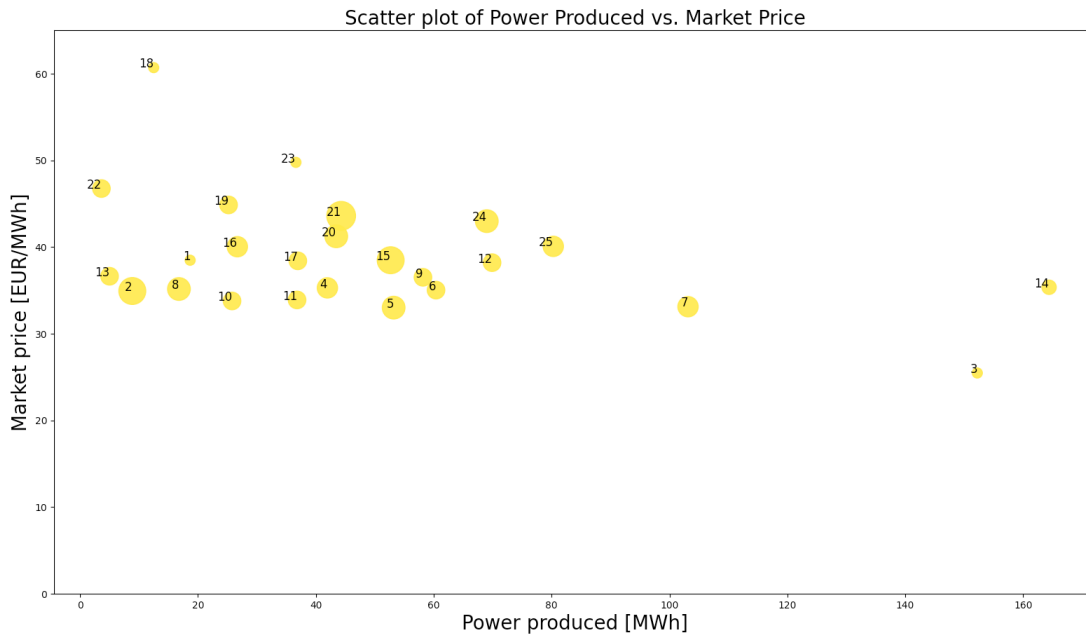


Figure 6.4: Scatter plot showing input data for 25 scenarios at 4-5 PM for the fall months. Each point is a scenario, and the size of the plot indicates its probability. The color is the same as the fall color from the 365 plot.

Figure 6.4 depicts the 25 scenario scatter plot for the fall at 4-5 PM. It can be observed that the general distribution centers around a market price of 40 EUR/MWh and a power produced of 10-80 MWh. Point 18 is an extreme point in the market price value direction and 3, 7 and 14 are extreme points for the power produced.

Table 6.1 presents the summary of all scenarios for all hours. From this table it is clear that the generated input values for the seasonal 25 scenario cases and for the seasonal 50 scenario cases are very similar. This can also be observed by comparing the fall scatter plot for 25 and 50 scenarios, shown in Figure 6.4 and 6.8 respectively. Hence, only the seasonal 25 scenario case for fall, is presented in this section. The rest of the seasonal scatter plots for the 25 scenario cases at 4-5 PM can be found in the Appendix A.3.

Winter

Key observations from the winter plot in Figure 6.5 is the even distribution across market price and power produced. It can be observed that the value difference within market price and power produced for the winter based scenarios is high, ranging from 35-60 EUR/MWh and 10-176 MWh. However, the probability is also evenly distributed, as seen in Section 6.1.4 which summarizes the different cases. For the winter case, as many as 8 scenarios yielded the identical highest probability, and many other scenarios with lower probability also yielded equal. This gives a clear indication of where one can expect the price and production to be at this time of the year.

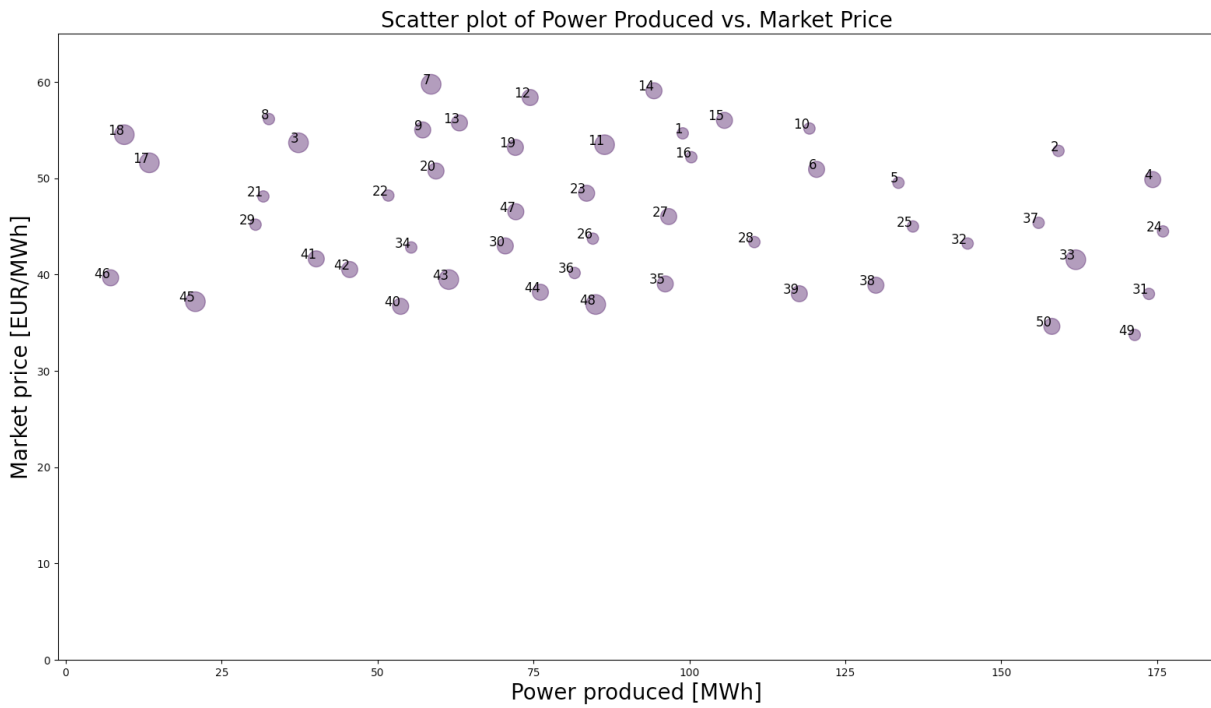


Figure 6.5: Scatter plot showing input data for 50 scenarios at 4-5 PM for the winter months. Each point is a scenario, and the size of the plot indicates its probability. The color is the same as the winter color from the 365 plot.

Spring

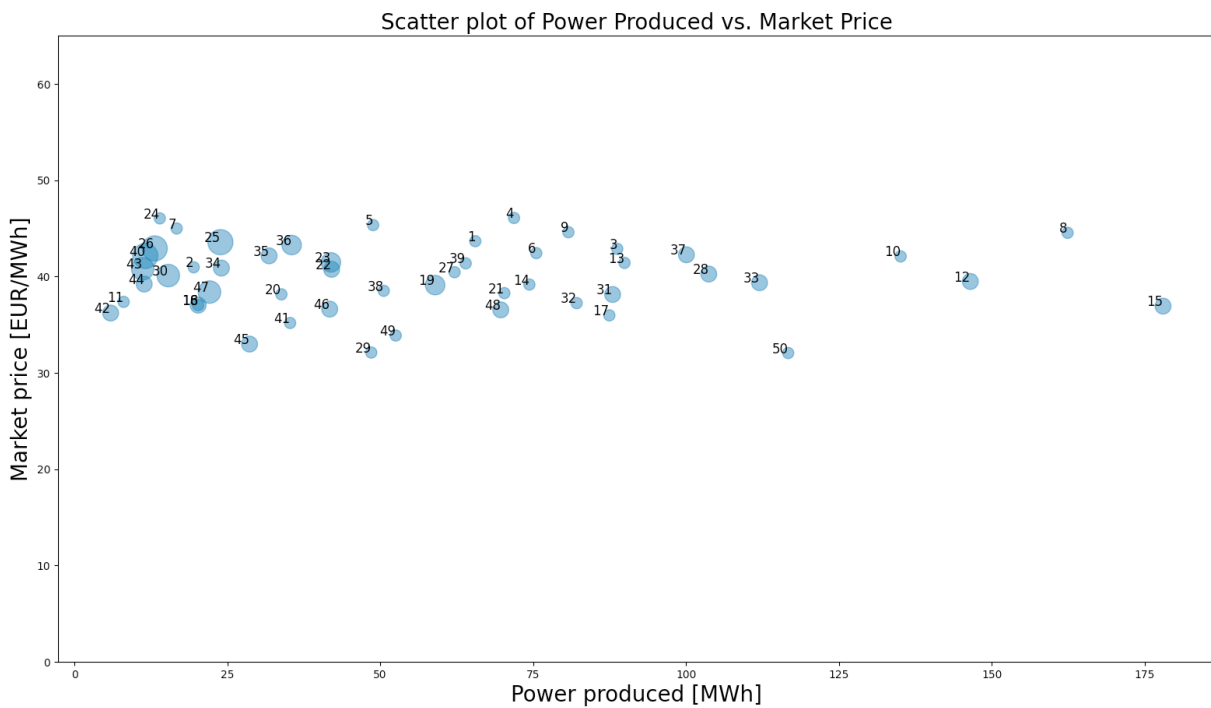


Figure 6.6: Scatter plot showing input data for 50 scenarios at 4-5 PM for the spring months. Each point is a scenario, and the size of the plot indicates its probability. The color is the same as the spring color from the 365 plot.

Figure 6.6 depicts the 50 scenarios case for the spring season. For this case, the distribution of scenarios are centered more towards the left side of the production scale, indicating an expectation of low production.

However, there are some extreme points touching up to what is observed in the 365 plot in Figure 6.1 to be maximum production. The market price distribution is relatively even, spread between 32 EUR/MWh and 46 EUR/MWh. For this case, as for the winter case, there are multiple scenarios with the same high probability. These are centered around 42-44 EUR/MWh and a production between 15-25 MWh. Further investigation shows that most scenarios with high probability are located around these intervals.

Summer

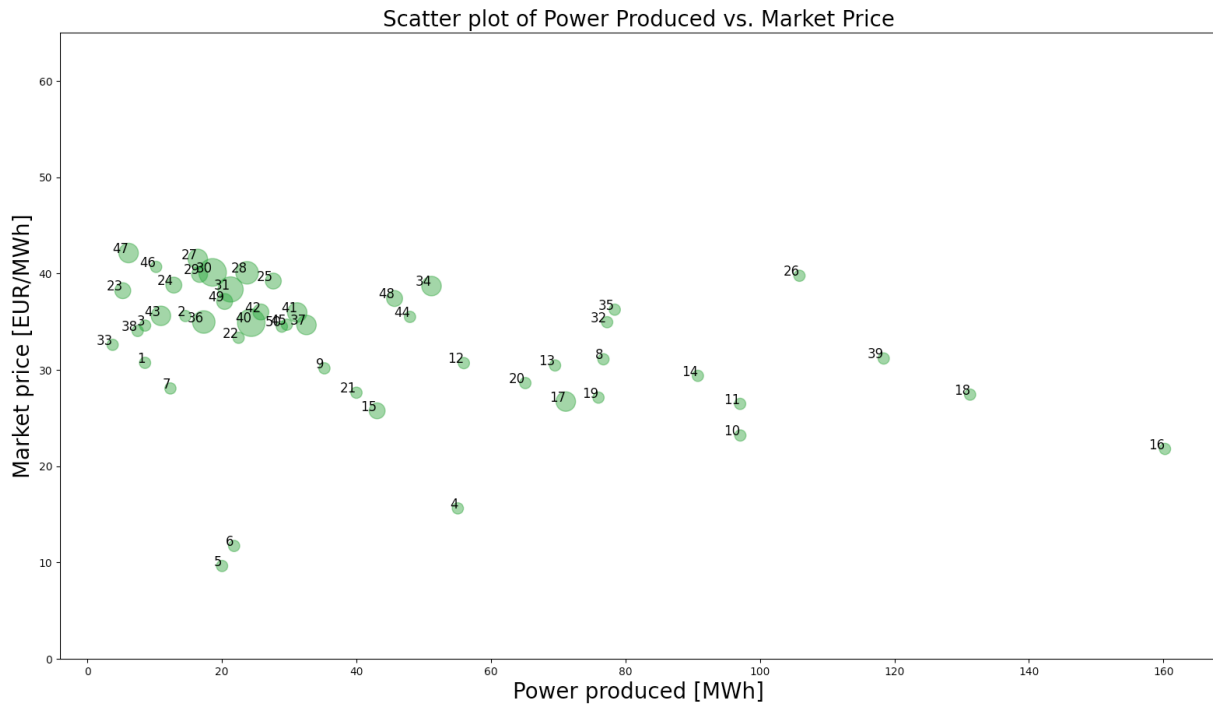


Figure 6.7: Scatter plot showing input data for 50 scenarios at 4-5 PM for the summer months. Each point is a scenario, and the size of the plot indicates its probability. The color is the same as the summer color from the 365 plot.

In Figure 6.7, where the summer months are represented in green, there is a clear trend for the market price value. This centers between 30 and 40 EUR/MWh. This is also where the highest probabilities lie. For power production, there are multiple scenarios distributed across the range, with the most data points below 80 MWh and the highest weight below 40 MWh. This shows that the general case for the summer is lower production at a lower price, with the occasional increase in production. As can be observed, there are also days with significantly lower market price value than the general case.

Fall

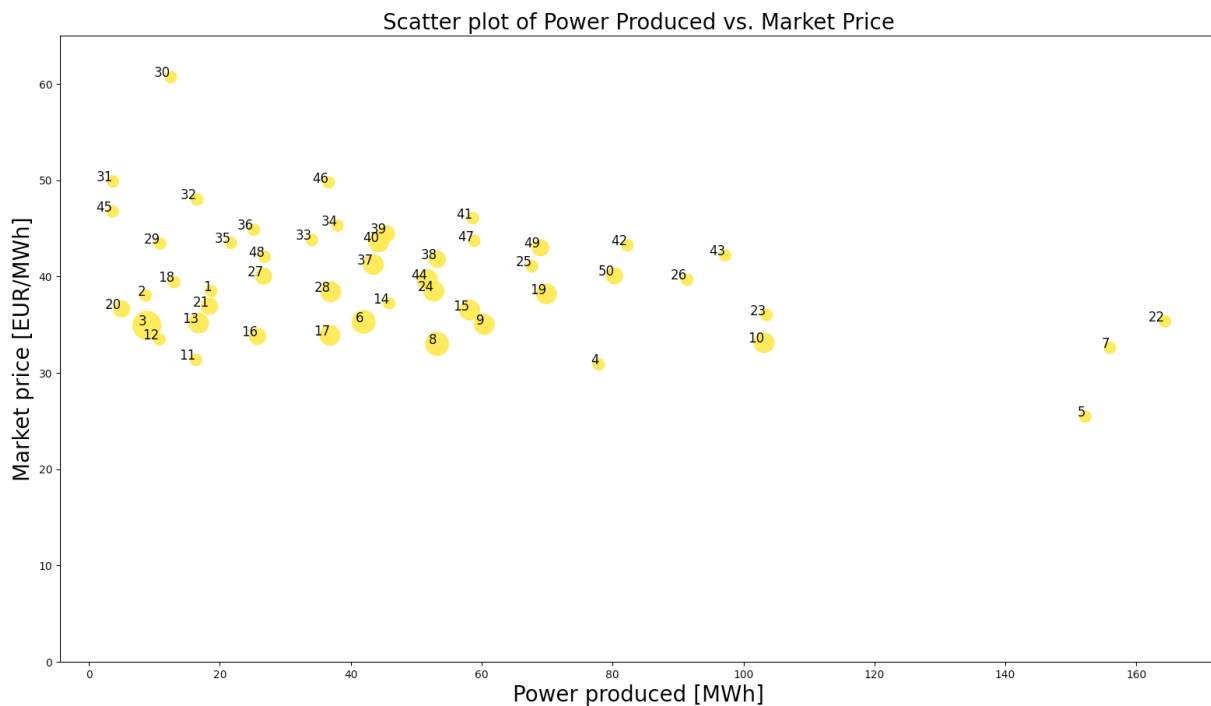


Figure 6.8: Scatter plot showing input data for 50 scenarios at 4-5 PM for the fall months. Each point is a scenario, and the size of the plot indicates its probability. The color is the same as the fall color from the 365 plot.

The 50 scenario case for the fall season is represented in Figure 6.8. Similarly to the previous cases, a trend can be observed, with extreme points indicating uncertainty in the expected production and market price. Here the general case for the market price is between 30 and 50 EUR/MWh, while the power produced is 5 to 100 MWh. Scenario number 3 clearly had the highest probability in this case, and the rest of the scenarios had a relatively even probability distribution. The observed extreme points differ noticeably for both the market price and the power produced. However, the probability for these scenarios is relatively low. Just like the spring case, this means that one can expect production and price within the general distribution, but with a slightly higher degree of uncertainty.

6.1.4 Summary of all input scenario cases

Table 6.1 summarizes the observations made in the input scenario scatter plots. This also includes observations made for the plots depicting 8-9 AM and 12-1 PM for the yearly 25, 50 and 365 scenario cases, as well as the seasonal 25 scenarios cases for 4-5 PM not shown in this results section. The table is organized in the following order from start to end.

- Yearly 25 and 50 scenario cases for all hours
- Seasonal 25 and 50 scenario cases for 4-5 PM

The 25 and 50 scenario cases with yearly data points are sequentially depicted at the three distinct hour intervals. The seasonal cases are presented sequentially, corresponding to the seasons' order, encompassing the 25 and 50 scenario cases within each seasonal depiction.

Additionally, the table gives an overview of the minimum and maximum market price values, and the scenario with the highest probability and its corresponding market price and power production values.

Table 6.1: A summary of the input values for 25 and 50 scenario cases for all hours. The respective scatter plots are either presented in the Chapter 6 or in Appendix A.3.

Case	Max. price [EUR/MWh]	Min. price [EUR/MWh]	Avg. price [EUR/MWh]	Max. prod. [MWh]	Avg. prod. [MWh]	Highest prob. and values
25, 8-9 AM	53.0	11.9	39.3	173.7	63.5	7, 43.8 EUR/MWh, 18.7 MWh
50, 8-9 AM	58.7	11.9	39.0	176.0	67.5	22, 44.2 EUR/MWh, 4.0 MWh
25, 12-1 PM	49.9	14.6	35.3	178.0	78.4	12, 28.0 EUR/MWh, 19.4 MWh
50, 12-1 PM	49.9	14.6	35.4	178.0	73.2	17, 28.0 EUR/MWh, 19.4 MWh
25, 4-5 PM	56.0	29.5	40.5	178.0	71.0	11, 40.8 EUR/MWh, 18.8 MWh
50, 4-5 PM	56.0	11.7	39.6	178.0	66.8	39, 35.7 EUR/MWh, 35.3 MWh
25, 4-5 PM winter	59.8	34.6	47.3	174.3	79.7	24, 36.9 EUR/MWh, 85.0 MWh
50, 4-5 PM winter	59.8	33.7	46.6	175.9	89.0	multiple*
25, 4-5 PM spring	46.1	32.1	39.8	178.0	64.3	9, 41.5 EUR/MWh, 41.9 MWh
50, 4-5 PM spring	46.1	32.1	39.9	178.0	58.3	multiple*
25, 4-5 PM summer	42.1	9.7	31.0	160.2	54.7	21, 34.9 EUR/MWh, 24.4 MWh
50, 4-5 PM summer	42.1	9.7	32.5	160.2	43.8	multiple*
25, 4-5 PM fall	60.7	25.5	38.9	164.4	49.9	21, 43.6 EUR/MWh, 44.3 MWh
50, 4-5 PM fall	60.7	25.5	39.7	164.4	49.1	3, 34.9 EUR/MWh, 8.9 MWh

* The case has multiple scenarios with the same probability. They are as follows:

- 50, 4-5 PM winter : 8 different scenarios; 3, 7, 11, 17, 18, 33, 43, 48.
- 50, 4-5 PM spring : 3 different scenarios; 25, 26, 40.
- 50, 4-5 PM summer : 2 different scenarios; 30, 40.

For the market price, it can be observed from Table 6.1 that the maximum power price is higher for winter and fall than summer and spring. For the yearly scenario cases, the maximum power price is somewhere in the middle of these two. The minimum market price is lower for summer and fall than for winter and spring. All scenario cases with yearly based input data have included the minimum extreme points. However, observations from the scatter plots in the Appendix, A.3.2, of the yearly scenario cases show that this captured minimum value is a single extreme point that significantly differs from the general trend. For all cases, the average market price follows the same trend observed in the maximum and minimum values, especially the seasonal scenario cases.

The yearly scenarios for the power produced seem to have captured the extreme points of high production, with maximum values across most scenarios at approximately 178.0 MWh. For the seasonal scenario cases, the power produced in the summer and fall is less than that produced during the winter and spring. The average production for winter is also significantly higher for any other seasonal cases. Spring has the second highest average production, and summer has the lowest across all cases.

Investigation of the scenario with the highest probability for all cases shows that it differs greatly from case to case. For the seasonal 50 scenario cases the number of points with the same probability increase to multiple points for winter, spring and summer. This could be because of the reduction from 365 to 90 input data points as compared to the yearly case. Further observations show that the two 12-1 PM cases are actually the same data points but with different numbering caused by the increase in scenarios. Apart from this hour the market price and power produced differ significantly from case to case.

6.2 Results from the *Wind Optimization Model*

This section provides an overview of the results when using the generated input scenario cases to check the functionality of the *Wind Optimization Model* and investigate the impact of varying up-regulation prices.

6.2.1 Expected power production, power price and profit

The expected power production, power price and profit for each scenario case can be calculated by Eq. (5.4), (5.5) and (5.6), respectively. Table 6.2, 6.3 and 6.4 shows these values for the yearly data, while Table 6.5 shows the seasonal results.

Table 6.2: Expected production, power price and profit for the yearly scenario cases at 8-9 AM.

Scenario case	Expected prod. [MWh]	Expected price [EUR/MWh]	Expected profit [EUR]
25	51.59	41.03	2100.43
50	51.00	40.06	2035.93
365	51.22	40.92	2120.63

Table 6.3: Expected production, power price and profit for the yearly scenario cases at 12-1 PM.

Scenario case	Expected prod. [MWh]	Expected price [EUR/MWh]	Expected profit [EUR]
25	53.40	36.33	1928.52
50	54.33	36.26	1953.01
365	54.16	39.89	2174.03

Table 6.4: Expected production, power price and profit for the yearly scenario cases at 4-5 PM.

Scenario case	Expected prod [MWh]	Expected price [EUR/MWh]	Expected profit [EUR]
25	52.11	39.66	2098.11
50	52.47	39.49	2102.68
365	53.41	39.62	2150.69

Table 6.5: Expected production, power price and profit for the seasonal scenario cases at 4-5 PM.

Season	Scenario case	Expected prod. [MWh]	Expected price [EUR/MWh]	Expected profit [EUR]
Winter	25	81.16	46.63	3717.91
	50	82.07	46.75	3771.61
Spring	25	50.05	40.15	1989.40
	50	49.23	40.13	1960.27
Summer	25	35.38	35.09	1150.46
	50	35.36	34.59	1138.11
Fall	25	46.39	38.44	1744.48
	50	46.83	38.60	1765.15

The SD is calculated and presented in Table 6.6 and 6.7, for yearly and seasonal input scenario data. This was done to be able to investigate the volatility in the distribution of the input scenarios.

It can be observed that the SD in production for summer and fall is notably lower than for winter and spring. It is also worth noting that the production's SD is approximately the same for both the yearly and seasonal 25 and 50 scenario cases. When it comes to the market price the SD is around 7-8 EUR/MWh for the yearly cases. By further comparison between the yearly cases one can also note that while the SD for 8-9 AM and 12-1 PM reduces from the 25 scenario case to the 50 scenario case, the deviation of price and production data at 4-5 PM has a significant increase from 25 to 50 scenarios. This is most likely related to the volatility within the investigated hours during the year. Further, one can observe that the seasonal cases have larger variations from season to season and from 25 scenarios to 50 scenarios. The former is logical as the different seasons have their own unique price patterns, and the latter could be a result of including more scenarios and hence getting more accurate distributions. Spring and fall prominently stand out compared to winter and summer, with much lower SD in price, at approximately 3 and 5 EUR/MWh.

Table 6.6: Standard deviation for the yearly 25 and 50 scenario cases across all hours.

Hour	Scenario case	SD price [EUR/MWh]	SD prod. [MWh]
8-9 AM	25	7.9	46.9
	50	7.2	47.7
12-1 PM	25	7.9	53.6
	50	6.6	52.0
4-5 PM	25	7.8	53.3
	50	8.8	51.1

Table 6.7: Standard deviation for the seasonal scenario cases at 4-5 PM.

Season	Scenario case	SD price [EUR/MWh]	SD prod. [MWh]
Winter	25	7.6	44.6
	50	7.5	46.1
Spring	25	3.0	41.9
	50	3.0	41.4
Summer	25	9.4	30.2
	50	6.2	30.0
Fall	25	4.9	32.2
	50	5.1	33.6

6.2.2 The impact of up and down regulation prices, yearly data

The *Wind Optimization Model* was tested with different up-regulation prices, starting at 110 EUR/MWh and decreasing by 5 EUR/MWh until the closest maximum DAM price in the scenario case. This is because, as mentioned in Section 5.3.2, the code is not functional if the up-regulation price is lower than the DAM price. Three distinct scenario cases were examined, consisting of 25 scenarios, 50 scenarios, and 365 scenarios. These scenario cases were tested using input scenario data obtained from the time periods of 8-9 AM, 12-1 PM, and 4-5 PM.

The results when running the 25, 50 and 365 scenarios cases based on yearly scenario data from the hour of 4-5 PM, are shown in Table 6.8, 6.9 and 6.10, respectively. The results for the similar scenario cases for hours 8-9 AM and 12-1 PM are presented in Appendix A.4. The tables show the optimal power bid into the DAM, including the profit earned with the given power production and power prices. It also shows the difference in profit compared to the expected profit calculated in Section 6.2.1 and the decrease shown in percentage.

Table 6.8: Results from running the *Wind Optimization Model* with 25 scenarios from data between 4-5 PM. The input data is shown in Figure 6.2.

Up-regulation price [EUR/MWh]	Down-regulation price [EUR/MWh]	Power bid [MWh]	Profit [EUR]	Difference [EUR]	Percentage decrease in profit
110	10	20.42	937.21	-1160.90	55.33%
105	10	20.42	946.69	-1151.42	54.88%
100	10	20.42	956.17	-1141.99	54.43%
95	10	20.42	965.65	-1131.46	53.93%
90	10	24.20	981.18	-1116.93	53.20%
85	10	35.35	1009.48	-1088.63	51.89%
80	10	35.35	1046.81	-1051.30	50.11%
75	10	40.17	1091.17	-1006.94	47.99%
70	10	41.96	1139.64	-958.47	45.68%
65	10	41.96	1191.80	-906.31	43.19%

Table 6.9: Results from running the *Wind Optimization Model* with 50 scenarios from data between 4-5 PM. The input data is shown in Figure 6.3.

Up-regulation price [EUR/MWh]	Down-regulation price [EUR/MWh]	Power bid [MWh]	Profit [EUR]	Difference [EUR]	Percentage decrease in profit
110	10	21.83	916.83	-1185.85	55.14%
105	10	23.87	931.86	-1170.82	54.44%
100	10	24.20	947.94	-1154.74	53.69%
95	10	25.19	964.91	-1137.77	52.90%
90	10	25.78	983.56	-1119.12	52.04%
85	10	33.38	1007.89	-1094.79	50.90%
80	10	35.35	1045.00	-1057.68	49.18%
75	10	35.53	1082.37	-1020.31	47.44%
70	10	40.17	1125.61	-977.07	45.43%
65	10	41.96	1177.15	-925.53	43.03%

Table 6.10: Results from running the *Wind Optimization Model* with 365 scenarios from data between 4-5 PM. The input data is shown in Figure 6.1.

Up-regulation price [EUR/MWh]	Down-regulation price [EUR/MWh]	Power bid [MWh]	Profit [EUR]	Difference [EUR]	Percentage decrease in profit
110	10	22.95	937.36	-1213.33	56.4%
105	10	23.81	952.04	-1198.65	55.7%
100	10	24.57	967.78	-1182.91	55.0%
95	10	25.81	985.21	-1165.48	54.2%
90	10	28.63	1005.60	-1145.09	53.2%
85	10	31.24	1031.38	-1119.31	52.0%
80	10	34.00	1062.60	-1088.09	50.6%
75	10	37.32	1100.20	-1050.49	48.8%
70	10	41.96	1148.33	-1002.36	46.6%
65	10	45.69	1206.35	-944.34	43.9%

Figure 6.9 presents the difference in profit when running the *Wind Optimization Model* with a different number of scenarios for the yearly data from 4-5 PM.

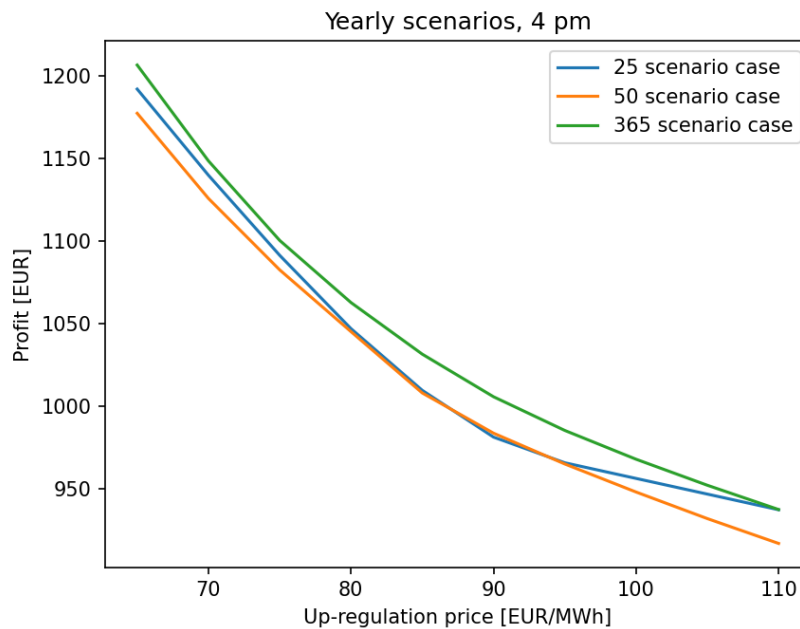


Figure 6.9: Profit when running the *Wind Optimization Model* with 25, 50 and 365 scenarios from yearly data points at 4-5 PM.

6.2.3 The impact of up and down regulation prices at 4-5 PM, seasonal data

The results when running the 25 and 50 scenario cases in the *Wind Optimization Model*, based on seasonal scenario data from the hour of 4-5 PM for winter, spring, summer and fall, are both shown in Table 6.11, 6.12, 6.13 and 6.14, respectively. The tables show the optimal power bid in the DAM, the corresponding profit and the percentage decrease in profit compared to the expected profit for both the 25 and 50 scenario cases. A comparison of the profit gained from the 25 and 50 scenario cases in the given seasons is shown in Figures 6.10, 6.11, 6.12 and 6.13.

As explained in the previous section, the scatter plots representing the seasonal 25 scenario cases can be found in the Appendix A.3 as they were quite similar to the 50 scenario cases.

Winter

Results from the *Wind Optimization Model* based on the input scenario data from winter shown for the 25 and 50 scenario cases in Figures A.7 and 6.5, respectively. The difference in profit for the 25 and 50 scenario cases based on winter scenarios is compared in 6.10.

Table 6.11: Result from the *Wind Optimization Model* with both 25 and 50 input scenario cases based on data from the winter season at 4-5 PM.

Up-regulation price	Down-regulation price	Power bid in DAM [MWh] 25 scenarios	Objective value [EUR/MWh] 25 scenarios	Percentage decrease in profit 25 scenarios	Power bid in DAM [MWh] 50 scenarios	Objective value [EUR/MWh] 50 scenarios	Percentage decrease in profit 50 scenarios
110	10	61.42	2203.15	40.74 %	61.42	2168.16	42.51 %
105	10	63.13	2247.35	39.55 %	61.42	2213.64	41.31 %
100	10	63.13	2293.51	38.31 %	63.13	2262.12	40.02 %
95	10	70.48	2345.14	36.92 %	70.48	2324.17	38.38 %
90	10	70.48	2406.81	35.26 %	72.17	2391.48	36.59 %
85	10	72.17	2471.24	33.53 %	74.47	2461.17	34.74 %
80	10	84.98	2547.84	31.47 %	81.6	2538.17	32.70 %
75	10	84.98	2646.2	28.83 %	84.52	2634.33	30.15 %
70	10	86.4	2745.46	26.16 %	86.4	2736.07	27.46 %
65	10	86.4	2848.08	23.40 %	96.13	2857.47	24.24 %
60	10	98.93	2983.17	19.76 %	105.62	3003.99	20.35 %

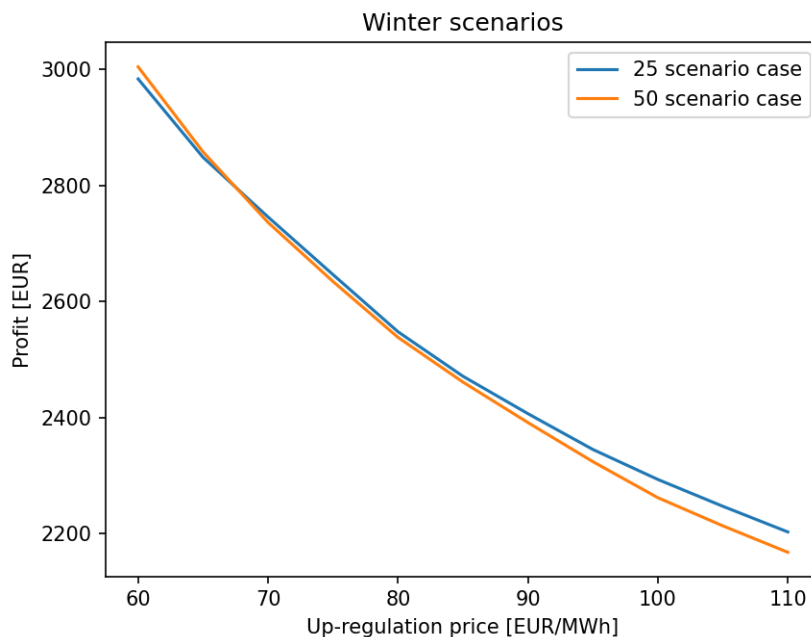


Figure 6.10: A comparison of the profits from running the 25 and 50 scenario case in the *Wind Optimization Model* for data based on the winter season at 4-5 PM.

Spring

Results from the *Wind Optimization Model* based on the input scenario data from spring shown for the 25 and 50 scenario cases in Figures A.8 and 6.6, respectively. The difference in profit for the 25 and 50 scenario cases based on spring scenarios is compared in 6.11.

Table 6.12: Result from the *Wind Optimization Model* with both 25 and 50 input scenario cases based on data from the spring season at 4-5 PM.

Up-regulation price	Down-regulation price	Power bid in DAM [MWh] 25 scenarios	Objective value [EUR/MWh] 25 scenarios	Percentage decrease in profit 25 scenarios	Power bid in DAM [MWh] 50 scenarios	Objective value [EUR/MWh] 50 scenarios	Percentage decrease in profit 50 scenarios
110	10	20.23	880.78	55.07 %	20.23	916.32	53.94 %
105	10	22.08	892.19	54.49 %	20.23	926.01	53.45 %
100	10	22.08	906.16	53.77 %	22.08	937.22	52.89 %
95	10	22.08	920.14	53.06 %	22.08	949.92	52.25 %
90	10	23.87	936.69	52.22 %	22.08	962.63	51.61 %
85	10	23.87	953.88	51.34 %	23.87	978.26	50.83 %
80	10	24.03	971.27	50.45 %	23.87	994.37	50.02 %
75	10	31.83	998.86	49.04 %	28.63	1019.56	48.75 %
70	10	35.52	1037.73	47.06 %	35.52	1056.14	46.91 %
65	10	41.74	1086.71	44.56 %	41.74	1108.18	44.30 %
60	10	42.05	1147.59	41.46 %	41.94	1167.81	41.30 %
55	10	58.98	1237.87	36.85 %	58.98	1258.02	36.76 %
50	10	71.88	1374.89	29.86 %	69.71	1388.97	30.18 %

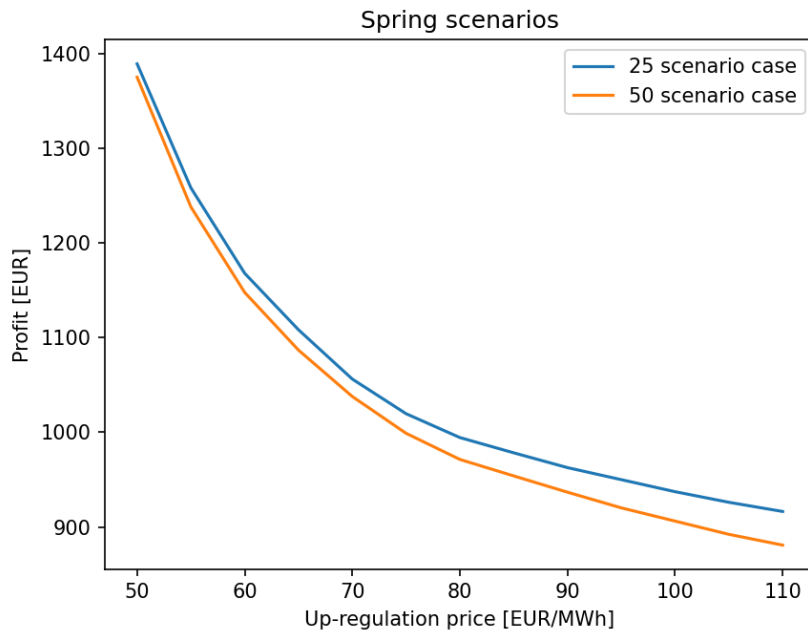


Figure 6.11: A comparison of the profits from running the 25 and 50 scenario case in the *Wind Optimization Model* for data based on the spring season at 4-5 PM.

Summer

Results from the *Wind Optimization Model* based on the input scenario data from summer shown for the 25 and 50 scenario cases in Figures A.9 and 6.7, respectively. The difference in profit for the 25 and 50 scenario cases based on summer scenarios is compared in 6.12.

Table 6.13: Result from the *Wind Optimization Model* with both 25 and 50 input scenario cases based on data from the summer season at 4-5 PM.

Up-regulation price	Down-regulation price	Power bid in DAM [MWh] 25 scenarios	Objective value [EUR/MWh] 25 scenarios	Percentage decrease in profit 25 scenarios	Power bid in DAM [MWh] 50 scenarios	Objective value [EUR/MWh] 50 scenarios	Percentage decrease in profit 50 scenarios
110	10	16.43	625.02	45.67 %	17.32	627.1	44.90 %
105	10	16.43	632.08	45.06 %	17.32	634.74	44.23 %
100	10	16.43	639.15	44.44 %	17.32	642.38	43.56 %
95	10	18.63	648.53	43.63 %	18.63	650.75	42.82 %
90	10	18.63	658.7	42.74 %	18.63	660.25	41.99 %
85	10	18.63	668.87	41.86 %	18.63	669.74	41.15 %
80	10	20.04	680.08	40.89 %	20.04	679.56	40.29 %
75	10	21.31	694.94	39.59 %	20.42	691.99	39.20 %
70	10	21.31	709.84	38.30 %	21.31	706.18	37.95 %
65	10	21.83	725.04	36.98 %	22.5	722.9	36.48 %
60	10	24.38	746.84	35.08 %	23.76	740.06	34.97 %
55	10	24.38	768.72	33.18 %	24.38	761.17	33.12 %
50	10	28.93	797.9	30.64 %	28.93	787.71	30.79 %

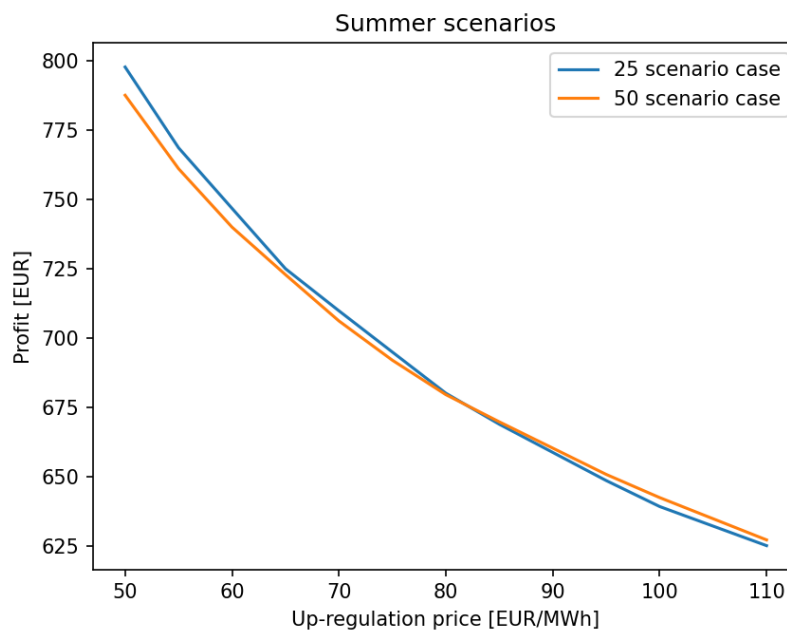


Figure 6.12: A comparison of the profits from running the 25 and 50 scenario case in the *Wind Optimization Model* for data based on the summer season at 4-5 PM.

Fall

Results from the *Wind Optimization Model* based on the input scenario data from fall shown for the 25 and 50 scenario cases in Figures 6.4 and 6.8, respectively. The difference in profit for the 25 and 50 scenario cases based on fall scenarios is compared in 6.13.

Table 6.14: Result from the *Wind Optimization Model* with both 25 and 50 input scenario cases based on data from the fall season at 4-5 PM.

Up-regulation price	Down-regulation price	Power bid in DAM [MWh] 25 scenarios	Objective value [EUR/MWh] 25 scenarios	Percentage decrease in profit 25 scenarios	Power bid in DAM [MWh] 50 scenarios	Objective value [EUR/MWh] 50 scenarios	Percentage decrease in profit 50 scenarios
110	10	25.78	854.64	51.01 %	25.78	849.57	51.87 %
105	10	26.68	872.93	49.96 %	26.68	867.75	50.84 %
100	10	26.68	891.35	48.90 %	26.68	886.92	49.75 %
95	10	36.62	913.79	47.62 %	34.08	910.29	48.43 %
90	10	36.62	948.82	45.61 %	36.81	945.08	46.46 %
85	10	36.62	984.01	43.59 %	36.81	981.11	44.42 %
80	10	36.62	1019.39	41.56 %	36.81	1017.35	42.36 %
75	10	41.96	1064.78	38.96 %	41.96	1057.94	40.07 %
70	10	43.46	1112.46	36.23 %	43.46	1105.26	37.38 %
65	10	44.29	1261.94	27.66 %	44.29	1156.45	34.48 %

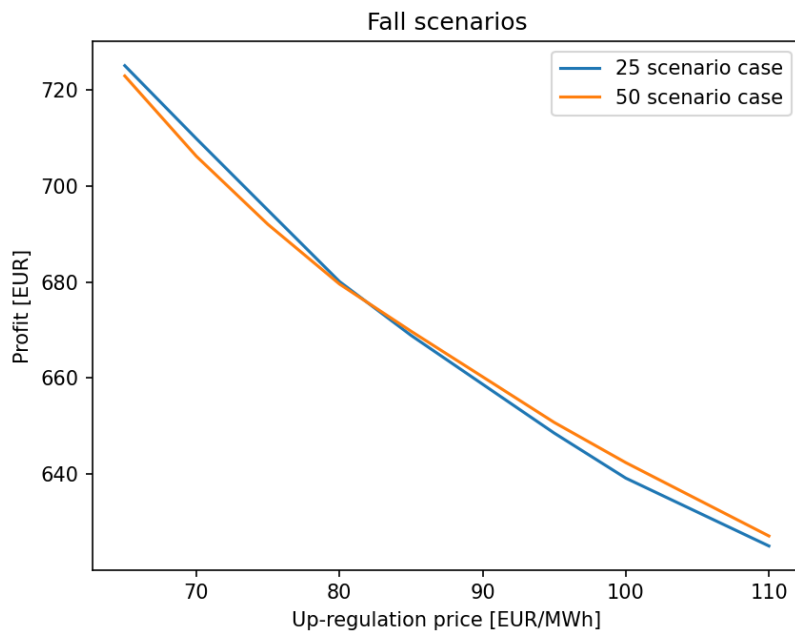


Figure 6.13: A comparison of the profits from running the 25 and 50 scenario case in the *Wind Optimization Model* for data based on the fall season at 4-5 PM.

Chapter 7

Discussion

This chapter will discuss the observations from the results through identified key topics. Additionally, limitations derived from the lack of sufficient input data and by using a hydropower specific optimization tool are commented and discussed.

7.1 Seasonal dependency

The *Wind Optimization Model* was initially run with input scenarios based on data from one whole year. The model results for 4-5 PM are shown in Section 6.2.2 while the results from 8-9 AM and 12-1 PM are shown in Appendix A.4. From these results, one can observe that the reduction in profit compared to the case with perfect information varies from 58% to 43% across the different times of the day. This significant decrease in profits has substantial implications for windpower producers. A reason for this significant reduction is the large price and production variation in the different scenarios when basing the scenarios on data from the entire year. As elaborated in Section 3.7, power prices in Norway are seasonally dependent because of the large penetration of hydropower production in the power grid and seasonal load fluctuations. This can be observed by looking at Figure 6.1, which depicts all 365 data points for 4-5 PM. From this scatter plot, one can also observe that the scenarios for different seasons share similar values. This can also be observed in Table 6.6, where the SD in price and production for the 25 and 50 scenario cases at 4-5 PM is relatively high compared to 8-9 AM and 12-1 PM. Incorporating scenarios based on the power prices from the whole year can therefore insert the model with more uncertainty than the windpower producer actually experiences when deciding what to bid into the DAM. To mitigate this issue, a decision was made to generate scenarios based on historical data from each distinct season to see if this decreases the reduction in profit.

From Figure 6.1, one can observe the trend of general higher power production and power prices during winter and less production and lower prices during the summer season. The results from running the *Wind Optimization Model* with seasonal input scenarios based on data from 4-5 PM are presented in Section 6.2.3. From these results, one can observe that the percentage decrease in profit is relatively smaller during all seasons compared to the scenario cases with input scenarios for the whole year. From Table 6.7, one can also observe a decrease in SD across all seasons because of the reduced uncertainty in seasonally based input scenarios. The season with the lowest decrease in profit compared to the perfect information case is the winter, which varies from approximately 20-40%. While spring and fall vary the most by approximately 30-55%, which is still lower than the variation of the yearly scenario case.

As the Norwegian power system historically has been dominated by hydropower, so has the market price. This means that the prices used in this case study follow hydropower production trends, which in 2019 mainly consisted of hydropower plants in the price zone NO3. The uncertainty in price and production is relatively low in the winter because the producer knows that inflow is usually low, meaning that the stored water is the only available water for production. As seen from Figure 7.2, the load is also relatively stable within the season. However, uncertainty increases during spring because of the difficulty predicting what time the snow melting will start and if the season will be dry or wet. Summer is more certain again, with a high degree of filling in the reservoir allowing for more flexibility. Fall is similar to spring, with uncertainty

related to the weather in terms of precipitation, temperature and consequently, the load demand. However, in recent years hydropower is no longer the only market participant because of the introduction of windpower installations. Since these windpower installations had yet to be installed during data used for 2019, one would presume the seasonal uncertainty price development explained above. Despite that, Table 6.7 shows that the standard deviation for the market price is the lowest for the spring season. A contradiction of the general understanding of seasonal price fluctuations. However, the percentage decrease in profit is highest during spring and fall, indicating higher uncertainty levels during these seasons. This can be attributed to the fact that there are some volatility factors in the market price that have not been considered in this thesis. Another reason could be that windpower production is independent of hydropower production in the way the power system works today. Hence, the profit for the windpower producer is evidently more dependent on windpower production rather than market price. This might be the main reason for the observed volatility in the wind producers' profit in the spring case, where the standard deviation in market price is low. As mentioned, the market price is higher in the winter season compared to spring. This means that even though the standard deviation is low during spring, the relative deviation compared to winter is higher than initially estimated.

From the expected profit during different seasons, shown in Table 6.5, one can see that the profit is significantly higher during winter than summer, while profit is similar during spring and fall. The high power prices during winter derive from the decreasing degree of filling in the hydropower reservoirs during this season, as seen by Figure 7.1. From Table 7.1, it can be observed that 2019 was a relatively wet year, and one can therefore expect to have seen lower market prices compared to years with a lower degree of filling. The average degree of filling might not give an accurate picture of the power prices during the year since it does not include hydropower production or seasonal variability in the degree of filling. However, it does provide general information on the price level of the given year in a hydro-dominated market. Another cause for the observed higher prices is the high load demand necessary for heating during a cold season like winter in Norway, as seen in Figure 7.2 depicting the yearly load variability in price zone NO3. The low prices in the summer come from an excess of water in the reservoirs, after being filled by the spring floods. A hydropower producer will then utilize tools such as SHOP to produce power at a level that maximizes profit while avoiding spillage, often resulting in high levels of production. This high degree of hydropower production will, in a price zone with a high enough penetration rate of hydropower, lower the prices in a market.

The analysis of Table 6.5 reveals that expected windpower production during the winter season is significantly greater compared to the other seasons. Summer demonstrates the lowest levels of production. Examination of data presented in [110] from January 2010 to January 2021 corroborates this pattern, indicating that low summer and high winter production is a recurring trend in Norwegian windpower generation. This results in higher profits for wind producers in Norway during winter. It also documents the benefits of splitting the scenario input generation to look at seasonal data instead of yearly, to obtain a more realistic production estimation for a windpower producer submitting their DAM bid.

7.2 Benefits of including uncertainty

In this thesis, all scenario cases with uncertainty have seen a reduced profit compared to the case with perfect information. This is because of the high up-regulation cost assumed in the *Wind Optimization Model*. This assumption has been made based on the BM prices observed in Nord Pool. Increased VRE production combined with the cut-off of Russian gas has made BM prices rise in recent years. Taking into account these factors, it is reasonable to assume that prices in the BM will remain high and possibly rise even more. This would reduce the windpower producer's profit even more compared to the perfect information case.

The examination of forecasting methods for windpower production has not been explored extensively in this thesis. The scenarios used as input into the *Wind Optimization Model* are derived from historical data. Another approach to scenario generation is to look at the accuracy of the forecasting methods at the time the windpower producers submit their bids into the DAM. By generating scenarios for estimated windpower

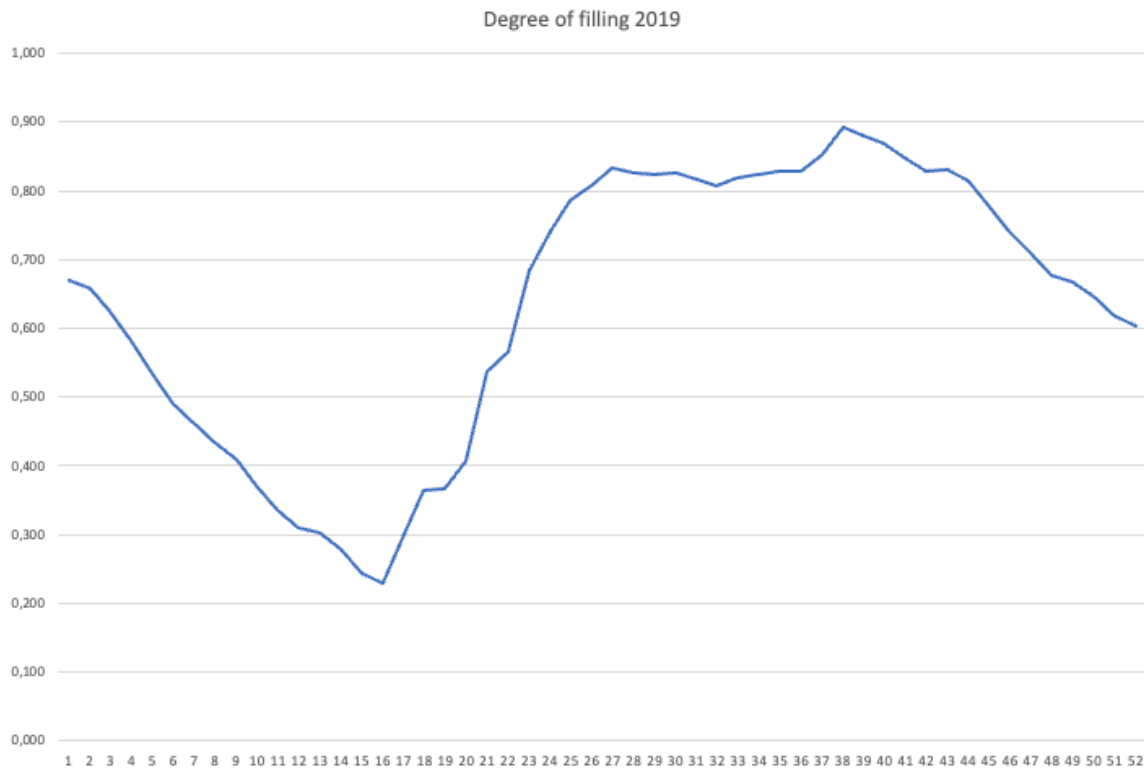


Figure 7.1: Degree of filling for 2019. Values provided by reservoir statistics by NVE [47].

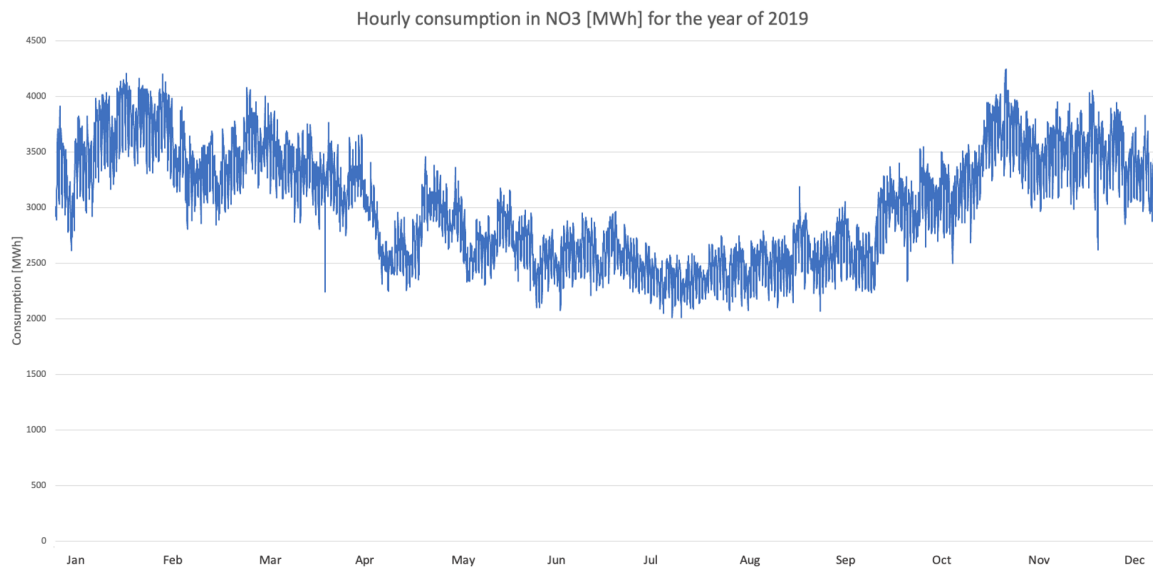


Figure 7.2: Graph showing the yearly consumption [MWh] in price zone NO3.

Table 7.1: Average degree of filling in reservoirs located in NO3.

Year	Average degree of filling
2023 (up to June 6th)	0.297
2022	0.609
2021	0.603
2020	0.678
2019	0.634
2018	0.552
2017	0.598
2016	0.559
2015	0.615
2014	0.600
2013	0.570
2012	0.658
2011	0.614
2010	0.484
2009	0.577
2008	0.643
2007	0.677
2006	0.499
2005	0.612
2004	0.595
2003	0.504
2002	0.606
2001	0.551
2000	0.655

production, DAM prices and BM prices based on the information one has at this time, the *Wind Optimization Model* yields more realistic results on how the consideration of uncertainty affects the windpower producers' profit. Running the *Wind Optimization Model* with this input information could potentially result in reduced uncertainty, assuming that the available information is less uncertain compared to assuming production for a random day within a season. However, it should be noted that acquiring this information is not easy to access. Through services like yr.no [111], a weather forecasting service that provides climate data from locations in Norway and around the world, it is possible to extract some information on wind speed forecasting. Regarding Geitfjellet Vindpark it is not possible to find wind speeds from the exact site, but from the closest town Orkanger. The weather forecasting service also provides historical wind speed data for some locations like Orkanger from one year back. However, this data would not be exact for Geitfjellet Vindpark, nor is it available for 2019.

The inclusion of uncertainty regarding power prices is a significant factor in this model. Prices have varied a lot during recent years. The merit order effect, mentioned in Section 3.5, is a factor that increases the volatility of power prices. Faults in the power grid, sudden changes in climate and fuel prices are other factors contributing to uncertainty in power prices. Norwegian power prices are also affected by supply and demand in other European countries, an effect that has strengthened by the installation of international cables described in Section 3.8. Since the market price uncertainty is expected to continue, it is essential to correctly include stochasticity in the *Wind Optimization Model*.

7.3 Number of scenarios included

In this master thesis, the case study at Geitfjellet Vindpark has been run for 365 scenarios, 25 scenarios and 50 scenarios. Table 6.1 in Section 6.1.4 summarizes and compares the input market price and power

produced for the 25 and 50 scenario cases. Sections 6.2.2 and 6.2.3 provides the results when running the *Wind Optimization Model*.

As can be observed in Sections 6.2.2 and 6.2.3, the power bid schedule obtained from the 50 scenario cases is more detailed than the ones for the 25 scenario cases. Meaning that in most cases, the power bid changes for each price step in the up-regulation price. For the 365 scenario cases, the bids are even more detailed. This observation applies to both the yearly and seasonal cases. Consequently, the bidding schedule becomes substantially more accurate. This indicates the significant advantage of including more scenarios in the optimization problem.

Figure 6.9 depicts the profit compared to the up-regulation price for the yearly scenario cases. Investigation of the graphs shows that the 365 and 50 scenario case have an approximately equal slope. However, the profit for the 50 scenario case is lower. Looking at the 25 scenario graph, which lies between the 365 and 50 graphs, the slope has a much more varying and unstable shape. A reason for the notable difference between the 25 and 50 scenario graphs could be that 25 scenarios are too few to capture the necessary information for an accurate result. Because the 50 scenario graph is almost equal to the 365 scenario graph, it could mean that the "optimal" number of scenarios for a yearly investigation lies somewhere between 25 and 50 scenarios.

The differences in profits between running 25 versus 50 scenarios vary more in the case of yearly input data than seasonal input data, as can be seen by observing Figure 6.9 compared to Figures 6.10 or 6.12 for 4-5 PM. This is interesting because the input values to the *Wind Optimization Model* from the scenario reduction algorithm are very similar. This can be observed in Table 6.1. A critical factor to acknowledge in this stage is that the input scenario generation had 365 data points for the yearly cases, while the seasonal input scenario generation had 90 data points. Additionally, the input data for the yearly case is taken from days across the whole year regardless of seasons, meaning that the data for market price and power produced sent into the *Wind Optimization Model* had a much greater variation than for the seasonal cases. Having had price and production data from several years could have improved accuracy within the model by creating more realistic input scenarios.

Another way of obtaining additional data could be to include data from all hours during the day in the scenario reduction algorithm. One would then have a more extensive database to generate input scenarios from that would still be seasonally dependent. The drawback of this approach is that especially the DAM price data would include the intraday variations in price. A decision was made not to include data from all hours during the days within a season to keep the input power market prices within a likely level. This can be seen by the difference between the expected price calculated for the 50 scenario case for data based on 8-9 AM and 12-1 PM in Table 6.2 and 6.3. The expected market price here varies with 3.8 EUR/MWh, a difference that would be larger if compared to an hour in the middle of the night when prices typically are even lower. A windpower producer would likely not expect that big of a difference in power prices when placing their bid into the DAM. From these tables, one can also observe that the expected production from windpower does not vary much during the day.

The input values for the seasonal 25 and 50 scenario cases were observed to be relatively equal. This led to only presenting the 50 scenario seasonal scatter plots in the results chapter. Furthermore, looking at the results from the *Wind Optimization Model* for the seasonal cases, it can be observed that for each season the profit renders almost the same across the up-regulation prices for both the 25 and 50 scenarios. See Figure 6.10, 6.11, 6.12 and 6.13, in addition to their respective tables. If computational time is an issue for the user, one can conclude that there are no additional values by increasing the number of scenarios for the seasons. As mentioned, for the seasonal cases the data basis for scenario generation has decreased from 365 days to approximately 90 days. This could be the reasoning behind why the 25 scenario cases and 50 scenario cases for each season are more similar compared to when the investigation was done over the whole year. Figure 6.9 shows a graph of the profit based on yearly input data for 4-5 PM.

Another interesting observation is that the 25 scenario case generally has higher profit than the 50 scenario case within each analyzed hour and for each season. A case containing more scenarios would also contain more extreme points, as can be observed when comparing the 25 scenario Figure 6.2 to the 50 scenario Figure 6.3. Extreme points go in both directions of higher and lower market prices, with more windpower produced and less windpower produced. Hence, the negative impact that extreme points have on the profit is normally balanced by the positive impact that an equally positive point has on the profit. This means that including more scenarios should not necessarily decrease the profit in the manner that is observed. Further observations of the figures also show that the distribution is relatively similar, which creates another question regarding the difference in profit. Unfortunately, there is no clear way to identify why. One reason could be how the scenarios are generated in the scenario reduction algorithm, somehow causing an underestimation in the uncertainty for the 50 scenario cases. The concluding remark is that the reason remains unknown and could be a potential for investigation in the future.

7.4 Input values

As mentioned in Section 5.1.1 and 5.1.2, the market price data and production data used in the case study at Geitfjellet Vindpark were taken from the year of 2019. This is because this was the only year provided by Renewables.ninja for windpower production, and no power producers were willing to share production from other years due to security reasons. This has resulted in several inaccuracies in the analysis done in this thesis.

Geitfjellet Vindpark was still under construction in 2019. This means that the production data provided by Renewables.ninja is an approximation based on the wind speed on the site and the given technical specifications given by the authors into the program. There are also no opportunities to verify that the given production data is sound. It is therefore important to be aware that this analysis is only based on one year. Ideally, an analysis such as this should have covered several years of data to reduce the yearly variations of load, production, prices and other intangible influences. By including any years after the wind farm operations started, one could also do a more accurate analysis of the impact the windpower penetration has had on the power system and power prices.

Numbers provided by Statistics Norway show that the windpower generation nationwide has significantly increased in recent years [112]. This could be used to investigate the occurrence of "wind rich" and "wind poor" years. However, this statistical data needs to be read carefully as the main reason for the increased windpower generation is a result of the growth of operating wind farms. Meaning that the increased windpower production is mainly linked to an increased number of production units rather than more wind and production time. Hence, this data can not directly account for the yearly wind production variations mentioned above. Without access to meteorological data at Geitfjellet Vindpark it is challenging to investigate whether 2019 was a "wind rich" or "wind poor" year. Thus it becomes accordingly difficult to say if the wind speed data and the corresponding production are at an expected or extreme level.

The energy crisis is a recent phenomenon observed in Europe and was not yet in motion in 2019. Increased CO₂-taxes in Europe, coupled with the ban on Russian gas initiated by the Ukraine-Russian war, has significantly increased power prices across all European countries. Furthermore, to combat climate change, most industries have slowly started their electrification process, putting additional strain on the power system. Even with the increased integration of solar and windpower in the system, the prices have yet to see a significant reduction. However, most of this did not affect the power market prices in 2019. Hence, the results produced in Chapter 6 could be even more distinct by using recent volatile market prices as they would significantly impact the bidding strategy.

Historical market price data for IDM and BM has been removed from Nord Pool beyond the recent year. This means that the up-regulation prices used in this thesis are merely an example of how the *Wind Optimization Model* works. For this master thesis, it was not necessary to have "real" market data, as the results show on a principal level how the increase or decrease of the up-regulation prices impacts the bidding

strategy and consequently the wind producers' profit. However, for any future extensive investigation, it would be beneficial to have the correct market data for a more accurate profit estimation, especially with the mentioned variability in the recent prices.

Investigations of the production year 2019 show a high degree of filling in the reservoirs and low market prices. From Table 7.1 in the Appendix it can be observed that the degree of filling in the reservoirs in price zone NO3 was relatively high compared to the other investigated years from 2000 to 2022. A high degree of filling generally means that the reservoirs had much inflow. Hydropower producers tend to avoid spillage from reservoirs by producing instead. Therefore, wet years typically have low market power prices. This was investigated in the preliminary power market analysis performed in the author's project thesis [6], where it was clear that years with a high degree of filling (wet years) had generally lower market prices than years with a low degree of filling (dry years). In [6] 2010 and 2020 were compared.

7.5 Challenges with using SHOP

The SHOP tool is intended for hydropower scheduling and thus has no inbuilt tools for simulating a wind turbine. This created challenges and limitations for what the program could achieve in terms of the scope of this master thesis. SHOP usually represents hydropower systems as one interconnected system. This resulted in the code crashing when multiple wind turbines were modeled separately in the same system to make up a wind farm. As a result, the wind farm was modeled as one entity instead of multiple individual wind turbines. This was done under the assumption of a linear relationship between windpower production and number of wind turbines. By doing this, the independent attributes of the wind turbines have potentially been lost. Wake losses and individual yaw control, mentioned in Sections 2.1.4 and 2.1.5, are then aspects that are not considered in the production data from Geitfjellet Vindpark. This also means that topology constraints are not included, but since this thesis uses the size of Geitfjellet Vindpark that was later installed, this is not an issue. However, this model approximation has not had any substantial effect on the study done in this thesis.

In the up-and-down ramping model, a reservoir with capacity was added. When using SHOP over multiple time steps, the optimization problem will look at the possibility of storing water for later time steps. This limits the code from correctly describing the system for more than one time step, as a wind turbine has no means for storing the energy. To expand windpower scheduling with uncertain production in SHOP to multiple time steps, a wind turbine object has to be added with corresponding attributes. In the *Wind Optimization Model* computational time is not an issue, as the system is simple and the problem is for one time step only. If a wind turbine object is implemented, the code will be able to run for many time steps. As described in Section 4.1.2 the addition of time steps increases the scenario tree, and this consequently increases the computational time. This is important to consider if the *Wind Optimization Model* is to be further developed. This is explored further in Chapter 9, Future work.

When working with different scenarios for inflow with a stand-alone wind turbine in SHOP, the production of the wind turbine can not exceed the lowest inflow scenario. This constraint arises from the need for a common decision across all scenarios, as windpower production is not a controllable decision variable in the same way as hydropower. Rather, it is determined by exogenous factors such as wind speed and direction. Consequently, the run-of-the-river plant cannot guarantee generation beyond the minimum inflow level. This makes the implementation of stochastic windpower production irrelevant if one does not do the solution of incorporating a reservoir with capacity, done in the *Wind Optimization Model*, where one is limited to a single time step.

In SHOP, there are no inbuilt functions that can convert wind speed and direction into power produced by a wind turbine. The power produced therefore has to be an input in the model. When simulating wind turbines, many functions in SHOP like turbine and generator efficiency curves and penstock losses, are not utilized. This makes the wind turbine model a simple approximation that does not utilize the full potential of SHOP. Creating the *Wind Optimization Model* might therefore be easier to implement without

the programming tool SHOP, like the model presented in 5.3.2. It should be said that this model has not been implemented and tested, but it could be used as a way of modeling a wind turbine object in SHOP. If one does not utilize SHOP it eliminates the possibility for investigations covering a broader theme, like the market integration in this master thesis.

Another challenge when utilizing SHOP to illustrate a wind farm is the lack of documentation. SINTEF has few available codes using the SHOP tool and only one example of SHARM in their documentation. Since documentation on coupled inflow and price scenarios in SHOP does not exist in SINTEFs' documentation, the *Wind Optimization Model* will be used as documentation by SINTEF going forward.

Chapter 8

Conclusion

This master thesis has utilized the short-term hydropower scheduling tool SHOP and the algorithm's hydropower attributes to develop a *Wind Optimization Model*. To do this, an extensive investigation of the basic principles of windpower and hydropower and a literature review of the Norwegian power market was performed. This thesis has also demonstrated and documented the use areas of the stochastic modeling extension, SHARM, through the *Wind Optimization Model*. The *Wind Optimization Model* has been tested on a case study based at Geitfjellet Vindpark. Here the impact of up-regulation prices on power bids for the windpower producer was investigated. This was initiated because in periods of high price differences between the DAM and IDM it is not optimal for windpower producers to bid their expected production due to the uncertainty in the wind. The results from the case study showed that the wind producer often bid under the expected production to avoid high price penalties. Using seasonal data points as input data rather than yearly data points reduced the uncertainty to a more realistic level. These bids also considered seasonal variability in load, production and market prices. The seasonal data points yielded production data closer to realistic expectations than the yearly data points. The *Wind Optimization Model* was also run with a different amount of scenarios to analyse the benefits of uncertainty inclusion.

A scenario reduction algorithm was used to adequately generate the input scenarios to the *Wind Optimization Model*. The data points for the algorithms were based on data from Renewables.ninja for the year of 2019. Because of the lack of price data and since the Geitfjellet Vindpark was not yet in operation in 2019, the profit estimation from this thesis can only be acknowledged as an approximation. However, the findings indicate that the proposed *Wind Optimization Model* successfully optimizes the windpower producer's bid to the market for the investigated time step.

To conclude, the model shows that the way the market works today does not allow for the distinct variability and uncertainty a windpower encounters in short-term scheduling. It could therefore be beneficial for the windpower producer to look into ways of balancing their bids by regulating through hydropower rather than balancing through the up-regulation price. Another solution would be to develop the proposed WHOP tool for joint scheduling. To build a working WHOP tool, an implementation of windpower related objects and attributes in SHOP is recommended.

Chapter 9

Future Work

This chapter will elaborate on the limitations identified in Chapter 7 and explain other possible extensions to the developed *Wind Optimization Model*, as well as recommendations for enabling a development of the WHOP tool. The sections below can be parts of future research through papers, project theses' and master theses'.

9.1 Expanding to WHOP

Forecasting and uncertainty models were not within the scope of this master thesis. However, as shown throughout this study, proper bidding within power markets is dependent on adequate forecasting and uncertainty reduction in windpower scheduling. Figure 9.1 shows the proposed flowchart for a future version of the WHOP tool. Windpower forecasting and uncertainty analysis using stochastic modeling should play an important part in the model both for the UC mode and the ULD mode. This master thesis has explored potential models for extension in Section 4.6. However, the implementation has been out of the scope of the work.

As stated in the collaboration paper written together with SINTEF and ANL "the traditional approach of decoupling wind and hydropower bidding is not always adequate to capture the full revenue potential for the owner of both wind and hydro", Appendix A.1. This master thesis has highlighted the financial shortcomings resulting from windpower producers not including uncertainty in their DAM bids. Including showing the financial potential of coordinating hydro and windpower production to meet system demand. This is especially relevant when the cost of regulation is less uncertain than the market price.

To better the coordination between the black hydropower parts and the blue wind optimization parts, illustrated in Figure 9.1, they must be properly interconnected. In this master thesis, the preliminary integration resulted in the two models running independently. Future work should investigate means of connecting the two producers in a way that accomplishes the desired outcome of windpower operating as the base load while the hydropower functions as the regulatory system as long as their environmental constraints are preserved without any violations.

9.2 Modifying SHOPs hydropower attributes

With the increased penetration of VRE sources like solar and windpower in the power system, there is a need for models that consider all participants for short-term scheduling. Some models trying to incorporate this were mentioned in Section 4.7. SHOP is one of the only models representing hydropower and market integration in the level of detail that has been necessary for areas dominated by hydropower production like the Norwegian power system.

To enable continuous usage of SHOP in the Nordic power system, SINTEF could consider extending their source code to also encompass objects and attributes specifically for windpower and solar power production. Objects like wind turbines and solar panels that act accordingly would solve some of the obstacles met

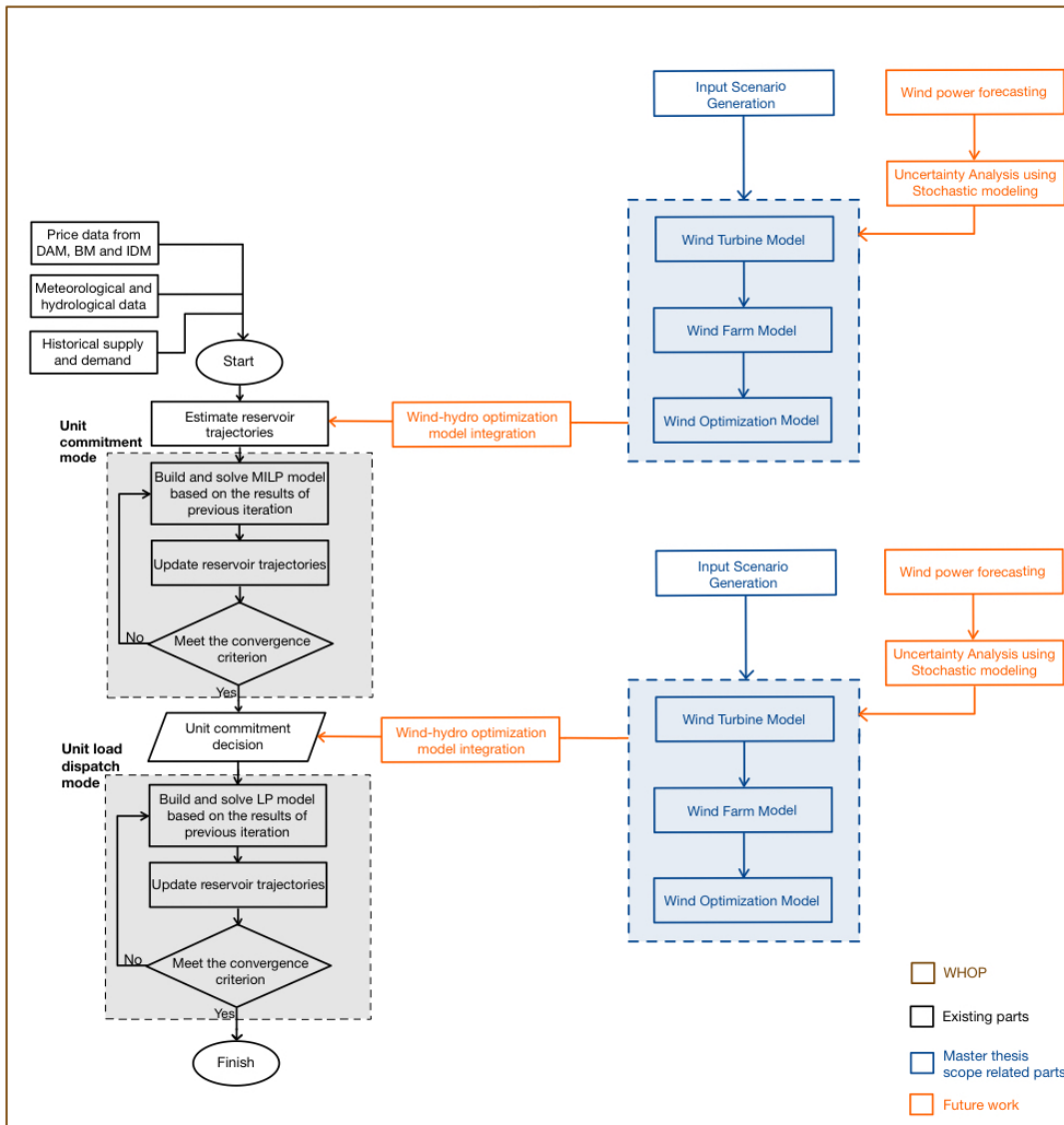


Figure 9.1: Proposal for future additions to the WHOP tool.

in the development of the *Wind Optimization Model*. SHARM would then have to be modified to correctly simulate uncertainty in windpower production that would not include the limitations that resulted in the *Wind Optimization Model* only being functional for a single time step. This addition to the SHOP would make the interconnection between wind and hydropower production easier by opening the possibility of adding attributes to a wind turbine that is not relevant to hydropower production. It would also make cooperation between wind and hydropower production in a future WHOP development less complicated.

9.3 Extending the input data to the case study

Future investigations could look into gathering data from recent years. As has been discussed in Section 7.4, there are several shortcomings in the sampled input data. The main takeaways is case data being limited to only one year and this year being before the operation start of Geitfjellet Vindpark. Therefore, a proposal for further work would be to cooperate with the local windpower production company to possibly gain access to weather data and production data. This way, the results from the case study would significantly gain validation. It would also make it easier to observe if there are any trends to depict from the wind farm related to weather circumstances, production, load demand and profit.

9.4 Connecting wind and hydro production

As mentioned, further development of the WHOP model involves building a connection between hydro and windpower production in the optimization model. The authors have two suggestions for implementing this. Firstly one could introduce a load that has to be fulfilled by either the hydro or windpower source. The goal here is for the WHOP model to prioritize fulfilling the load with windpower and have hydropower regulate its production with regard to this. The user could then vary the load to observe how windpower and hydropower production is affected. A second possibility is to make the DAM prices for hydropower be affected by the amount of windpower in the system. This would simulate how the DAM works. It should be noted that this has yet to be done in SHOP before, and it is not certain that it can be implemented. These two methods could be investigated by combining the *Wind Optimization Model* from this thesis with a hydropower system, or one could combine the hydropower system with a wind turbine object described in Section 9.2.

9.5 Large scale energy storage

As mentioned, the volatility in windpower generation combined with the lack of storage capacity is an issue when it comes to windpower scheduling. Large scale energy storage through batteries could assist during times of volatile prices and wind speed for power production. This could also help balance out the volatility in power sent to the market from the producer, as the batteries could supply energy if the producer realizes they are unable to meet their bids. Thus, they can bypass having to pay the up-regulation price. This can be further explored in terms of both economic and technical aspects if implemented into joint wind-hydro scheduling. Pumped hydro (PSH), mentioned in Section 2.2.6, could also be relevant to include.

Bibliography

- [1] F. Li and K. B., “Generation scheduling in a system with wind power,” in *2005 IEEE/PES Transmission Distribution Conference Exposition: Asia and Pacific*, 2005, pp. 1–6. DOI: 10.1109/TDC.2005.1547157.
- [2] E. F. Norway, the Norwegian ministry of petroleum, and energy. “The power market.” (n.d.), [Online]. Available: <https://energifaktanorge.no/en/norsk-energiforsyning/kraftmarkedet/> (visited on 15/5/2023).
- [3] H. I. Skjelbred. “Shop.” (2023), [Online]. Available: <https://www.sintef.no/programvare/shop/> (visited on 2/5/2023).
- [4] M. M. Belsnes. “The stochastic short-term model sharm.” (2023), [Online]. Available: <https://www.sintef.no/en/projects/2013/the-stochastic-short-term-model-sharm/> (visited on 2/5/2023).
- [5] NVE. “Hvor kommer strømmen fra?” (2023), [Online]. Available: <https://www.nve.no/energi/energisystem/kraftproduksjon/hvor-kommer-strommen-fra/> (visited on 7/6/2023).
- [6] H. B. Sletta and K. Serck-Hanssen, “Integration of renewable energy sources into electricity markets via optimized wind farm and hydropower scheduling,” 2022, Specialisation Project Report in the course "TET4510 - Electrical Energy and Power Systems", Department of Electric Energy, Norwegian University of Science and Technology (NTNU), Trondheim.
- [7] L. Li, “Understanding seismic body waves retrieved from noise correlations : Toward a passive deep earth imaging,” Ph.D. dissertation, Oct. 2018, p. 215.
- [8] G. M. Masters, *Renewable and Efficient Electric Power Systems, 2nd Edition*. Wiley IEEE Press, 2013, ISBN: 978-1-118-63350-2.
- [9] C. U. of Hawai'i. “Exploring our fluid earth - wind systems.” (n.d.), [Online]. Available: <https://manoa.hawaii.edu/exploringourfluidearth/physical/atmospheric-effects/wind-systems> (visited on 15/5/2023).
- [10] J. Machowski, Z. Lubosny, J. W. Bialek, and J. R. Bumby, *Power System Dynamics: Stability and Control, 3rd Edition*. Wiley, 2020, ISBN: 978-1-119-52636-0.
- [11] S. Djohra, K. Mustapha, and S. Hadji, “Technical and economic study of a stand-alone wind energy system for remote rural area electrification in algeria,” *Renewable Energy and Power Quality Journal*, pp. 638–643, Apr. 2014. DOI: 10.24084/repqj12.439.
- [12] A. L. R. James F. Manwell Jon G. McGowan, *Wind Energy Explained: Theory, Design and Application*. Wiley, 2005, ISBN: 10: 0-471-49972-2.
- [13] J. Li, “Capacity worth of energy storage system in renewable power generation plant,” *Engineering*, vol. 05, Jan. 2013. DOI: 10.4236/eng.2013.59B001.
- [14] O. Anya-Lara, J. O. Tande, K. Uhlen, and K. Merz, *Offshore Wind Energy Technology*. Wiley-Blackwell, 2018, ISBN: 9781119097761.
- [15] M. of Petroleum Energy. “The offshore energy act.” (2023), [Online]. Available: <https://www.regjeringen.no/en/dokumenter/offshore-energy-act/id2968375/> (visited on 5/6/2023).
- [16] Equinor. “First power from hywind tampen.” (2022), [Online]. Available: <https://www.equinor.com/news/20221114-first-power-from-hywind-tampen> (visited on 15/5/2023).

- [17] M. of Petroleum Energy. “Important step for offshore wind.” (2022), [Online]. Available: <https://www.regjeringen.no/en/aktuelt/regjeringen-gar-videre-i-sin-satsing-pa-havvind/id2949762/> (visited on 15/5/2023).
- [18] O. of The Prime Minister and M. of Petroleum Energy. “Announces the first competitions for offshore wind.” (2023), [Online]. Available: <https://www.regjeringen.no/en/aktuelt/announces-the-first-competitions-for-offshore-wind/id2969473/> (visited on 5/6/2023).
- [19] M. of Petroleum Energy. “Nye områder for havvind på norsk sokkel.” Norwegian. (2023), [Online]. Available: <https://www.regjeringen.no/no/aktuelt/nye-omrader-for-havvind-pa-norsk-sokkel/id2973609/> (visited on 3/5/2023).
- [20] O. of The Prime Minister. “Ambitious offshore wind initiative.” (2022), [Online]. Available: <https://www.regjeringen.no/en/aktuelt/ambitious-offshore-wind-power-initiative/id2912297/> (visited on 15/5/2023).
- [21] I. Andersen, E. S. Viseth, and L. Nohrstedt. “Sweden against norway, who develops offshore wind on a large scale first?” Norwegian. (2022), [Online]. Available: <https://www.tu.no/artikler/sverige-mot-norge-hvem-bygger-ut-havvind-i-stor-skala-forst/520313> (visited on 16/5/2023).
- [22] Statkraft. “Vannkraft.” Norwegian. (n.d.), [Online]. Available: <https://www.statkraft.no/var-virkksomhet/vannkraft/> (visited on 15/5/2023).
- [23] NVE. “Vannkraft.” Norwegian. (n.d.), [Online]. Available: <https://www.nve.no/energi/energisystem/vannkraft/> (visited on 15/5/2023).
- [24] M. Kanoglu, Y. Cengel, and J. Cimbala, *Fundamentals and Applications of Renewable Energy*, 1st ed. McGraw-Hill Education, 2019, ISBN: 1260455300,9781260455304.
- [25] K. S. Schmitz, “Chapter 2 - five important equations in thermodynamics,” in *Physical Chemistry*, K. S. Schmitz, Ed., Boston: Elsevier, 2017, pp. 41–98, ISBN: 978-0-12-800514-9. DOI: <https://doi.org/10.1016/B978-0-12-800514-9.00002-X>. [Online]. Available: <https://www.sciencedirect.com/science/article/pii/B978012800514900002X>.
- [26] K. A. Rosvold. “Elvekraftverk.” Norwegian. (2023), [Online]. Available: <https://snl.no/elvekraftverk> (visited on 5/6/2023).
- [27] U. department of energy: Office of Energy Efficiency Renewable Energy. “Types of hydropower plants.” (n.d.), [Online]. Available: <https://www.energy.gov/eere/water/types-hydropower-plants> (visited on 15/5/2023).
- [28] “Part ii: Corrosion topics,” in *Corrosion Atlas Case Studies*, ser. Corrosion Atlas Series, F. Khoshnaw and R. Gubner, Eds., Elsevier, 2020, pp. xliii–lxviii, ISBN: 978-0-12-818760-9. DOI: <https://doi.org/10.1016/B978-0-12-818760-9.02003-1>.
- [29] P. Kumar and R. Saini, “Study of cavitation in hydro turbines—a review,” *Renewable and Sustainable Energy Reviews*, vol. 14, no. 1, pp. 374–383, 2010, ISSN: 1364-0321. DOI: <https://doi.org/10.1016/j.rser.2009.07.024>. [Online]. Available: <https://www.sciencedirect.com/science/article/pii/S1364032109001609>.
- [30] M. M. Belsnes. “Norsk pumpekraft kan hjelpe med å stabilisere strømprisene.” Norwegian. (2022), [Online]. Available: <https://blogg.sintef.no/sintefenergy-nb/norsk-pumpekraft-kan-hjelpe-med-a-stabilisere-stromprisene/#comments> (visited on 15/5/2023).
- [31] A. Khodadadi, L. Herre, P. Shinde, R. Eriksson, L. Söder, and M. Amelin, “Nordic balancing markets: Overview of market rules,” in *2020 17th International Conference on the European Energy Market (EEM)*, 2020, pp. 1–6. DOI: 10.1109/EEM49802.2020.9221992.
- [32] E. B. Brose and A. S. Haugsbø, “Flow-based market coupling in the nordic power market,” 2019.

- [33] O. Wolfgang, A. Haugstad, B. Mo, A. Gjelsvik, I. Wangensteen, and G. Doorman, "Hydro reservoir handling in Norway before and after deregulation," *Energy*, vol. 34, no. 10, pp. 1642–1651, 2009, 11th Conference on Process Integration, Modelling and Optimisation for Energy Saving and Pollution Reduction, ISSN: 0360-5442. DOI: <https://doi.org/10.1016/j.energy.2009.07.025>. [Online]. Available: <https://www.sciencedirect.com/science/article/pii/S0360544209003119>.
- [34] D. Begg, G. Vernasca, S. Fischer, and R. Dornbusch, *Economics, 11th Edition*. McGraw Hill Higher Education, 2014, ISBN: 9780077154516.
- [35] N. Pool. "Price coupling of regions (pcr)." (n.d.), [Online]. Available: <https://www.nordpoolgroup.com/en/the-power-market/Day-ahead-market/Price-coupling-of-regions/> (visited on 15/5/2023).
- [36] N. committee. "Single day-ahead coupling (sdac)." (n.d.), [Online]. Available: <https://www.nemo-committee.eu/sdac> (visited on 15/5/2023).
- [37] N. Pool. "Intraday market." (n.d.), [Online]. Available: <https://www.nordpoolgroup.com/en/the-power-market/Intraday-market/> (visited on 15/5/2023).
- [38] D. Kirshen and G. Strbac, *Fundamentals of Power System Economics, 2nd Edition*. Wiley, 2018.
- [39] W. Antweiler and F. Muesgens, "On the long-term merit order effect of renewable energies," *Energy Economics*, vol. 99, p. 105 275, 2021, ISSN: 0140-9883. DOI: <https://doi.org/10.1016/j.eneco.2021.105275>. [Online]. Available: <https://www.sciencedirect.com/science/article/pii/S0140988321001808>.
- [40] N. C. Figueiredo and P. P. da Silva, "The "merit-order effect" of wind and solar power: Volatility and determinants," *Renewable and Sustainable Energy Reviews*, vol. 102, pp. 54–62, 2019, ISSN: 1364-0321. DOI: <https://doi.org/10.1016/j.rser.2018.11.042>. [Online]. Available: <https://www.sciencedirect.com/science/article/pii/S1364032118307950>.
- [41] C. Brancucci Martinez-Anido, G. Brinkman, and B.-M. Hodge, "The impact of wind power on electricity prices," *Renewable Energy*, vol. 94, pp. 474–487, 2016, ISSN: 0960-1481. DOI: <https://doi.org/10.1016/j.renene.2016.03.053>. [Online]. Available: <https://www.sciencedirect.com/science/article/pii/S0960148116302373>.
- [42] Statnett. "Tall og data fra kraftsystemet." Norwegian. (n.d.), [Online]. Available: <https://www.statnett.no/for-aktorer-i-kraftbransjen/tall-og-data-fra-kraftsystemet/#nordisk-kraftbalanse/> (visited on 15/5/2023).
- [43] NVE. "I kraftsystemet handler mye om fysikk." Norwegian. (2022), [Online]. Available: <https://www.nve.no/reguleringsmyndigheten/slik-fungerer-kraftsystemet/i-kraftsystemet-handler-mye-om-fysikk/> (visited on 16/5/2023).
- [44] N. B. Model. "Nordic balancing model." (n.d.), [Online]. Available: <https://nordicbalancingmodel.net/> (visited on 15/5/2023).
- [45] Statnett. "Tertiærreserver - mfr." Norwegian. (2023), [Online]. Available: <https://www.statnett.no/for-aktorer-i-kraftbransjen/systemansvaret/kraftmarkedet/reservemarkeder/tertiarreserver/> (visited on 15/1/2023).
- [46] H. Horne, A. Roos, I. H. Magnussen, M. Buvik, and B. Langseth. "Norge har et betydelig potensial for forbrukerfleksibilitet i sektorene bygg, transport og industri." Norwegian. (2020), [Online]. Available: https://publikasjoner.nve.no/faktaark/2020/faktaark2020_07.pdf?fbclid=IwAR0qixjgBI_fPttnjRG6qqi2N7GfHMJ8776ZZmRFFKo0k3UgjjFZP02XMos (visited on 15/5/2023).
- [47] NVE. "Magasinstatistikk." Norwegian. (n.d.), [Online]. Available: <https://www.nve.no/energi/analyser-og-statistikk/magasinstatistikk/> (visited on 15/5/2023).
- [48] E. F. Norway, the Norwegian ministry of petroleum, and energy. "Kraftproduksjon." Norwegian. (2022), [Online]. Available: <https://energifaktanorge.no/norsk-energiforsyning/kraftforsyningen/> (visited on 15/5/2023).
- [49] F. Vind. "Om fosen vind." Norwegian. (n.d.), [Online]. Available: <https://www.fosenvind.no/om-fosen-vind/> (visited on 15/5/2023).

- [50] NVE, *Data for utbygde vindkraftverk i norge*, Norwegian, n.d. [Online]. Available: <https://www.nve.no/energi/energisystem/vindkraft/data-for-utbygde-vindkraftverk-i-norge/> (visited on 15/5/2023).
- [51] Y.-K. Chen, H. Koduvere, P. A. Gunkel, J. G. Kirkerud, K. Skytte, H. Ravn, and T. F. Bolkesjø, “The role of cross-border power transmission in a renewable-rich power system – a model analysis for northwestern europe,” *Journal of Environmental Management*, vol. 261, p. 110 194, 2020, ISSN: 0301-4797. DOI: <https://doi.org/10.1016/j.jenvman.2020.110194>. [Online]. Available: <https://www.sciencedirect.com/science/article/pii/S0301479720301304>.
- [52] ENTSO-E. “Tyndp.” (2023), [Online]. Available: <https://tyndp.entsoe.eu/explore/what-is-the-tyndp-and-why-does-europe-need-a-plan-for-electricity-infrastructure-1> (visited on 15/5/2023).
- [53] NVE. “Nea – jarpstrømmen.” Norwegian. (2021), [Online]. Available: <https://www.nve.no/om-nve/nves-utvalgte-kulturminner/kraftledninger/nea-jarpstrommen/> (visited on 12/5/2023).
- [54] A. L. Brenna. “Sveriges strømmnett er norges flaskehals.” Norwegian. (2021), [Online]. Available: <https://www.europower.no/nett/sveriges-stromnett-er-norges-flaskehals/2-1-1094955> (visited on 12/5/2023).
- [55] Statnett. “North sea link.” (n.d.), [Online]. Available: <https://www.statnett.no/en/our-projects/interconnectors/north-sea-link/> (visited on 7/6/2023).
- [56] Statnett. “Nordlink.” (n.d.), [Online]. Available: <https://www.statnett.no/en/our-projects/interconnectors/nordlink/#about-the-projecthttps://www.statnett.no/vare-prosjekter/mellomlandsforbindelser/> (visited on 7/6/2023).
- [57] TenneT. “Norned.” (n.d.), [Online]. Available: <https://www.tennet.eu/projects/norned> (visited on 4/5/2023).
- [58] G. Andersson and M. Hyttinen, “Skagerrak the next generation,” *ABB Library*, 2015.
- [59] A. Helseth and A. C. G. de Melo. “Scheduling toolchains in hydro-dominated systems.” (2020), [Online]. Available: <https://sintef.brage.unit.no/sintef-xmlui/handle/11250/2672581> (visited on 15/5/2023).
- [60] F. S. Hillier and G. J. Lieberman, *Introduction to Operations Research, International edition*, 10th ed. McGrawHill, 2015, ISBN: 978-1-259-25318-8.
- [61] J. Lundgren, M. Rönnqvist, and P. Värbrand, *Optimization*, 1:2. Studentlitteratur, 2012, ISBN: 978-91-44-05308-0.
- [62] F. L. John R. Birge, “Introduction to stochastic programming,” in Springer New York, NY, 1997. DOI: 10.1007/978-3-642-02493-1_2. [Online]. Available: <https://doi.org/10.1007/978-1-4614-0237-4>.
- [63] J. L. Higle, “Stochastic programming: Optimization when uncertainty matters,” in Springer New York, NY, 2014. [Online]. Available: <https://doi.org/10.1287/educ.1053.0016>.
- [64] G. Gokayaz, S. Ahipasaoglu, and S. Galelli, “From probabilistic seasonal streamflow forecasts to optimal reservoir operations: A stochastic programming approach,” *IFAC-PapersOnLine*, vol. 52, pp. 1–8, Jan. 2019. DOI: 10.1016/j.ifacol.2019.11.001.
- [65] H. I. Skjelbred, “Unit-based short-term hydro scheduling in competitive electricity markets,” Ph.D. dissertation, Mar. 2019.
- [66] A. Borghetti, C. D’Ambrosio, A. Lodi, and S. Martello, “An milp approach for short-term hydro scheduling and unit commitment with head-dependent reservoir,” *IEEE Transactions on Power Systems*, vol. 23, no. 3, pp. 1115–1124, 2008. DOI: 10.1109/TPWRS.2008.926704.
- [67] J. Kong, H. I. Skjelbred, and O. B. Fosso, “An overview on formulations and optimization methods for the unit-based short-term hydro scheduling problem,” *Electric Power Systems Research*, vol. 178, p. 106 027, 2020, ISSN: 0378-7796. DOI: <https://doi.org/10.1016/j.epsr.2019.106027>. [Online]. Available: <https://www.sciencedirect.com/science/article/pii/S0378779619303463>.

- [68] A. Helseth, G. Warland, and B. Mo, “Long-term hydro-thermal scheduling including network constraints,” in *2010 7th International Conference on the European Energy Market*, 2010, pp. 1–6. DOI: 10.1109/EEM.2010.5558767.
- [69] A. Gjelsvik, B. Mo, and A. Haugstad, “Long- and medium-term operations planning and stochastic modelling in hydro-dominated power systems based on stochastic dual dynamic programming,” in *Handbook of Power Systems I*, P. M. Pardalos, S. Rebennack, M. V. F. Pereira, and N. A. Iliadis, Eds. Berlin, Heidelberg: Springer Berlin Heidelberg, 2010, pp. 33–55, ISBN: 978-3-642-02493-1. DOI: 10.1007/978-3-642-02493-1_2. [Online]. Available: https://doi.org/10.1007/978-3-642-02493-1_2.
- [70] M. Bussieck and S. Vigerske, “Minlp solver software,” in Jan. 2011, ISBN: 9780470400531. DOI: 10.1002/9780470400531.eorms0527.
- [71] R. M. Lima, M. G. Marcovecchio, A. Q. Novais, and I. E. Grossmann, “On the computational studies of deterministic global optimization of head dependent short-term hydro scheduling,” *IEEE Transactions on Power Systems*, vol. 28, no. 4, pp. 4336–4347, 2013. DOI: 10.1109/TPWRS.2013.2274559.
- [72] T. Follestad, O. Wolfgang, and M. Belsnes, “An approach for assessing the effect of scenario tree approximations in stochastic hydropower scheduling models,” *Proceeding - 17th Power Systems Computations Conference PSCC 2011*, vol. 74, pp. 271–277, 2011.
- [73] J. Matevosyan, M. Olsson, and L. Söder, “Hydropower planning coordinated with wind power in areas with congestion problems for trading on the spot and the regulating market,” *Electric Power Systems Research*, vol. 79, no. 1, pp. 39–48, 2009, ISSN: 0378-7796. DOI: <https://doi.org/10.1016/j.epsr.2008.05.019>. [Online]. Available: <https://www.sciencedirect.com/science/article/pii/S0378779608001521>.
- [74] C. D’Ambrosio, A. Lodi, and S. Martello, “Piecewise linear approximation of functions of two variables in milp models,” *Operations Research Letters*, vol. 38, no. 1, pp. 39–46, 2010, ISSN: 0167-6377. DOI: <https://doi.org/10.1016/j.orl.2009.09.005>. [Online]. Available: <https://www.sciencedirect.com/science/article/pii/S0167637709001072>.
- [75] H. I. Skjelbred, J. Kong, and O. B. Fosso, “Dynamic incorporation of nonlinearity into milp formulation for short-term hydro scheduling,” *International Journal of Electrical Power Energy Systems*, vol. 116, p. 105 530, 2020, ISSN: 0142-0615. DOI: <https://doi.org/10.1016/j.ijepes.2019.105530>. [Online]. Available: <https://www.sciencedirect.com/science/article/pii/S0142061519310105>.
- [76] J. P. S. Catalao, S. J. P. S. Mariano, V. M. F. Mendes, and L. A. F. M. Ferreira, “Scheduling of head-sensitive cascaded hydro systems: A nonlinear approach,” *IEEE Transactions on Power Systems*, vol. 24, no. 1, pp. 337–346, 2009. DOI: 10.1109/TPWRS.2008.2005708.
- [77] M. Nazari-Heris, B. Mohammadi-Ivatloo, and G. B. Gharehpetian, “Short-term scheduling of hydro-based power plants considering application of heuristic algorithms: A comprehensive review,” *Renewable and Sustainable Energy Reviews*, vol. 74, pp. 116–129, 2017, ISSN: 1364-0321. DOI: <https://doi.org/10.1016/j.rser.2017.02.043>. [Online]. Available: <https://www.sciencedirect.com/science/article/pii/S1364032117302605>.
- [78] M. Belsnes, O. Wolfgang, T. Follestad, and E. Aasgård, “Applying successive linear programming for stochastic short-term hydropower optimization,” *Electric Power Systems Research*, vol. 130, pp. 167–180, 2016, ISSN: 0378-7796. DOI: <https://doi.org/10.1016/j.epsr.2015.08.020>. [Online]. Available: <https://www.sciencedirect.com/science/article/pii/S0378779615002576>.
- [79] D. Vagner, J. Gunnerød, A. Kringstad, R. Korneliussen, L. Christiansen, and L. M. Hytten. “Kortsiktig markedsanalyse 2022-2027.” Norwegian. (2022), [Online]. Available: <https://www.statnett.no/globalassets/for-aktorer-i-kraftsystemet/planer-og-analyser/kma2022-2027.pdf> (visited on 8/5/2023).

- [80] “Comparing bidding methods for hydropower,” *Energy Procedia*, vol. 87, pp. 181–188, 2016, 5th International Workshop on Hydro Scheduling in Competitive Electricity Markets, ISSN: 1876-6102. DOI: <https://doi.org/10.1016/j.egypro.2015.12.349>. [Online]. Available: <https://www.sciencedirect.com/science/article/pii/S1876610215030386>.
- [81] E. K. Aasgård, G. S. Andersen, S.-E. Fleten, and D. Haugstvedt, “Evaluating a stochastic-programming-based bidding model for a multireservoir system,” *IEEE Transactions on Power Systems*, vol. 29, no. 4, pp. 1748–1757, 2014. DOI: 10.1109/TPWRS.2014.2298311.
- [82] S.-E. Fleten and T. K. Kristoffersen, “Stochastic programming for optimizing bidding strategies of a nordic hydropower producer,” *European Journal of Operational Research*, vol. 181, no. 2, pp. 916–928, 2007, ISSN: 0377-2217. DOI: <https://doi.org/10.1016/j.ejor.2006.08.023>. [Online]. Available: <https://www.sciencedirect.com/science/article/pii/S0377221706005807>.
- [83] N. Nhede. “Three-quarters of 2020 see negative power prices in europe.” (2020), [Online]. Available: <https://www.powerengineeringint.com/world-regions/europe/three-quarters-of-2020-see-negative-power-prices-in-europe/> (visited on 22/3/2023).
- [84] J. Yan, C. Möhrlein, T. Göçmen, M. Kelly, A. Wessel, and G. Giebel, “Uncovering wind power forecasting uncertainty sources and their propagation through the whole modelling chain,” *Renewable and Sustainable Energy Reviews*, vol. 165, p. 112519, 2022, ISSN: 1364-0321. DOI: <https://doi.org/10.1016/j.rser.2022.112519>. [Online]. Available: <https://www.sciencedirect.com/science/article/pii/S1364032122004221>.
- [85] Z. Zhao, C. Wang, M. Nokleby, and C. J. Miller, “Improving short-term electricity price forecasting using day-ahead lmp with arima models,” in *2017 IEEE Power Energy Society General Meeting*, 2017, pp. 1–5. DOI: 10.1109/PESGM.2017.8274124.
- [86] J. Jung and R. P. Broadwater, “Current status and future advances for wind speed and power forecasting,” *Renewable and Sustainable Energy Reviews*, vol. 31, pp. 762–777, 2014, ISSN: 1364-0321. DOI: <https://doi.org/10.1016/j.rser.2013.12.054>. [Online]. Available: <https://www.sciencedirect.com/science/article/pii/S1364032114000094>.
- [87] L. Chen and X. Lai, “Comparison between arima and ann models used in short-term wind speed forecasting,” in *2011 Asia-Pacific Power and Energy Engineering Conference*, 2011, pp. 1–4. DOI: 10.1109/APPEEC.2011.5748446.
- [88] Y. Wang, D. L. Wu, C. X. Guo, Q. H. Wu, W. Z. Qian, and J. Yang, “Short-term wind speed prediction using support vector regression,” in *IEEE PES General Meeting*, 2010, pp. 1–6. DOI: 10.1109/PES.2010.5589418.
- [89] L. Zhu, Q. H. Wu, and L. Jiang, “Mathematical morphology-based short-term wind speed prediction using support vector regression,” in *IEEE PES Innovative Smart Grid Technologies, Europe*, 2014, pp. 1–6. DOI: 10.1109/ISGTEurope.2014.7028795.
- [90] K. Methaprayoon, C. Yingvivanapong, W.-J. Lee, and J. R. Liao, “An integration of ann wind power estimation into unit commitment considering the forecasting uncertainty,” *IEEE Transactions on Industry Applications*, vol. 43, no. 6, pp. 1441–1448, 2007. DOI: 10.1109/TIA.2007.908203.
- [91] M. A. Mohandes, S. Rehman, and T. O. Halawani, “A neural networks approach for wind speed prediction,” *Renewable Energy*, vol. 13, no. 3, pp. 345–354, 1998, ISSN: 0960-1481. DOI: [https://doi.org/10.1016/S0960-1481\(98\)00001-9](https://doi.org/10.1016/S0960-1481(98)00001-9). [Online]. Available: <https://www.sciencedirect.com/science/article/pii/S0960148198000019>.
- [92] S. Shamshirband, T. Rabczuk, and K.-W. Chau, “A survey of deep learning techniques: Application in wind and solar energy resources,” *IEEE Access*, vol. 7, pp. 164 650–164 666, 2019. DOI: 10.1109/ACCESS.2019.2951750.
- [93] J. Tu, G. Yeoh, and C. Liu, *Computational Fluid Dynamics - A Practical Approach 3rd Edition*. Butterworth-Heinemann, 2018, ISBN: 978-0081011270.

- [94] “A preliminary study of assimilating numerical weather prediction data into computational fluid dynamics models for wind prediction,” *Journal of Wind Engineering and Industrial Aerodynamics*, vol. 99, no. 4, pp. 320–329, 2011, The Fifth International Symposium on Computational Wind Engineering, ISSN: 0167-6105. DOI: <https://doi.org/10.1016/j.jweia.2011.01.023>. [Online]. Available: <https://www.sciencedirect.com/science/article/pii/S0167610511000250>.
- [95] A. U. Department of Development Planning. “Wilmar planning tool.” (n.d.), [Online]. Available: <https://www.energyplan.eu/othertools/global/wilmar-planning-tool/> (visited on 1/2/2023).
- [96] A. U. Department of Development Planning. “Other tools.” (n.d.), [Online]. Available: <https://www.energyplan.eu/othertools/> (visited on 23/2/2023).
- [97] A. N. Laboratory. “Power system modeling with a-leaf: The argonne low-carbon electricity analysis framework.” (n.d.), [Online]. Available: <https://www.anl.gov/esia/a-leaf> (visited on 31/1/2023).
- [98] E. Exemplar. “Plexos - the energy analytics and decision platform for all systems.” (n.d.), [Online]. Available: <https://www.energyexemplar.com/plexos> (visited on 9/2/2023).
- [99] E. Exemplar. “Empowering transformative energy decisions.” (n.d.), [Online]. Available: <https://www.energyexemplar.com/plexos> (visited on 9/2/2023).
- [100] N. R. E. Laboratory. “Floris wake modeling wind farm controls.” (n.d.), [Online]. Available: <https://nrel.github.io/floris/intro.html> (visited on 22/2/2023).
- [101] Statkraft. “Vindparkene.” Norwegian. (n.d.), [Online]. Available: <https://www.fosenvind.no/vindparkene/> (visited on 15/2/2023).
- [102] Vestas. “V136-4.2.” (n.d.), [Online]. Available: <https://www.vestas.com/en/products/4-mw-platform/V136-4-2-MW> (visited on 15/2/2023).
- [103] S. Pfenninger and I. Staffell, “Long-term patterns of european pv output using 30 years of validated hourly reanalysis and satellite data,” *Energy*, vol. 114, pp. 1251–1265, 2016. DOI: 10.1016/j.energy.2016.08.060.
- [104] I. Staffell and S. Pfenninger, “Using bias-corrected reanalysis to simulate current and future wind power output,” *Energy*, vol. 114, pp. 1224–1239, 2016. DOI: 10.1016/j.energy.2016.08.068.
- [105] Renewables.ninja. “Renewables.ninja home page.” (n.d.), [Online]. Available: <https://www.renewables.ninja> (visited on 1/6/2023).
- [106] G. Modelling and A. Office. “Modern-era retrospective analysis for research and applications, version 2.” (n.d.), [Online]. Available: <https://gmao.gsfc.nasa.gov/reanalysis/MERRA-2/> (visited on 2/5/2023).
- [107] G. Maps. “Location of geitfjellet vindpark.” (2023), [Online]. Available: <https://goo.gl/maps/5Jt51mGUupG9nk4JA> (visited on 1/6/2023).
- [108] N. Growe-Kuska, H. Heitsch, and W. Romisch, “Scenario reduction and scenario tree construction for power management problems,” in *2003 IEEE Bologna Power Tech Conference Proceedings*, vol. 3, 2003, 7 pp. Vol.3-. DOI: 10.1109/PTC.2003.1304379.
- [109] ANEO. “Let’s create energy.” Norwegian. (n.d.), [Online]. Available: <https://www.aneo.com/> (visited on 5/6/2023).
- [110] J. G. Idsø, “Growth and economic performance of the norwegian wind power industry and some aspects of the nordic electricity market,” 2021. DOI: <https://doi.org/10.3390/en14092701>.
- [111] N. M. Institute and N. B. (NRK). “Historical weather orkanger.” (n.d.), [Online]. Available: <https://www.yr.no/en/statistics/graph/1-210753/Norway/Tr%C3%B8ndelag/Orkland/Orkanger> (visited on 1/6/2023).
- [112] M. Holstad. “Nedgang i vindkraftproduksjon for første gang siden 2016.” Norwegian. (2023), [Online]. Available: <https://www.ssb.no/energi-og-industri/energi/statistikk/elektrisitet/artikler/nedgang-i-vindkraftproduksjon-for-forste-gang-siden-2016> (visited on 29/5/2023).

Appendix A

Appendix

A.1 Optimization of Wind Scheduling for Improved Power Market Integration

Optimization of Wind Scheduling for Improved Power Market Integration

Kristin Serck-Hanssen¹, Hanna Sletta¹, Umit Cali¹, Michael Belsnes², Jongwhan Kwon³, and Marthe Fogstad Dyngje¹

¹Norwegian University of Science and Technology (NTNU), Trondheim, Norway

²SINTEF Energy Research, Trondheim, Norway

³Argonne National Laboratory, Chicago, USA

Abstract—Increasing wind power penetration, along with other variable renewable energy (VRE) resources, provides considerable potential in terms of decarbonizing power grids. In particular, Norway’s power system is predominantly based on hydropower, and the country has significant potential for wind energy development. However, the efficient and reliable operation of VRE resources is challenging due to their inherent variability and uncertainty. This variability and uncertainty pose technical and economic challenges for integrating VRE resources into power systems as well. This study focuses on the optimal scheduling of wind power for one time step, taking into account the uncertainty of wind generation prediction, as well as the impact on outcomes for producer profit. The ultimate goal of the work is to expand an existing stochastic hydropower scheduling model and develop a joint wind-hydro scheduling tool that considers the dynamic interactions between the hydropower and wind power systems.

Index Terms—wind power, hydropower, scheduling, Optimal bidding, stochastic modeling

I. INTRODUCTION

As a way to combat climate change and lessen reliance on fossil fuels, interest in renewable energy sources like wind has significantly increased in recent years. To successfully support the transition to a low-carbon energy system and meet the rising energy demand, the supply of wind must rise in tandem with electrification [1]. The price of electricity may vary significantly both daily and seasonally due to changes in demand, the availability of different energy sources, and climatic conditions. This fluctuation in power prices affects power producers, especially for intermittent renewable energy sources without storage capabilities, like wind power. Given the fluctuating cost of energy, power producers need to optimize power production by considering markets in order to maximize their profit.

In particular, it is important to consider uncertainty in wind forecasts when determining the optimal bidding of wind farm operators. This study aims to maximize the operation of wind farms through stochastic optimization modeling. The framework developed in this study is linked to SHOP [2], a Short-term Hydropower Optimization Program developed by SINTEF for scheduling hydropower output and market bidding. Several components from the hydropower scheduling algorithm in SHOP can be used for scheduling wind farm operations, including market interaction, and stochastic modeling

[3] to account for multiple scenarios and uncertainty. Adopting these techniques can provide a quick route to improved wind power integration. In a hydropower-dominated power system, like Norway, this strategy can be advantageous to power producers looking to include wind power in their portfolio. In order to develop the model for wind farm operation an extensive review has been conducted, covering aspects related to power markets, hydropower technology, wind power technology, and optimization and scheduling methods for renewable power plants. Wind speed forecasts, stochastic modeling of various situations, and technical descriptions of the energy conversion are only a few of the processes involved in the operation scheduling.

For flexible energy sources like hydropower, where one can schedule a certain generation in advance, the Day Ahead Market (DAM) performs well. However, it is more challenging to anticipate generation 12-36 hours prior to the bid deadline for VREs such as wind power. Using forecasting techniques improves the accuracy of this prediction, but still, it does not provide perfect information. As a result, the intraday market (IDM) was introduced and has become important to wind power producers. It provides the producers with a better picture of the system generation by opening two hours after the DAM closes and closing one hour before each production start. This allows producers to adjust production, and trade themselves into balance in real-time according to the latest information regarding weather conditions, consumption or outages [4]. In addition, there is the regulation market for reserves that are activated to stabilise the frequency. In the Nordic market, every balance-responsible participant in the power market must fulfil its obligation in other markets. So if a wind power producer is not in balance in the combination of DAM and IDM the deficit will be settled to the balancing price. If the wind generation is above the bid value, the wind power producer will continue to produce as long as the balance price is above zero, but if he has a negative balance buying balancing power can be expensive.

The way electricity prices are determined in a power pool has altered as a result of the expansion of VRE sources like wind. This type of energy source is reliant on the presence of stochastic wind speeds [5]. It is also advantageous to produce even when the price of electricity is low because of the low

levelized cost of electricity (LCOE) compared to hydropower [6]. This means that in a perfectly functioning market, these VREs should be given precedence in order to produce at cheap costs, whereas power plants like hydro or nuclear that have greater start-up costs should halt production.

In 2022 Norway experienced periods with significant discrepancies between the DAM and the balancing market (BM). At a randomly chosen day post summer, on August 14th 2022, the average up-regulation price given by Nord Pool for price zone NO3 was 63.80 EUR/MWh whereas the average DAM price was at 19.38 EUR/MWh. Increased electrification, the energy crisis, the invasion of Ukraine and low degree of inflow to the reservoirs could all play a part. These price differences impact the producers' willingness to bid high production in case of high costs if they have to go through the balancing market to meet their bids. This is especially the case for a wind power producer who operates under uncertain and stochastic conditions. Optimizing production for the wind power producer by also considering the hydro generation could result in notable economical savings and potentially improved market integration and utilization of the wind farm. With this regard, the main contributions of this study are as follows:

- Development of a wind power scheduling tool in a stochastic setting that incorporates market bidding and optimal scheduling techniques.
- Extending the existing stochastic hydropower scheduling model (SHOP) to develop a joint wind-hydro scheduling tool (WHOP) that takes into account the dynamic interactions of the hydropower and wind power systems.
- Demonstration of the findings of the techno-economic analysis based on multiple scenarios in which the proposed models are applied.

II. METHODOLOGY

The main goal of this study is to examine the methods to enhance the SHOP software and specifically focus on scheduling wind power output in the market context. It is essential to find ways to improve the efficiency and accuracy of wind power scheduling to ensure that it meets the needs of the market while also ensuring the profitability of wind producers. The methodology for attaining the objectives will be provided in this section in the form of data collection and a flowchart detailing the suggested approach to problem-solving. For a detailed explanation of the optimization model that is created in SHOP and the existing SHOP software see [2], [7].

A. Wind-Hydro Optimization Program

WHOP is a co-scheduling and cooperative planning method for wind and hydropower, built on the foundation of an existing hydropower scheduling tool; SHOP, illustrated in black in the flowchart in Figure 1. WHOP will enhance SHOP by adding the possibility for wind power optimization and thus meet the aim of this study of developing a method for wind power optimization in SHOP. The preliminary proposed solution approach for the WHOP model is shown in Figure 1. First, a single wind turbine model was developed in the

SHOP Virtual Laboratory [8], before being further extended to a full wind farm. This paper presents the wind optimization model for one-time step. The scope of this study is presented in blue in Figure 1. The wind optimization problem is yet to be integrated into the combined wind and hydro model, as can be observed in yellow in the flowchart and is currently working as a stand-alone framework. Furthermore, forecasting is essential for determining the best time to schedule the generation of wind plants [14], therefore, there is a need to include a realistic wind power model in SHOP considering the uncertainty and stochastic behavior of the wind. However, further research on this, represented in yellow in Figure 1, is out of the scope of this study.

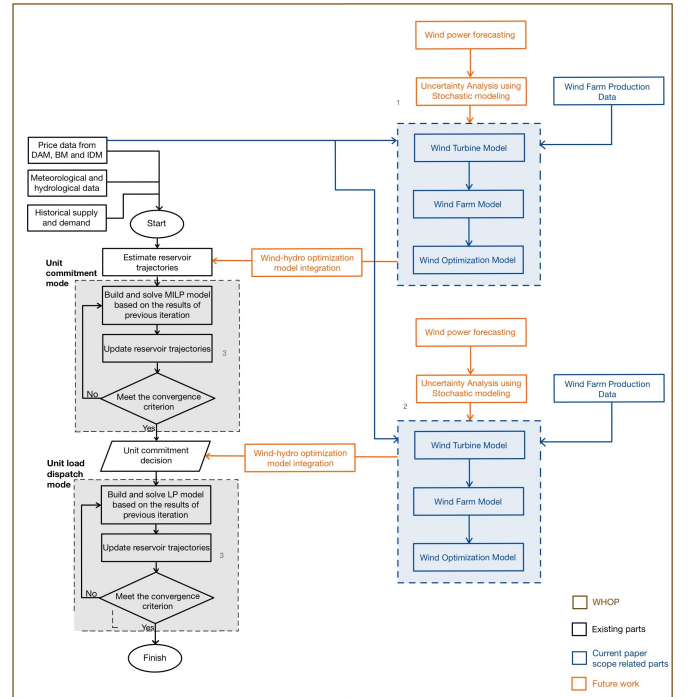


Fig. 1. Flowchart showing the solution strategy in the extended WHOP model. The black-marked SHOP part of the flow chart is based on the solution strategy for SHOP in [9].

The WHOP model possesses a number of key features that make it a valuable resource for optimizing wind and hydropower operations. These features include:

- 1) The wind speed forecasts' accuracy is less than perfect, this approach nevertheless allows wind producers to calculate a rough generation schedule that will be supplied to the SHOP tool. This allows the hydropower producer to more accurately include wind power uncertainty in their unit-commitment calculation in case it is optimal for the producer to do that.
- 2) The wind power optimization model repeatedly enters the SHOP model before the unit load dispatch mode. The wind hydropower generation optimization model entering the unit load dispatch stage has a higher degree of precision than the estimation made for the day-

ahead market since wind power forecasts are more accurate for short-term predictions of just a few hours. The hydropower producer can now adjust their output accordingly to actual wind production including relevant trades in IDM.

- 3) In the unit commitment and unit load dispatch modes, the hydro reservoir trajectories are updated at the same time as the updated wind energy trajectories. The production of wind energy will be updated here in relation to that of hydropower. Making sure that market bids for both wind and hydro are satisfied is crucial. It is possible to do minor adaptations in hydro production in the unit load dispatch mode as long as the UC is unchanged and the marginal status of the system will indicate the opportunity or need to change position IDM and the balancing markets.

B. Data processing

In this study, we have investigated two cases for a given location, Geitfjellet Wind Farm, for the year 2019. This is a case of 10 different scenarios and a case of 30 different scenarios. The DAM price data have been gathered from Nord Pool for price zone NO3, while wind production data have been gathered using *Renewables.ninja* [10] at latitude 63.365 and longitude 9.497. The scenario input data for each case is shown in the scatter plot in Figures 2 and 3 for the 10 and 30 scenario cases respectively. The scatter plot shows the power produced versus the market price and the size of the points represents the probability of the scenario. The color represents the different scenarios.

A scenario reduction algorithm is applied to select a set of weighted scenarios for wind output and market prices. There are various methods to select scenarios, including time series analysis, machine learning techniques like decision trees or neural networks, and clustering methods, as comprehensively reviewed in [11]. In this study, we employ a backward scenario reduction algorithm from [12] to select sets of scenarios. The inputs to the algorithm are the time series data of wind availability and market prices. The algorithm iteratively removes scenarios based on their similarity to the remaining scenarios until the desired number of representative days is reached. The output of the algorithm is a set of selected scenarios along with their associated probabilities.

C. Optimal market bidding for a wind power producer

The decision variable in SHOP is each hydropower plant's production in all time steps. When working with wind power this decision is decided by the turbine type, wind speed, and wind direction. A decision that could be made by the wind producer is how much power should be bid into the market based on wind forecasting. This decision depends on the cost of buying power from the reserve market during the wind farm's power deficits. This model looks at different reserve market prices and when they change the wind producers' optimal bid in the DAM.

$$P_h[MW] \cdot 10^6 = Q[m/s^3] \cdot (\eta \cdot \rho \cdot g \cdot H_n) \quad (1)$$

In this study, we model a physical wind turbine (Figure 4) using the hydropower system modeling language SHOP (Figure 5). In the model, the wind that hits the turbine is represented by the inflow into a reservoir. The conversion from the power produced to inflow into the reservoir is shown in (1). To simplify the model, the net height of the reservoir is set to a value that equals the inflow rate in m^3/s to the power output in MW. At the start of the first time step, the reservoir is assumed to have a maximum capacity such that any excess inflow would result in spillage, making it beneficial to produce power from all inflow. To explore different scenarios, we use the SHOP expansion SHARM to include different inflow scenarios that result in different power production scenarios for the wind farm. SHARM (Short-term Hydropower Application with Risk Modelling) is a stochastic formulation of a successive linear programming method and is made for SHOP [13]. These scenarios are also coupled with different pricing scenarios. The water stored in the upper reservoir is included to be used if the inflow scenario is not sufficient to produce the power bid into the DAM market. SHOP is able to value this water at an up-regulation price. This model is only functional in one-time step because of the possibility of water being stored in this reservoir if stored water has been used in previous time steps. If the inflow scenario exceeds the power bid into DAM, the model allows the water to travel to a lower reservoir that values the water at a down-regulation price. If the up-regulation price is set to a value lower than the DAM price the model becomes dysfunctional. The system can then can buy power from the BM and sell it to the DAM, something that does not work in the real world. The model is scaled up to represent a wind farm.

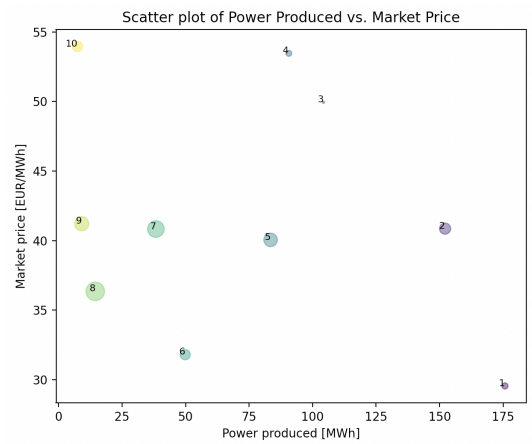


Fig. 2. Input data for ten scenarios. Each point is a scenario. The size of the points represents the probability of the scenario and the color represents the different scenarios.

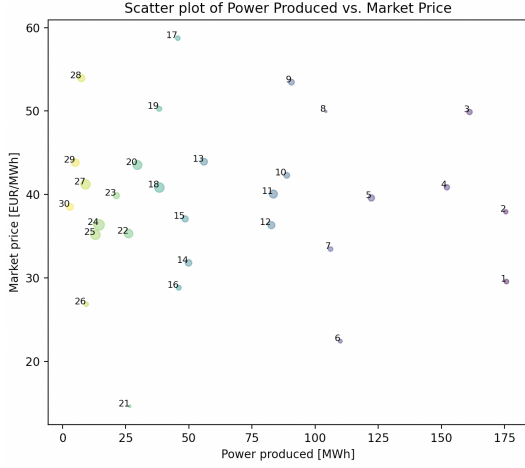


Fig. 3. Input data for thirty scenarios. Each point is a scenario. The size of the points represents the probability of the scenario and the color represents the different scenarios.

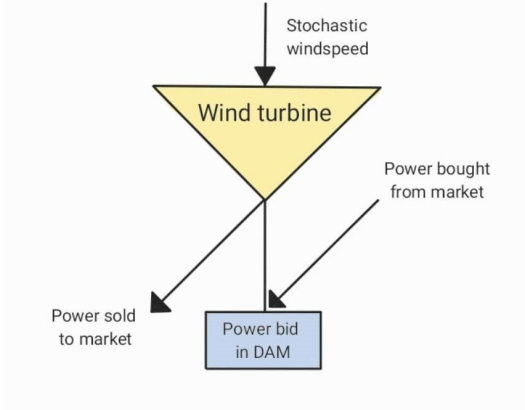


Fig. 4. The physical system that the model is to represent

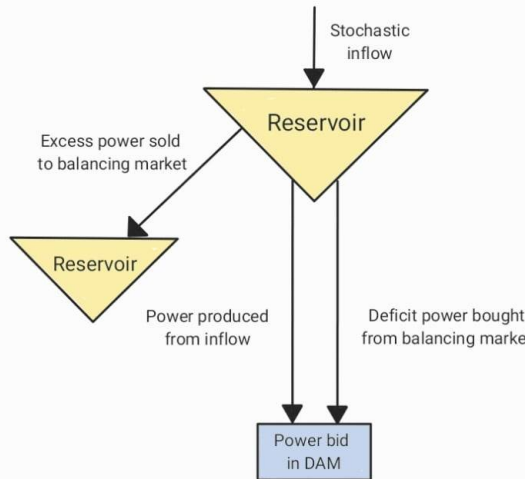


Fig. 5. System created in SHOP

III. RESULTS

Table I and II present the optimal power bid and profit obtained from the simulation of 10 and 30 scenarios, respectively. The up-regulation prices vary from 60 to 100 EUR/MWh. It can be observed from both tables that the wind producers' bids increase as the up-regulation price decreases in the scenario cases. One can then also observe that the down-regulation price is so low that it does not affect the result in this case study. The down-regulation price was kept at this constant level of 10 EUR/MWh as the focus of this paper was to investigate the impact of the up-regulation price on the bid decision.

Figure 2 and 3 represent the input data, as mentioned. The 10-scenario case has a maximum market price value around 54 EUR/MWh and a minimum value around 30 EUR/MWh. The probability of scenario 8 yielded the highest with market price value of 36 EUR/MWh and power production of 15 MWh. For the 30-scenario case the maximum market price value is 58 EUR/MWh and the minimum value is 15 EUR/MWh. Here the probability of scenario 24 yielded the highest with market price value of 37 EUR/MWh and power production of 13 MWh.

Further analysis of Figure 2 and 3 it is apparent that the input price scenarios for both cases center around a price of 40 EUR/MWh. However, the 30-scenario case has more extreme high and low scenarios. The power bid schedule obtained from the case with 30 scenarios is more detailed, indicating the advantage of including more scenarios in the optimization problem.

The expected bid for the two cases were found by averaging over probability and power production. For the 10 scenarios it is 47.93 MWh, while for the 30 scenarios, it is 48.39 MWh. By comparing the calculated expected bid volumes to the volumes presented in the Table I and II it can be observed that the maximum power bid happening at an up-regulation price of 60 EUR/MWh does not exceed the expected bid. A lower up-regulation price of 50 EUR/MWh and less has not been analysed as this price level would be lower than the market price.

TABLE I
RESULTS SHOWING THE SOLUTION TO THE OPTIMIZATION PROBLEM WITH VARYING UP-REGULATION COSTS WITH TEN SCENARIOS

Up-regulation price [EUR/MWh]	Down-regulation price [EUR/MWh]	Power bid [MWh]	Profit [EUR]
100	10	14,45	797,87
90	10	14,45	810,67
80	10	14,45	823,48
70	10	38,32	893,75
60	10	38,32	1016,41

IV. DISCUSSION

A. Discussing the results

The results show that the wind producer would bid in under the expected production to avoid high production penalties

TABLE II
RESULTS SHOWING THE SOLUTION TO THE OPTIMIZATION PROBLEM WITH
VARYING UP-REGULATION COSTS WITH THIRTY SCENARIOS

Up-regulation price [EUR/MWh]	Down-regulation price [EUR/MWh]	Power bid [MWh]	Profit [EUR]
100	10	14,45	767,46
90	10	21,29	792,87
80	10	26,13	847,03
70	10	29,64	917,24
60	10	45,62	1031,73

when the up-regulation price is high. Also, the modeled wind farm does not produce more or equal power compared to the expected production in both scenarios. This is because the penalties for producing less than the bid is worse than the benefits for producing more than the bid. Lastly, the results show that the profit varies more with 30 scenarios due to the higher volatility captured in the 30-scenario case compared to the 10-scenario case.

The wind producer would bid below the anticipated output when the up-regulation price is high to avoid excessive production fines. When compared to the expected production, neither scenario produces more or the same amount of power. This is so because there are greater consequences for producing less than the bid than there are rewards for generating more. With 30 situations, the profit is more variable. This is due to the fact that the extreme possibilities have a significant impact on the best offer in the 30-scenario case compared to the 10-scenario case where the scenarios vary less.

B. Limitations of SHOP

SHOP is a hydropower tool developed for hydropower producers to optimally schedule their production on a short-time basis. As all commands, objects, and attributes have been made for this purpose, it is challenging to model wind turbine attributes. As explained in Section IID, the turbines have instead been modeled as hydropower plants using a conversion (Eq. (1)) from inflow to power produced. This limits the possibility to model additional details about the technical specifications of wind turbines. On the other hand, it makes it easier to perform simple model analysis.

The scenarios have been selected based on one year of data, due to a lack of generation data on the *Renewables.ninja* website. If more data were used the scenarios would be a more accurate representation of the relationship between power produced and market price. This is especially important due to the recent large velocity in power prices.

V. CONCLUSION AND FURTHER WORK

The traditional approach of bidding the expected value of wind power into the market is not optimal when there are significant differences between the spot price and regulation price. The uncertainty in wind forecast and forecast should be included in the bidding strategy for wind power assets as demonstrated in this work.

The importance of an adequate representation of the scenarios is also demonstrated in I and II where the use of more

information about the uncertainty, and application of more scenarios, shows how the proposed method of wind power bidding can give a detailed strategy for different possible outcomes. The value of stochastic wind power bidding depends on the price differences between the market products but it will always be there.

The current model using SHOP VLAB makes use of the components available for hydropower modelling, resulting in the decoupling of time intervals in the optimization. While wind is decoupled, hydropower is not, so to capture a better value of the joint planning of wind and hydro resources wind should have its own module in the hydropower model.

The work shows the importance of an adequate representation of wind and price uncertainty in the stochastic model, having joint scenarios for wind, precipitation and prices will be computationally demanding a wind module will solve that. The input to the stochastic wind model is critical. This study presents the first stage of a consistent model with modeling of a generic wind farm, as well as the possibility for enhancement of the wind forecasting tools required for full usage of the model for individual turbines or the entire wind farm.

The traditional approach of decoupling wind and hydropower bidding is not always adequate to capture the full revenue potential for the owner of both wind and hydropower. This work can be extended to investigate the value of being able to regulate on own hydropower where the uncertainty about regulation cost is lower than that of the market.

Currently, there are not many tools available for consistent forecasting of prices for multiple energy and reserve products. This forecasting and modelling challenge needs to be addressed properly to harvest the potential of the wind model presented in this work. The model developed throughout this article indicates that wind power producers could benefit from a joint operation of hydro as up-regulation rather than purchasing from the power market. The proposed approach demonstrates a highly essential contribution to the Norwegian economy by optimizing the joint operation of wind and hydroelectric power plants since Norway has a very high potential for hydropower in addition to the increasing investments in wind power.

ACKNOWLEDGEMENT

This work has been supported by NorthWind (2021-2029), a Centre for Environmental-friendly Energy Research co-financed by the Research Council of Norway (contract 321954). Besides, the U.S. Department of Energy and Norway's Royal Ministry of Petroleum and Energy collaborate on hydropower R&D through an Annex to a 2004 memorandum of understanding (MOU). This MOU Annex signed in 2020, brings together the DOE's EERE Water Power Technologies Office (WPTO) and the Norwegian Research Centre for Hydropower Technology (HydroCen) to plan and coordinate hydropower R&D activities.

REFERENCES

- [1] F. Li and K. B., "Generation scheduling in a system with wind power," in 2005 IEEE/PES Transmission Distribution Conference Exposition: Asia and Pacific, 2005, pp. 1–6. DOI: 10.1109/TDC.2005.1547157
- [2] O. B. Fosso and M. M. Belsnes, "Short-term hydro scheduling in a liberalized power system," 2004 International Conference on Power System Technology, 2004. PowerCon 2004., Singapore, 2004, pp. 1321-1326 Vol.2, doi: 10.1109/ICPST.2004.1460206.
- [3] M. M. Belsnes, O. Wolfgang, T. Follestad, E. K. Aasgård, "Applying successive linear programming for stochastic short-term hydropower optimization." *Electric power systems research*, 2016 Volume 130, p. 167-180
- [4] Nord Pool. "Intraday market". Available: <https://www.nordpoolgroup.com/en/the-power-market/Intraday-market/> (Visited on 20-10-2022)
- [5] J. Machowski, Z. Lubosny, J. W. Bialek, and J. R. Bumby, "Power System Dynamics: Stability and Control", 3rd Edition. Wiley, 2020, ISBN: 978-1-119-52636-0
- [6] IRENA (2022), "Renewable Power Generation Costs in 2021", International Renewable Energy Agency, Abu Dhabi. ISBN 978-92-9260-452-3
- [7] H. I. Skjelbred, J. Kong, O. B. Fosso, "Dynamic incorporation of nonlinearity into MILP formulation for short-term hydro scheduling", *International Journal of Electrical Power & Energy Systems*, Volume 116, 2020, 105530, ISSN 0142-0615, <https://doi.org/10.1016/j.ijepes.2019.105530>
- [8] SHOP Virtual Laboratory (SHOP VLAB) <https://www.sintef.no/en/sintef-energy/energylabs/sintef-energy-virtual-lab/> (Visited on 25-04-2023)
- [9] H. I. Skjelbred, "Unit-based short-term hydro scheduling in competitive electricity markets," (Doctoral thesis, Norwegian University of Science and Technology, Trondheim, Norway) pp. 49, Mar. 2019.
- [10] S. P. Staffell and S. Pfenniger, "Renewables ninja," 2016.
- [11] H. Li et al., "A review of scenario analysis methods in planning and operation of modern power systems: Methodologies, applications, and challenges," *Electric Power Systems Research*, vol. 205, p. 107722, Apr. 2022, doi: 10.1016/j.epr.2021.107722.
- [12] N. Growe-Kuska, H. Heitsch, and W. Romisch, "Scenario reduction and scenario tree construction for power management problems," in *Power Tech Conference Proceedings, 2003 IEEE Bologna*, Jun. 2003, p. 7 pp. Vol.3-. doi: 10.1109/PTC.2003.1304379
- [13] M. M. Belsnes, "The stochastic short-term model SHARM" <https://www.sintef.no/en/projects/2013/the-stochastic-short-term-model-sharm/> (Visited on 29/04/2023)
- [14] U.Cali, "Grid and market integration of large-scale wind farms using advanced wind power Forecasting: technical and energy economic aspects", Kassel university press GmbH, vol. 17, 2011.

A.2 V136-4.2MW Turbine

The brochure for the V136-4.2 MW Turbine [102].

V136-4.2 MW™

IEC IIB/IEC S

Facts & figures

POWER REGULATION

Pitch regulated with variable speed

OPERATING DATA

Rated power	4,000 kW/4,200 kW
Cut-in wind speed	3m/s
Cut-out wind speed	25m/s
Re cut-in wind speed	23m/s
Wind class	IEC IIB/IEC S
Standard operating temperature range from -20°C to +45°C with de-rating above 30°C (4,000 kW)	

*Subject to different temperature options

SOUND POWER

Maximum 103.9 dB(A)**

**Sound Optimised Modes available dependent on site and country

ROTOR

Rotor diameter	136m
Swept area	14,527m ²
Air brake	full blade feathering with 3 pitch cylinders

ELECTRICAL

Frequency	50/60Hz
Converter	full scale

GEARBOX

Type	two planetary stages and one helical stage
------	--

TOWER

Hub heights	Site and country specific
-------------	---------------------------

NACELLE DIMENSIONS

Height for transport	3.4m
Height installed (incl. CoolerTop®)	6.9m
Length	12.8m
Width	4.2m

HUB DIMENSIONS

Max. transport height	3.8m
Max. transport width	3.8m
Max. transport length	5.5m

BLADE DIMENSIONS

Length	66.7m
Max. chord	4.1m

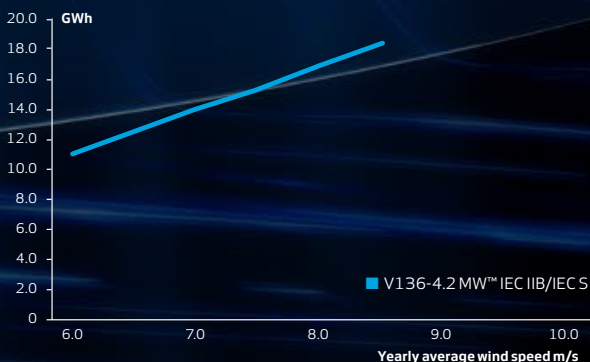
Max. weight per unit for transportation* 70 metric tonnes

*Excluding tower

TURBINE OPTIONS

- Lightning Detection
- Large Diameter Steel Tower (LDST)
- 4.2 MW Power Optimised Mode (site specific)
- Load Optimised Modes down to 3.6 MW
- Condition Monitoring System
- High Wind Operation
- Vestas Ice Detection
- Low Temperature Operation to - 30°C
- Fire Suppression
- Shadow Detection
- Increased Cut-In
- Aviation Lights
- Aviation Markings on the Blades

ANNUAL ENERGY PRODUCTION



Assumptions

One wind turbine, 100% availability, 0% losses, k factor = 2, Standard air density = 1.225, wind speed at hub height.

© 2019 Vestas Wind Systems A/S. All rights reserved.

This document was created by Vestas Wind Systems A/S on behalf of the Vestas Group and contains copyrighted material, trademarks and other proprietary information. This document or parts thereof may not be reproduced, altered or copied in any form or by any means without the prior written permission of Vestas Wind Systems A/S. All specifications are for information only and are subject to change without notice. Vestas Wind Systems A/S does not make any representations or extend any warranties, expressed or implied, as to the adequacy or accuracy of this information. This document may exist in multiple language versions. In case of inconsistencies between language versions the English version shall prevail. Certain technical options, services and wind turbine models may not be available in all locations/countries.

A.3 Input scenario generation for 8-9 AM and 12-1 PM across all yearly cases

A.3.1 365 scenario cases

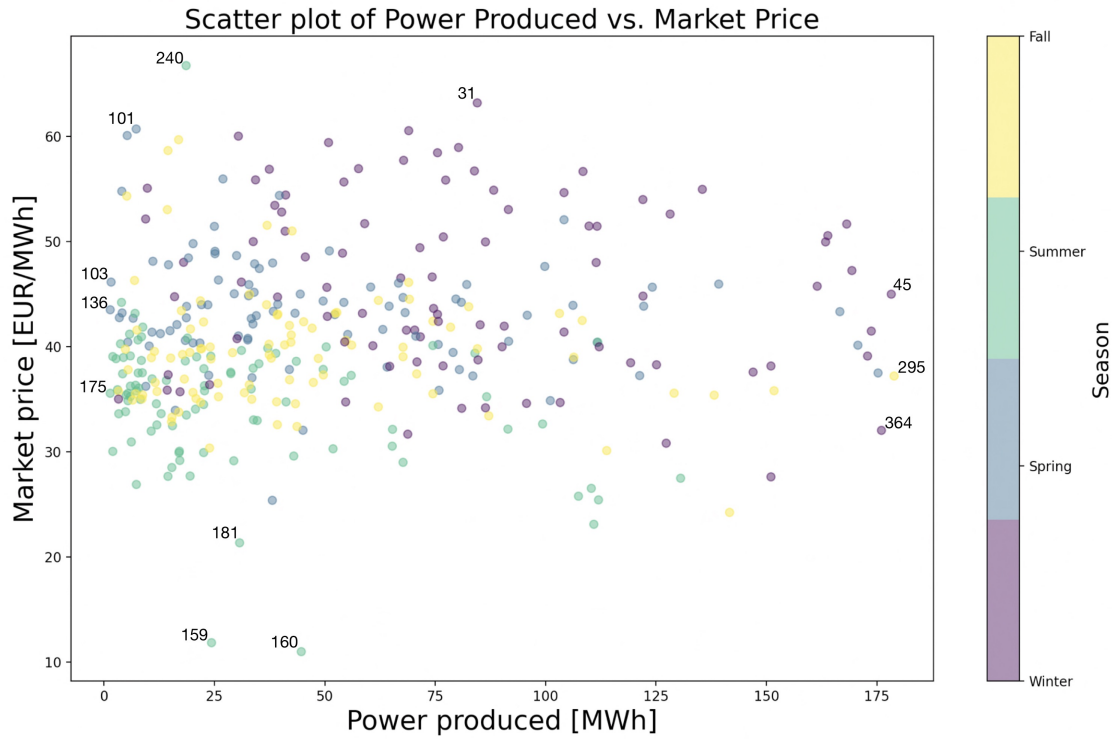


Figure A.1: Scatter plot showing input data for 365 scenarios at 8-9 AM. Each point is a scenario, each with the same probability. The colors represent the four seasons and the scenarios within as shown in the bar to the right. Extreme points are numbered.

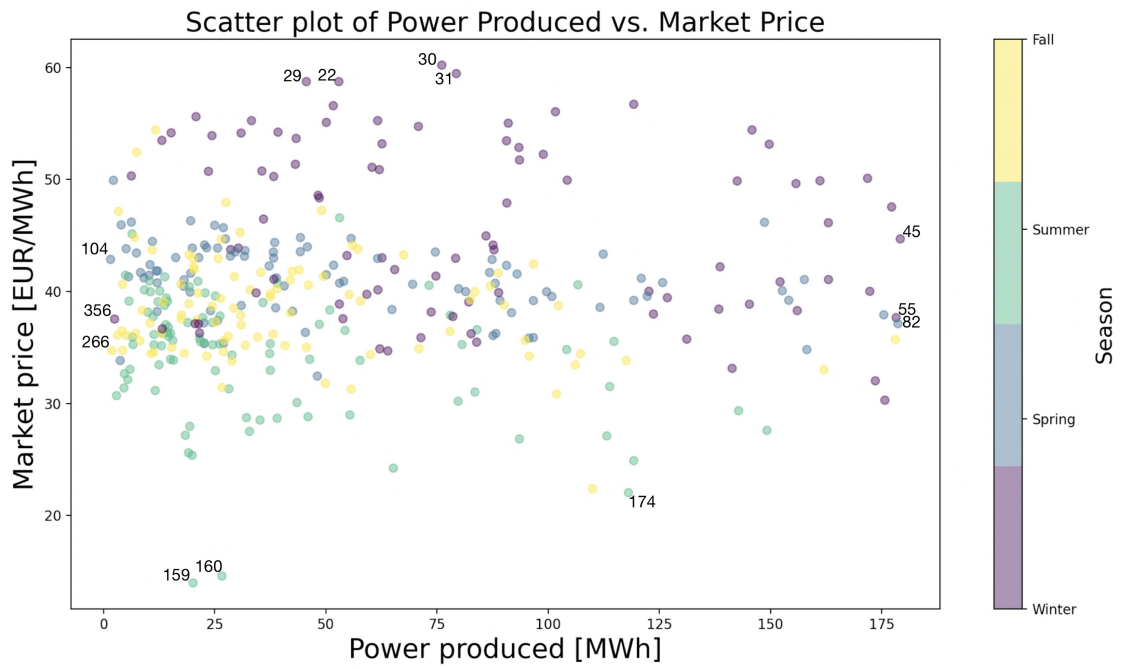


Figure A.2: Scatter plot showing input data for 365 scenarios at 12-1 PM. Each point is a scenario, each with the same probability. The colors represent the four seasons and the scenarios within as shown in the bar to the right. Extreme points are numbered.

A.3.2 Yearly 25 and 50 scenario cases for 8-9 AM and 12-1 PM

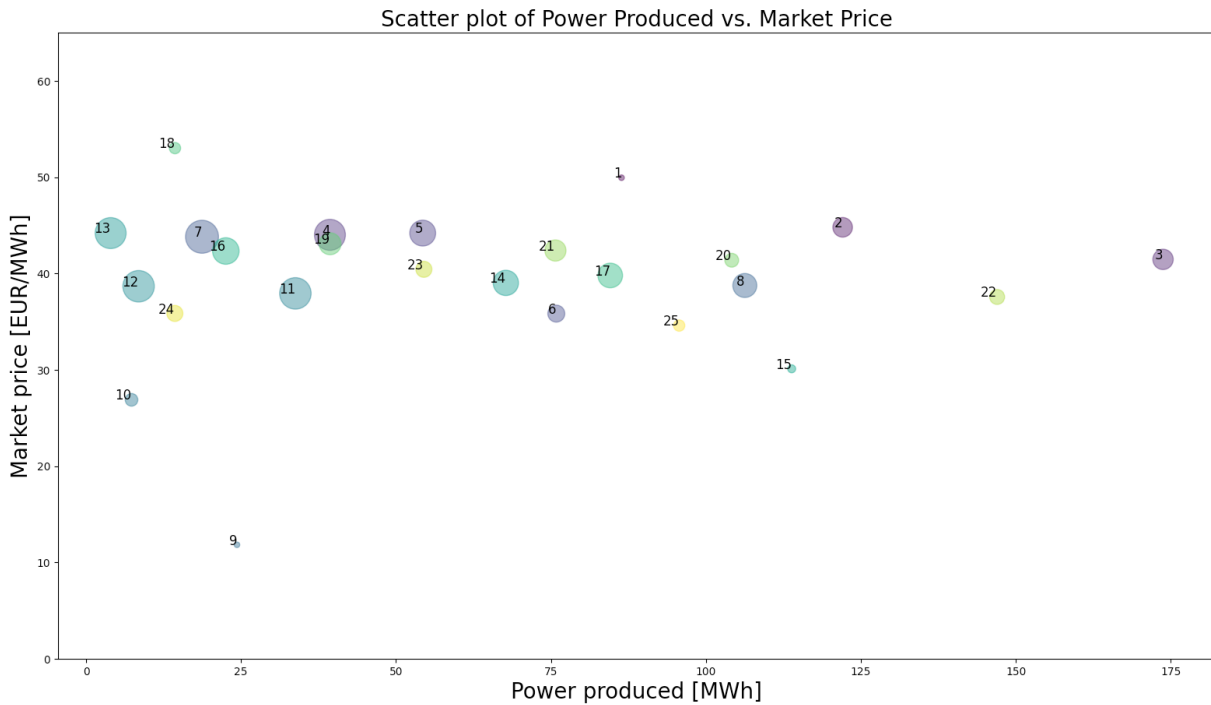


Figure A.3: Scatter plot showing input data for 25 scenarios at 8-9 AM. Each point is a scenario, and the size of the plot indicates its probability. The color represent the different scenarios.

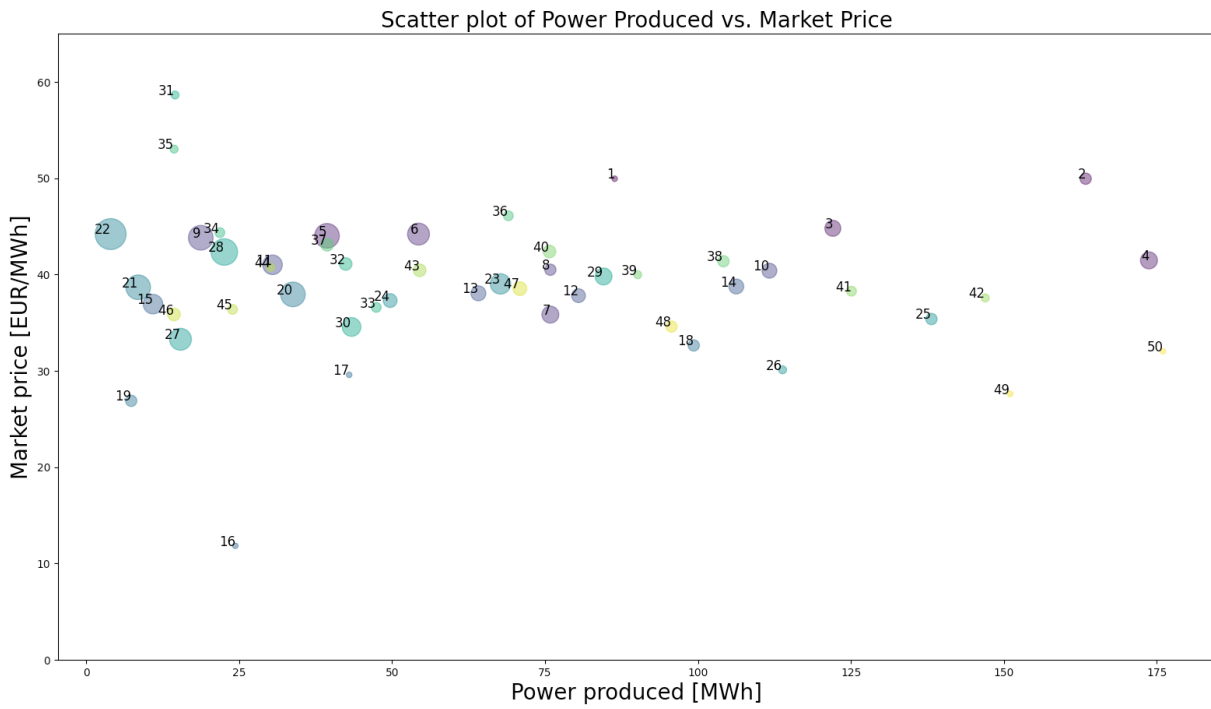


Figure A.4: Scatter plot showing input data for 50 scenarios at 8-9 AM. Each point is a scenario, and the size of the plot indicates its probability. The color represent the different scenarios.

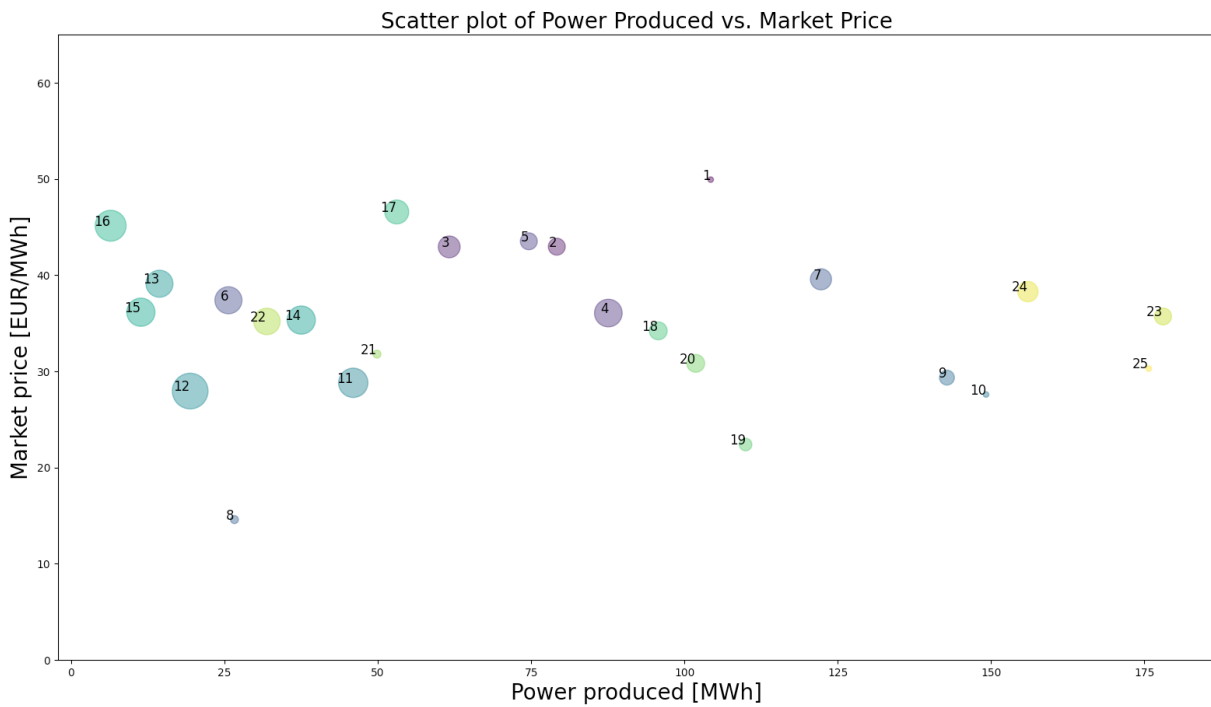


Figure A.5: Scatter plot showing input data for 25 scenarios at 12-1 PM. Each point is a scenario, and the size of the plot indicates its probability. The color represent the different scenarios.

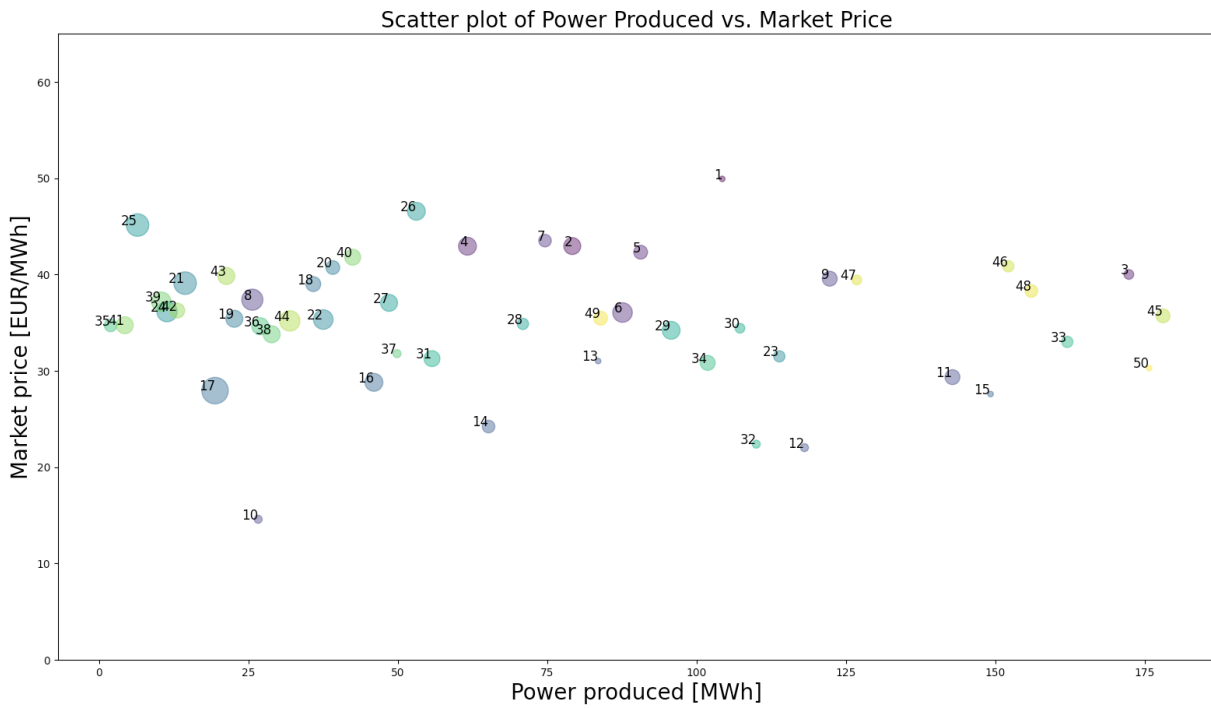


Figure A.6: Scatter plot showing input data for 50 scenarios at 12-1 PM. Each point is a scenario, and the size of the plot indicates its probability. The color represent the different scenarios.

A.3.3 Seasonal 25 scenario cases for 4-5 PM for winter, spring and summer

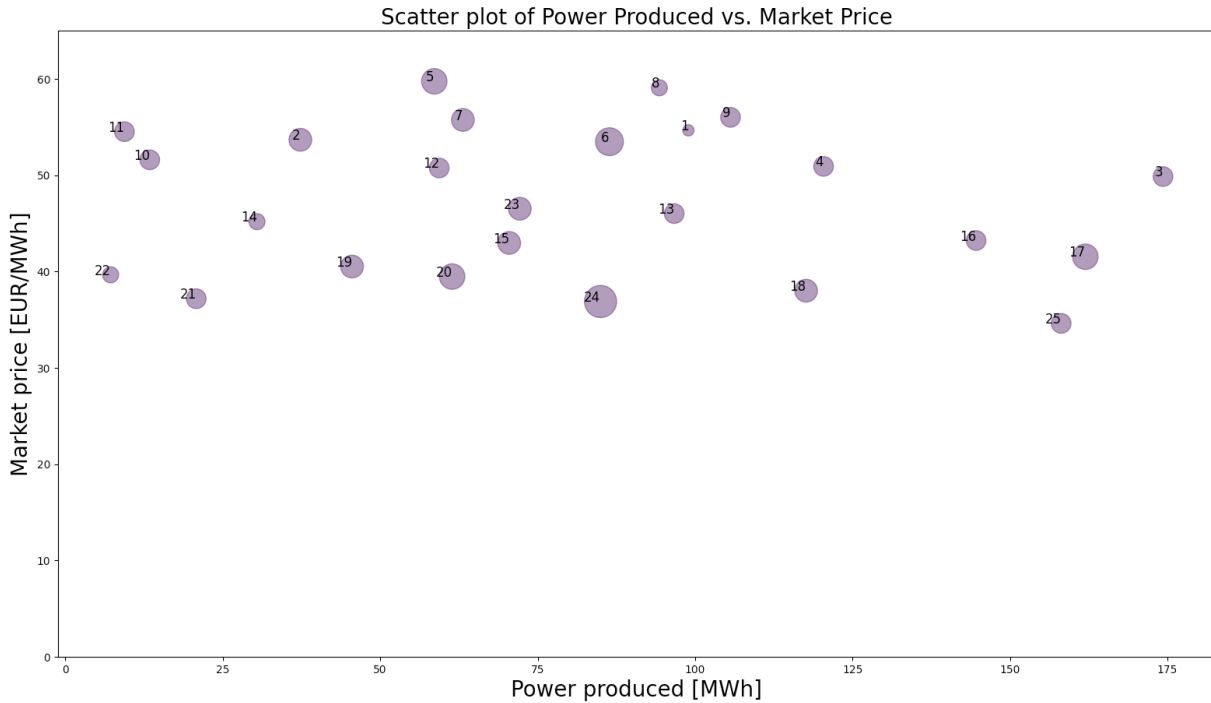


Figure A.7: Scatter plot showing input data for 25 scenarios at 4-5 PM for the winter months. Each point is a scenario, and the size of the plot indicates its probability. The color is the same as the winter color from the 365 plot.

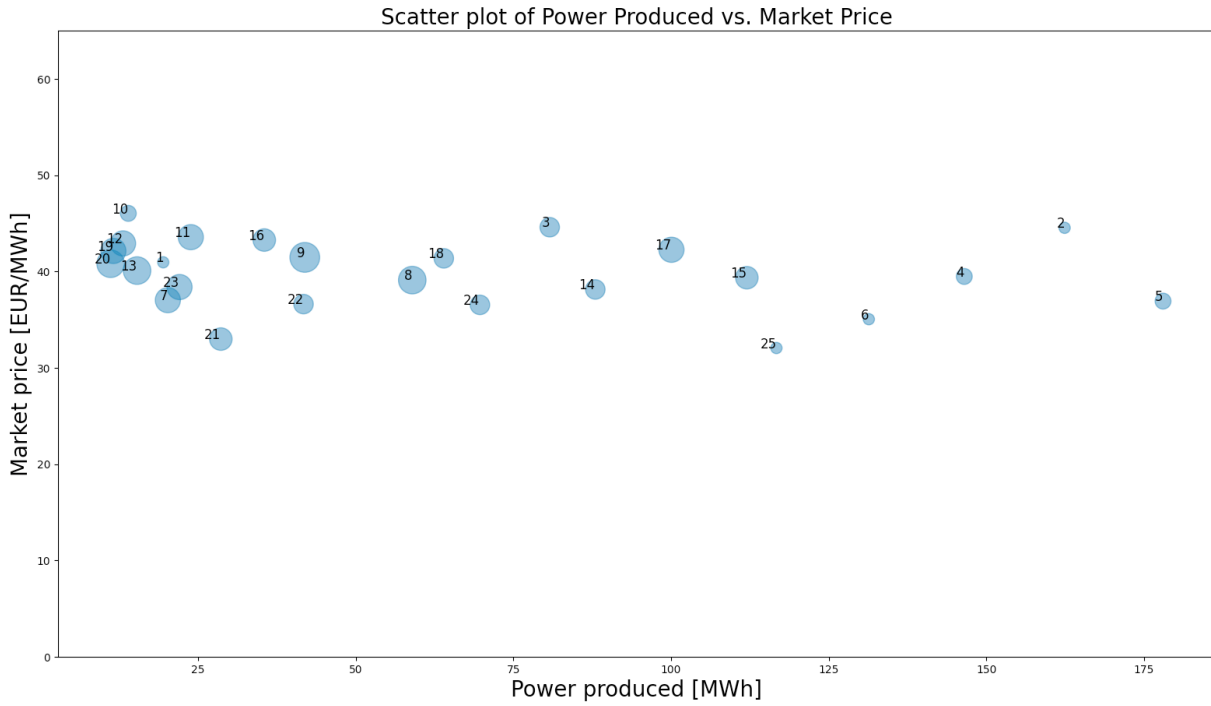


Figure A.8: Scatter plot showing input data for 25 scenarios at 4-5 PM for the spring months. Each point is a scenario, and the size of the plot indicates its probability. The color is the same as the spring color from the 365 plot.

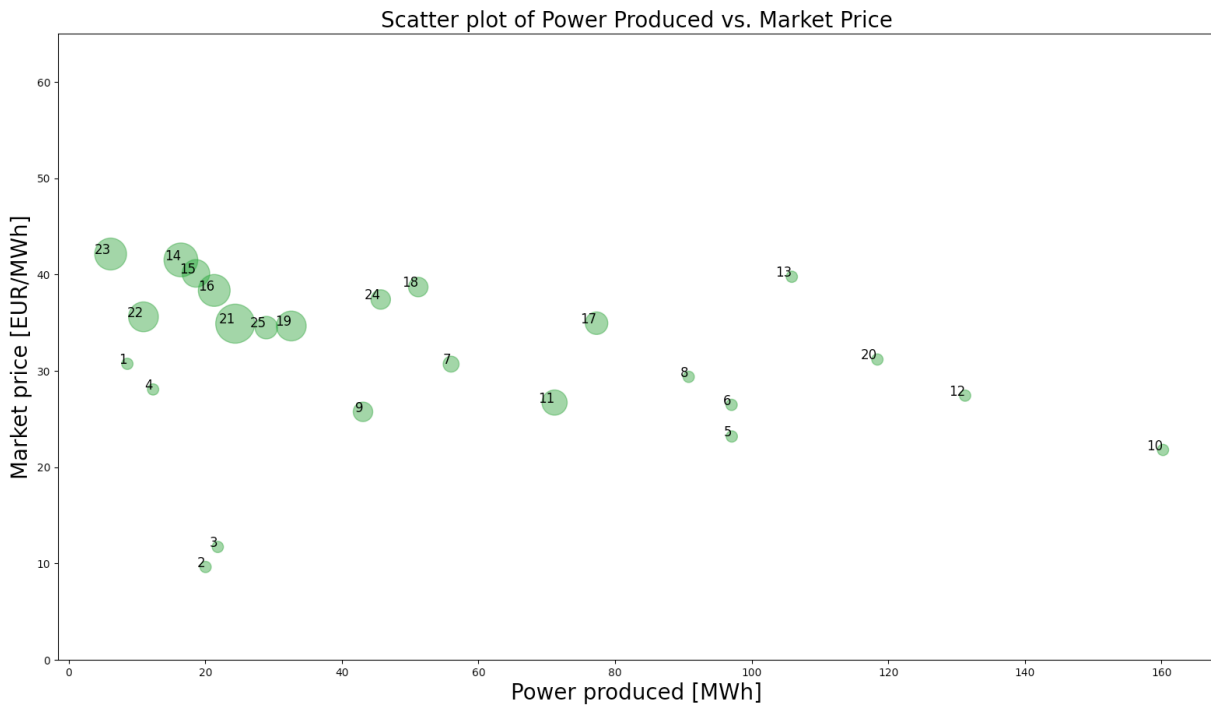


Figure A.9: Scatter plot showing input data for 25 scenarios at 4-5 PM for the summer months. Each point is a scenario, and the size of the plot indicates its probability. The color is the same as the summer color from the 365 plot.

A.4 Yearly model results from 8-9 PM and 12-1 PM for 25, 50 and 365 scenarios

Table A.1: Results from running the *Wind Optimization Model* with 25 scenarios from data between 8-9 AM. The input data is shown in Figure A.3.

Up-regulation price [EUR/MWh]	Down-regulation price [EUR/MWh]	Power bid in DAM [MWh]	Profit [EUR]	Difference [EUR]	Percentage decrease in profit
110	10	22.55	859.93	-1240.50	59.06 %
105	10	22.55	877.72	-1222.71	58.21 %
100	10	22.55	895.52	-1204.91	57.36 %
95	10	22.55	914.32	-1186.11	56.47 %
90	10	33.77	947.72	-1152.71	54.88 %
85	10	33.77	986.24	-1114.19	53.05 %
80	10	33.77	1024.77	-1075.66	51.21 %
75	10	39.34	1071.49	-1028.94	48.99 %
70	10	39.34	1122.67	-977.76	46.55 %
65	10	39.34	1173.91	-926.52	44.11 %
60	10	54.31	1256.99	-843.44	40.16 %

Table A.2: Results from running the *Wind Optimization Model* with 50 scenarios from data between 8-9 AM. The input data is shown in Figure A.4.

Up-regulation price [EUR/MWh]	Down-regulation price [EUR/MWh]	Power bid [MWh]	Profit [EUR]	Difference [EUR]	Percentage decrease in profit
110	10	21.83	837	-1198.93	58.89 %
105	10	22.55	854.3	-1181.63	58.04 %
100	10	22.55	871.86	-1164.07	57.18 %
95	10	22.55	889.42	-1146.51	56.31 %
90	10	30.12	908.51	-1127.42	55.38 %
85	10	30.44	940.67	-1095.26	53.80 %
80	10	33.77	976.63	-1059.30	52.03 %
75	10	33.77	1015.81	-1020.12	50.11 %
70	10	39.34	1066.77	-969.16	47.60 %
65	10	42.97	1121.52	-914.41	44.91 %
60	10	49.67	1190.75	-845.18	41.51 %

Table A.3: Results from running the *Wind Optimization Model* with 365 scenarios from data between 8-9 AM. The input data is shown in Figure A.1.

Up-regulation price [EUR/MWh]	Down-regulation price [EUR/MWh]	Power bid in DAM [MWh]	Profit [EUR]	Difference [EUR]	Percentage decrease in profit
110	10	21.89	860.06	-1260.57	59.44 %
105	10	22.57	877.11	-1243.52	58.64 %
100	10	23.91	895.72	-1224.91	57.76 %
95	10	25.14	916.53	-1204.10	56.78 %
90	10	29.50	942.78	-1177.85	55.54 %
85	10	32.55	975.18	-1145.45	54.01 %
80	10	33.77	1012.6	-1108.03	52.25 %
75	10	37.08	1053.9	-1066.73	50.30 %
70	10	39.37	1103.65	-1016.98	47.96 %

Table A.4: Results from running the *Wind Optimization Model* with 25 scenarios from data between 12-1 PM. The input data is shown in Figure A.5.

Up-regulation price [EUR/MWh]	Down-regulation price [EUR/MWh]	Power bid [MWh]	Profit [EUR]	Difference [EUR]	Percentage decrease in profit
110	10	19.4	851.46	-1077.06	55.85 %
105	10	19.40	861.13	-1067.39	55.35 %
100	10	19.40	870.79	-1057.73	54.85 %
95	10	19.40	880.46	-1048.06	54.35 %
90	10	25.64	893.01	-1035.51	53.69 %
85	10	25.64	912.76	-1015.76	52.67 %
80	10	25.64	932.51	-996.01	51.65 %
75	10	31.91	957.99	-970.53	50.33 %
70	10	31.91	989.99	-938.53	48.67 %

Table A.5: Results from running the wind optimization model with 50 scenarios from data between 12-1 PM. The input data is shown in Figure A.6.

Up-regulation price [EUR/MWh]	Down-regulation price [EUR/MWh]	Power bid [MWh]	Profit [EUR]	Difference [EUR]	Percentage decrease in profit
110	10	19.40	842.32	-1110.69	56.87 %
105	10	21.29	853.27	-1099.74	56.31 %
100	10	21.29	866.38	-1086.63	55.64 %
95	10	22.63	880.65	-1072.36	54.91 %
90	10	25.64	896.94	-1056.07	54.07 %
85	10	25.64	916.91	-1036.10	53.05 %
80	10	26.98	938	-1015.01	51.97 %
75	10	28.88	961.91	-991.10	50.75 %
70	10	31.90	991.88	-961.13	49.21 %

Table A.6: Results from running the *Wind Optimization Model* with 365 scenarios from data between 12-1 PM. The input data is shown in Figure A.2.

Up-regulation price [EUR/MWh]	Down-regulation price [EUR/MWh]	Power bid [MWh]	Profit [EUR]	Difference [EUR]	Percentage decrease in profit
110	10	21.84	912.42	-1261.61	58.03 %
105	10	22.73	927.46	-1246.57	57.34 %
100	10	24.47	944.24	-1229.79	56.57 %
95	10	25.64	963.27	-1210.76	55.69 %
90	10	26.64	984.45	-1189.58	54.72 %
85	10	28.52	1008.01	-1166.02	53.63 %
80	10	30.94	1036.08	-1137.95	52.34 %
75	10	35.20	1070.56	-1103.47	50.76 %
70	10	38.27	1115.28	-1058.75	48.70 %



 **NTNU**

Norwegian University of
Science and Technology